Mesenteric Lymphatic Targeting of Antiretroviral agents for Improved Treatment of HIV/AIDS

<u>YenJu Chu</u>

School of Pharmacy

University of Nottingham

Nottingham

United Kingdom

Thesis submitted to The University of Nottingham for the degree of Doctor in Philosophy

Table of Contents

ACKNOWLEDGEMENTS

Rome was not built by a single person, as this Ph.D cannot be done without concerted efforts. First of all, I would like to express my sincere appreciation, gratitude, and respect to my supervisor Associate Professor Pavel Gershkovich for his patience, passion, motivation, creation, wisdom, rigour, and immense knowledge in supervision throughout my Ph.D and for supporting my future career in academia. His impressive thinking process has been deeply implanted in my soul and will certainly benefit my future career. Furthermore, I want to extend my gratitude to Professor Peter Fischer and Professor Michael Stocks for their precious guidance and support in chemistry work.

I am particularly grateful to my wife, Ms. Chim Lih Shin, who has supported and provided warm emotional and mental support throughout my Ph.D study. As a paediatrician, she sometimes gave me academic advice allowing me to progress in my project. Moreover, she brought my son into this world during the final year of Ph.D. Without her, I might not be able to start and finish my study. I want to give special gratitude to my adorable son, master Roller Chu, who is the best chapter of my Ph.D and the best gift in my life. His smile released my tiredness, and crying inspired me to be a better father. I would also like to thank my parents, brothers, and sister-in-laws for their emotional support.

I have the great pleasures in working with my lab colleagues, university members, and friends at the University of Nottingham. I gratefully

acknowledge Dr. Chaolong Qin and Dr. Wanshan Feng, who guided and helped me throughout my entire Ph.D. I also want to sincerely thank the valuable contributions from Dr. Joseph Ali, Dr. Carlos Sanders-Velvez, Dr. Adelaide Jewell, Miss. Alice Brookes, Ms. Abgail Wong, Mr. Liuhang Ji, Mr. Haojie Chen, Miss. Sarah Sulaiman, Miss. Graziamarina Sinatra, and Mr. Branislav Vukovic. I am also very grateful to Dr. Aimie Garces, Dr. Eleonora Comeo, Dr. Kok Zhi Yuan, and Mr. Ta-Chi Su for their assistance in the chemistry lab. I am also grateful to the undergraduate and MSc students Miss. Ying Ying Lam, Mr. Charles Sheriston, Miss. Yu Jane Khor, Miss. Concepción Medrano-Padial, and Miss. Sheikh Rahman, who participated and contributed to my project. Additionally, I want to thank Mr. Lee Hibbett, Ms. Ann Williams, and Mr. Paul Cooling for their technical support in the labs. I would also like to thank the Bio-Support Unit (BSU) team in the University of Nottingham for excellent technical assistance for animal studies in this Ph.D project.

Finally, I am deeply grateful to the Ministry of National Defence, R.O.C. for the financial support of this Ph.D study.

LIST OF PUBLICATIONS

1. List of publication originating from this thesis:

Chu, Y., Qin, C., Feng, W., Sheriston, C., Jane Khor, Y., Medrano-Padial, C., Watson, B., Chan, T., Ling, B., Stocks, M., Fischer, P., Gershkovich, P. (2021) Oral administration of tipranavir with long-chain triglyceride results in moderate intestinal lymph targeting but no efficient delivery to HIV-1 reservoir in mesenteric lymph nodes. *International Journal of Pharmaceutics*, 602, p.120621.

Chu Y., Wong, A., Chen, H., Ji, L., Qin, C., Feng, W., Stocks, M. J., Gershkovich, P. (2023). Development of lipophilic ester prodrugs of dolutegravir for intestinal lymphatic transport. *European Journal of Pharmaceutics and Biopharmaceutics*. Online ahead of print.

2. Additional publications

Qin, C., Feng, W., **Chu, Y.**, Lee, J., Berton, M., Bettonte, S., Teo, Y., Stocks, M., Fischer, P. and Gershkovich, P. (2020). Development and validation of a cost-effective and sensitive bioanalytical HPLC-UV method for determination of lopinavir in rat and human plasma. *Biomedical Chromatography*, 34 (11), e4934.

Qin, C., **Chu, Y.**, Feng, W., Fromont, C., He, S., Ali, J., Lee, J., Zgair, A., Berton, M., Bettonte, S., Liu, R., Yang, L., Monmaturapoj, T., Medrano-Padial, C., Ugalde, A., Vetrugno, D., Ee, S.Y., Sheriston, C., Wu, Y.,

Stocks, M., Fischer, P. and Gershkovich, P. (2020). Targeted delivery of lopinavir to HIV reservoirs in the mesenteric lymphatic system by lipophilic ester prodrug approach. *Journal of Controlled release*, 329, pp.1077-1089.

Feng, W., Qin, C., **Chu, Y.**, Berton, M., Lee, J. B., Zgair, A., Bettonte, S., Stocks, M., Constantinescu, C., Barrett, D., Fischer, P., Gershkovich, P. (2021) Natural sesame oil is superior to pre-digested lipid formulations and purified triglycerides in promoting the intestinal lymphatic transport and systemic bioavailability of cannabidiol. *European Journal of Pharmaceutics and Biopharmaceutics*, 162, pp.43-49.

Feng, W., Qin, C., Cipolla, E., Lee, J. B., Zgair, A., **Chu, Y.**, Ortori, C., Stocks, M., Constantinescu, C., Barrett, D., Fischer, P., Gershkovich, P. (2021) Inclusion of Medium-Chain Triglyceride in Lipid-Based Formulation of Cannabidiol Facilitates Micellar Solubilization In Vitro, but In Vivo Performance Remains Superior with Pure Sesame Oil Vehicle. *Pharmaceutics*, 13(9), p.1349.

Feng, W., Qin, C., Abdelrazig, S., Bai, Z., Raji, M., Darwish, R., **Chu, Y.**, Ji, L., Gray, D., Stocks, M., Constantinescu, C., Barrett, D., Fischer, P., Gershkovich, P. (2022) Vegetable oils composition affects the intestinal lymphatic transport and systemic bioavailability of co-administered lipophilic drug cannabidiol. *International Journal of Pharmaceutics*, 624, p.121947.

LIST OF ABBREVIATIONS

AIDS	Acquired immunodeficiency syndrome
ARV	Antiretroviral drug
ART	Antiretroviral therapy
AUC	Area under curves
AZT	Azidothymidine or zidovudine
BBB	Brain-blood barrier
BCB	Blood-cerebral spinal fluid-barrier
BMI	Body mass index
cART	Combination antiretroviral therapy
CBD	Cannabidiol
CCR5	Chemokine co-receptors 5
CETPi	Cholesterol ester transfer protein inhibitor
CM	Chylomicrons
CNS	Central nervous system
CSF	Cerebrospinal fluid
CV	Column volume
CXCR4	CXC-chemokine receptor
CYP3A4	Cytochrome P450 3A4
C_{max}	Maximum plasma drug concentration
C_0	Concentration extrapolated to time zero
CL	Clearance
DDT	dichlorodiphenyltrichloroethane
DMSO	Dimethyl sulfoxide
DMF	N,N-Dimethylformamide
DNA	Deoxyribonucleic acid

DPBS	Dulbecco’s phosphate buffered saline
DTG	Dolutegravir
EDTA	Ethylenediaminetetraacetic acid
ESI	Electrospray ionization
EVG	Elvitegravir
FaSSIF	Fasted state simulated intestinal fluid
FaSSGF	Fasted state simulated gastric fluid
FDA	Food and Drug Administration (US)
FI	Fusion inhibitor
F_{oral}	Oral bioavailability
Gag	Golyprotein
GALT	Gut-associated lymphoid tissue
GI	Gastrointestinal
HAND	HIV-associated neurocognitive disorders
HIV	Human immunodeficiency virus
HPLC	High-performance liquid chromatography
IC_{90}	90% inhibition concentration
IM	Intramuscular
INSTI	Integrase strand transfer inhibitor
IS	Internal standard
IV	Intravenous
IVIVC	*In vitro-in vivo* correlation
KBr	Potassium bromide
LCT	Long-chain triglyceride
LC-MS/MS	Liquid Chromatography-tandem mass spectrometry
LLOQ	Lower limit of quantification
LPV	Lopinavir
LPV/r	Lopinavir/ritonavir
LRA	Latency-reversing agents
MCT	Medium-chain triglyceride

MLNs	Mesenteric lymph nodes
MPA	Mycophenolic acid
MRM	Multiple reaction monitoring
MTBE	Methyl tertiary butyl ether
NaCl	Sodium chloride
NaOH	Sodium hydroxide
NaF	Sodium fluoride
NaTc	Sodium taurocholate hydrate
NaH_2PO_4	Sodium phosphate monobasic
NFV	Nelfinavir
NMDTG	Nano-formulated myristoylated DTG
NMR	Nuclear magnetic resonance
NNRTI	Non-nucleoside reverse transcriptase inhibitor
NRTI	Nucleoside reverse transcriptase inhibitor
PAI	Post-attachment inhibitor
PA-IC_{90}	Protein adjusted 90% inhibition concentration
PBS	Phosphate-buffered saline
PE	Pharmacokinetic enhancer
PEG-400	Polyethylene glycol 400
P-gp	P-glycoprotein
PIs	Protease inhibitors
Ppm	Parts per million
RAL	Raltegravir
RNA	Ribonucleic acid
RSE	Relative standard errors
RSD	Relative standard deviation
RTV	Ritonavir
SCT	Short-chain triglyceride
SD	Standard deviation

SEDDS	Self-emulsifying drug delivery system
SIV	Simian immunodeficiency virus
Super-SNEDDS	Supersaturated self-nanoemulsifying drug delivery system
TPV	Tipranavir
$t_{1/2}$	Half-life
t_{max}	Time to reach plasma peak concentration
$t_{max\text{-}1h}$	One hour before t_{max}
TG	Triglyceride
THC	Δ9-tetrahydrocannabinol
TLC	Thin layer chromatography
UGT1A1	Orthologous UDP glucuronosyltransferase 1A1
UV	Ultra-violet
VLDL	Very low density lipoproteins
V_{ss}	Volume of distribution at steady state

ABSTRACT

Human immunodeficiency virus (HIV) is a worldwide pandemic that causes irreversible and unstoppable disease progression. Antiretroviral therapy (ART) can efficiently suppress viral replication and control the pace of HIV infection. However, discontinuing ART usually leads to rebound viremia and drug resistance when resuming ART. This is primarily due to establishment of latent HIV reservoirs in cellular and anatomical sites. Suboptimal levels of ART in viral reservoirs might allow the persistence of latent infection. Gut-associated lymphoid tissue (GALT), in particular mesenteric lymph nodes (MLNs), is the largest immune system in the body and an important HIV reservoir. This study selects two antiretroviral agents (ARVs), tipranavir (TPV) and dolutegravir (DTG), as candidate drugs for targeted delivery to the mesenteric lymphatic system. In view of the different physicochemical properties between TPV and DTG, this study was conducted by two different approaches: (1) Targeting of lipophilic drug TPV to mesenteric lymphatics by means of intestinal lymphatic transport using a long-chain triglyceride (LCT)-based formulation approach; (2) Developing a lipophilic ester prodrug system of hydrophilic drug DTG, combined with LCT-based formulation to target DTG to mesenteric lymph and MLNs.

The introduction of combination antiretroviral therapy (cART) led to substantial improvement in mortality and morbidity of HIV-1 infection. However, the poor penetration of ARVs to HIV-1 reservoirs limits the ability of the ARVs to eliminate the virus. MLNs are one of the main HIV-1 reservoirs in patients under suppressive ART. The intestinal lymphatic

absorption pathway substantially increases the concentration of lipophilic drugs in mesenteric lymph and MLNs when they are co-administered with LCT. Chylomicrons (CM) play a crucial role in intestinal lymphatic absorption as they transport drugs to the lymph lacteals rather than blood capillary by forming drug-CM complexes in the enterocytes. Thus, lipophilic antiretroviral drugs could potentially be delivered to HIV-1 reservoirs in MLNs by an LCT-based formulation approach. In this study, protease inhibitors (PIs) were initially screened for their potential for intestinal lymphatic targeting using a computational model. The candidates were further assessed for their experimental affinity to CM. TPV was the only-candidate with substantial affinity to both artificial and natural CM *in vitro* and *ex vivo*. Pharmacokinetics and biodistribution studies were then performed to evaluate the oral bioavailability and intestinal lymphatic targeting of TPV in rats. The results showed similar oral bioavailability of TPV with and without co-administration of LCT vehicle. Although LCT-based formulation led to 3-fold higher concentrations of TPV in mesenteric lymph compared to plasma, the levels of the drug in MLNs were similar to plasma in both LCT-based and lipid-free formulation groups. Thus, LCT-based formulation approach alone was not sufficient for effective delivery of TPV to MLNs. Future efforts should be directed to a combined highly lipophilic prodrugs/lipid-based formulation approach to target TPV, other PIs and potentially other classes of antiretroviral agents to viral reservoirs within the mesenteric lymphatic system.

A number of alkyl ester prodrugs of DTG were designed based on the *in silico* predicted affinity to chylomicrons (CM), and six promising prodrugs were selected and synthesised. The synthesised prodrugs were further assessed for their intestinal lymphatic transport potential and biotransformation in biorelevant media *in vitro* and *ex vivo*. DTG and one most promising prodrug (prodrug 5) were then assessed in pharmacokinetics and biodistribution studies in rats. Although oral administration of an allometrically scaled dose (5 mg/kg) of unmodified DTG with or without lipids achieved concentrations above protein binding-adjusted IC_{90} (PA-IC_{90}) (64 ng/mL) in most tissues, it was not selectively targeted to MLNs. The combination of lipophilic ester prodrug and LCT-based formulation approach improved the targeting selectivity of DTG to MLNs by 4.8-fold compared to unmodified DTG. However, systemic exposure to DTG was limited by poor intestinal absorption of the prodrug following oral administration. *In vitro* lipolysis showed a good correlation between micellar solubilisation of the prodrug and *in vivo* systemic exposure to DTG in rats. Thus, it is prudent to include *in vitro* lipolysis in the early assessment of orally administered drugs and prodrugs in lipidic formulations, even when intestinal lymphatic transport is involved in the absorption pathway. Further studies are needed to clarify the underlying mechanisms of low systemic bioavailability of DTG following oral administration of the prodrug and potential ways to overcome this limitation.

In conclusion, this PhD work focuses on targeting two ARVs, TPV and DTG, to an important HIV reservoir in MLNs by means of drug-CM

association-driven intestinal lymphatic transport. When formulated with LCT, oral administration of TPV to rats has achieved substantial drug levels in mesenteric lymph fluid, suggesting intestinal lymphatic transport of TPV in the presence of lipids. However, the concentration of TPV in the mesenteric lymph is insufficient for drug targeting to MLNs, indicating that the LCT-based formulation approach alone does not lead to effective mesenteric lymphatic targeting of TPV or other ARVs. A combination approach of lipophilic ester prodrug and LCT-based formulation was applied to deliver hydrophilic DTG to mesenteric lymphatic transport. Although the oral administration of the selected prodrug candidate in an LCT-based formulation improved the selectivity of mesenteric lymphatic targeting of DTG, the oral bioavailability of DTG was attenuated due to poor intestinal absorption.

LIST OF FIGURES

LIST OF TABLES

1. INTRODUCTION

1.1. Human immunodeficiency virus (HIV) and acquired immunodeficiency syndrome (AIDS)

1.1.1. Epidemiology of HIV/AIDS

HIV originated from the simian immunodeficiency virus (SIV), a member of the retrovirus [1], which primarily infects mammalian species. As early as 1920 to 1940, HIV transmitted from non-human primates into the human population [2, 3]. In 1981, the first case of AIDS brought HIV under the spotlight [4]. Two years later, the virus was isolated from a pre-AIDS patient [5]. Based on genetic diversity, HIV has two subtypes: HIV-1 and HIV-2. They share many similarities, such as transmission pathways, life cycle in host cells, and the leading to AIDS. HIV-1 is more transmissible and progressive than HIV-2 [6]. The transmission of HIV is by direct contact with infected body fluids with mucous membranes or damaged skin [7-9]. Risk factors include high-risk sexual behaviours, blood transfusions, needle sharing, and vertical mother-to-child transmission [10-15].

According to WHO statistics, HIV has infected more than 84.2 million people and claimed 40.1 million lives globally since the pandemic. In 2021, the morbidity and mortality of HIV infection were reported as the population of 38.4 million and 650,000, respectively, and 1.5 million people were newly infected with HIV worldwide (**Table 1-1**). Compared to 2010, the incidence of HIV infection and deaths in 2021 decreased by 32% and 52%, respectively. Although 75% of HIV-infected people are under treatment of antiretroviral therapy (ART) and 92% of this treated

population have achieved viral suppression (< 200 copies/mL of blood), HIV/AIDS is still one of the major worldwide issues due to its irreversible disease progression [16].

	People living with HIV in 2021	People acquiring HIV in 2021	People dying from HIV-related causes in 2021
Total	**38.4 million (33.9-43.8 million)**	**1.5 million (1.1-2.0 million)**	**650,000 (510,000-860,000)**
Adults (15+ years)	**36.7 million (32.3-41.9 million)**	**1.3 million (990,000-1.8 million)**	**560,000 (430,000-740,000)**
Women (15+ years)	**19.7 million (17.6-22.4 million)**	**640,000 (480,000-870,000)**	**240,000 (180,000-320,000)**
Men (15+ years)	**16.9 million (14.6-19.7 million)**	**680,000 (500,000-920,000)**	**320,000 (250,000-430,000)**
Children (<15 years)	**1.7 million (1.3-2.1 million)**	**160,000 (110,000-230,000)**	**980,000 (67,000-140,000)**

Table 1-1. Summary of the global HIV epidemic in 2021. Modified from WHO [16].

1.1.2. The life cycle of HIV

The life cycle of HIV is well documented and divided into several critical stages that became the potential action sites of antiretroviral drugs (ARVs) (**Figure 1-1**) [17]. During the first stage, HIV virions identify the host $CD4^+$ T cells through the interactions between the viral surface envelope glycoproteins (gp120) and target cells' surface receptor proteins (CD4) [18-20], as well as chemokine co-receptors (CCR5 or CXCR4) [21-29]. The surface interaction leads to the fusion of HIV and the host cell, allowing the release of viral capsid into the cytosol [30-34]. After entering the host cell, the viral capsid breaks down and liberates the viral mRNA and enzymes. Viral single-stranded RNA is then reverse-transcribed to double-stranded DNA in the cytoplasm [35], which will then migrate into the host cell nucleus. With the aid of HIV integrase and

cofactors, viral DNA is inserted into the host chromosome to join the DNA replication event [36-39]. HIV mRNA is then produced through the cell-hosted transcription and disseminated to the cytoplasm for further translation into provirus polypeptides [40, 41]. Finally, viral mRNA and provirus particles assemble and exit from the host cell. HIV protease drives viral maturation by cleaving non-functional precursor polypeptides into functional proteins [42].

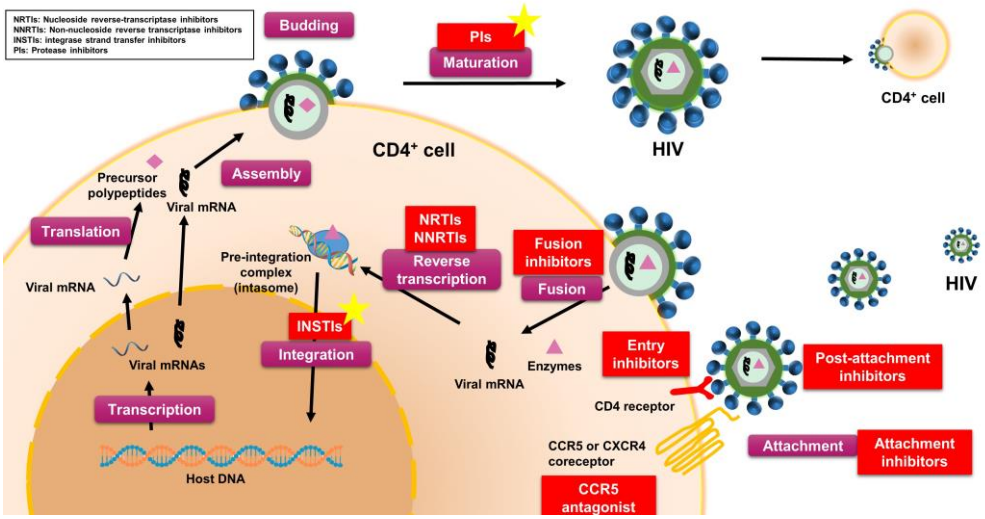

Figure 1-1. The HIV life cycle and potential therapeutic targets for ARVs. HIV initiates its life cycle by attaching to the CD4 receptor and CCR5 or CXCR4 co-receptor on the host cell's surface (stage 1 - attachment). The viral capsid liberates the viral genome and associated proteins into the cytosol (stage 2 - fusion). Viral mRNA is reverse transcribed into cDNA, which is then assembled with enzymes to form a pre-integration complex (intasome) and moved into the host cell nucleus (stage 3 – reverse transcription). HIV integrase helps viral cDNA to insert into host DNA sequence (stage 4 – integration) for transcription of viral mRNAs (stage 5 – transcription). Following the transcription, viral mRNAs disseminate into the cytosol for further translation to precursor polypeptides (stage 6 – translation). At the final stage, provirus precursors and viral mRNA assemble and exit the host cell (stage 7 – budding). HIV protease cleaves viral precursor polypeptides into functional enzymes (stage 8 – maturation). Modified from [17].

1.1.3. Stages of HIV infection

HIV gradually destroys the host immune system in three stages: (1) acute HIV infection; (2) chronic HIV infection; (3) acquired immunodeficiency syndrome (AIDS).

1.1.3.1. Acute HIV infection

After the acquisition of HIV, there is a short window, termed the ‘eclipse phase’, during which the virus replicates in mucosal and lymphoid tissues and remains undetectable in peripheral blood for 7 to 21 days without causing any symptom [43, 44]. This short interval currently cannot be identified as no diagnostic test can detect viral biomarkers [45]. Sustained local seroconversion eventually leads to systemic viral dissemination. Thereby, infected hosts may experience flu-like symptoms with a peak of viremia and a trough level of blood $CD4^+$ T cells [46, 47]. During the peak of viremia, the immune system responds to the acute HIV infection, leading to the recovery of $CD4^+$ T cell counts. At the same time, the viral load will decline to a certain level, termed the ‘viral set point’ [48-50]. The viral set point could be maintained for years by homeostasis between viral reproduction and host immune responses [51].

1.1.3.2. Chronic HIV infection and AIDS

After reaching the viral set point, HIV infection proceeds to the asymptomatic chronic infection stage. Persistent viral turnover leads to sustained immune activation, which contributes to the progressive depletion of $CD4^+$ T cells and subsequent immunodeficiency [17]. A chronic infection could take a decade or more to advance to AIDS when left untreated.

AIDS is the final stage of HIV infection when the immune system is severely paralysed. People with weakened immune systems are highly likely to acquire opportunistic infections or infection-related cancers, which could lead to serious disease consequences. According to US Centers for Disease Control and Prevention, AIDS is diagnosed in HIV-infected individuals with $CD4^+$ T cell counts below 200 cells/mm^3 or with certain opportunistic infections [52]. From the onset of AIDS, the life expectancy is about two years without ART intervention [53].

1.2. HIV reservoirs

HIV reservoirs are defined as HIV inactively persists in cells or anatomical compartments in a replication-competent form. Although ART effectively suppresses the virus in HIV-infected patients, it does not eradicate it due to the latent reservoirs. In general, there are two types of HIV reservoirs: cellular reservoir and anatomical reservoir.

1.2.1. Cellular reservoirs

HIV persists in $CD4^+$ T cells latently in patients receiving long-term suppressive ART [54-56]. Since HIV replication usually happens in activated $CD4^+$ T cells [57, 58], latent viral reservoirs are believed to be established in resting $CD4^+$ T cells (naïve and memory T cells) during the early stages of HIV infection [59-61]. These infected $CD4^+$ T cells can remain silent and house the viral genome throughout their natural life without being attacked by the host immune system [62]. Memory cells have long lifespans, allowing rapid responses to specific antigens they

have previously encountered. As HIV DNA is stably anchored in these long-lived memory cells, the half-life of these latent cellular reservoirs is quite long (an average of 43.9 months in HIV-infected adults on suppressive ART) [63].

In addition to resting $CD4^+$ T cells, other cell types have been reported to harbour latent HIV [64]. For example, myeloid lineage cells, particularly monocytes/macrophages, presenting CD4 receptor and CCR5 or CXCR4 co-receptors [65], are important latent viral reservoirs during HIV infection [66]. These cells are long-lived, resistant to HIV-mediated apoptosis, and widely distributed in almost every tissue [67, 68]. Thus, monocytes/macrophages are ideal targets for latent infection. Antigen-presenting dendritic cells also harbour low levels of viral DNA in HIV-infected individuals [69]. The infected dendritic cells will transfer the infection when presenting the virus to $CD4^+$ T cells, resulting in the depletion of the anti-HIV immune response [70]. It is important to note that HIV is also found to hide in the central nervous system (CNS). In previous studies, HIV DNA and RNA were found in astrocytes, macrophages and microglia isolated from the brain tissues of HIV-infected individuals with or without ART [71-74]. The diversity and wide distribution of cellular reservoirs constitute a major obstacle to HIV eradication.

1.2.2. Anatomical reservoirs

Persistent viral replication was observed in HIV-infected people receiving suppressive ART (viral load < 50 copies/mL of plasma) [75], indicating

the presence of tissue reservoirs. Since HIV-infected cells distribute throughout the body, multiple tissues could be populated by these infected cells and turned into anatomical reservoirs. The anatomical reservoirs include the CNS, lymphoid tissues (spleen, lymph nodes and gut-associated lymphoid tissues (GALT)), reproductive system and other deep tissues [76]. We will describe the CNS and lymphoid tissues, two of the most important and popular HIV reservoirs.

1.2.2.1. CNS

The CNS includes brain and cerebrospinal fluid (CSF). Studying HIV in the brain is difficult due to the limited access to brain tissues. Since CSF has a similar cellular composition to the brain and can reflect cerebral pathologic conditions [77], it has been used as a surrogate of the brain in HIV research. Human and non-human primate studies have shown that HIV rapidly invades the CNS within two weeks (as early as eight days) of the transmission event [78, 79]. The Trojan horse model has been used to describe the scenarios of HIV neuroinvasion that the virus hides in circulated immune cells to overcome the brain-blood barrier (BBB) and gain access to the brain [80]. During infections and inflammations, the permeability of BBB will increase, allowing monocytes/macrophages to cross the BBB and enter the brain. Once in the brain, HIV starts to infect glial cells (microglia and astrocytes): microglia is infected through the CD4/chemokine receptor-mediated infection [81], and astrocyte is infected through endocytosis [82]. The meningeal lymphatic system is another entry point, where infected

lymphocytes activate the inflammation responses, increasing the permeability of lymphatic vessels [80]. The infected lymphocytes can then easily enter the brain. Meningeal tissues have been proposed as a bridge between the brain and peripheral tissues, providing a pathway for HIV to migrate in and out of the brain [83, 84]. HIV can evolve and replicate independently in different anatomical sites, especially CNS [85-94]. The compartmentalisation of HIV in the CNS has been reported to associate with HIV-caused neuro-complications, including HIV-associated neurocognitive disorders (HAND) [95]. In the era of ART, the incidence of HIV-caused dementia has reduced from 25% to 5% in HIV-infected patients, and the severity of HAND symptoms has decreased [96, 97]. However, the CNS is the most difficult-to-penetrate anatomical compartment, as it is protected by the BBB and blood-cerebral spinal fluid (CSF)-barrier (BCB), which are major obstacles for substances to reach the CNS. Suboptimal levels of ARVs in this viral reservoir usually lead to viral escape. In HIV-infected patients on suppressive ART for years, a persistent-replicated viral population is detected in the CNS [98-102].

1.2.2.2. Lymphoid tissues

In a non-human primate study, more than 98% of the SIV viral load was presented in lymphoid tissues, including lymph nodes, spleen, and gut, before and during ART [103]. Furthermore, the GI tract has been reported as a central site of $CD4^+$ T cell depletion and sustained viral replication in SIV-infected non-human primates [104]. In long-term viral-

controlled patients, $CD4^+$ T cell depletion was observed not fully recover, and high viral DNA levels were present in GALT [105]. Thus, lymphoid tissues, particularly GALT, are thought to be the central anatomical reservoirs of HIV. It is important to note that more than half of the body's lymphocytes are housed in GALT [106, 107]. GALT comprises mesenteric lymph nodes (MLNs), peyer's patches and scattered isolated lymphoid follicles [108-110]. In particular, MLNs are the largest aggregates of lymph nodes in the body. The lymph draining from the GI system converges in MLNs before continuing into the thoracic duct and subsequently into the systemic circulation [106]. MLNs are responsible for inducing immunologic tolerance to ingested substances and preventing the systemic dissemination of live commensal microorganisms [111]. Once dendritic cells pick up foreign antigens at the intestinal epithelial surface, they will present these foreign antigens to lymphocytes in MLNs for immune priming or tolerisation [112]. Differentiated lymphocytes will then disseminate from MLNs into systemic circulation through the thoracic duct for further immune responses [111]. Therefore, MLNs are considered the central site of immune response in GALT. Hosting large amounts of lymphocytes, especially $CD4^+$ T cells, and the presence of anatomical and pharmacokinetic barriers make MLNs an ideal sanctuary for HIV [113]. In fact, the HIV viral loads and replication frequencies in MLNs were found to be higher compared to peripheral blood and other lymphoid tissues in non-human primates and humans [114-116].

1.2.3. The Last Gift Cohort

More recently, a cohort study, the Last Gift, has recruited HIV-infected people willing to contribute to HIV cure research at the end of life [117]. This study includes the collection of antemortem blood and a rapid autopsy across 28 anatomical tissues within six hours of the participant's death. Nineteen participants completed the autopsy, and the tissues from the first 6 participants were analysed for the characterisations and dynamics of HIV reservoirs [118]. According to the results, the blood, gut, and lymphoid tissues are the primary sources of persistent viral dissemination. Notably, two patients stopped the treatment before death, allowing the observations of rebounded viremia and HIV repopulation into tissues. Furthermore, the study found that HIV can exchange within CNS or between CNS and systemic circulation, suggesting HIV can cross the BBB bidirectionally [118]. The Last Gift has revealed valuable information on HIV reservoirs and viral repopulation throughout the body and more studies are in progress.

1.2.4. Poor penetration of ART into HIV reservoirs

Early initiation of ART (within three months of the infection) can reduce the size of HIV reservoirs [119-126] and rapidly suppress viremia [127]. In a longitudinal study, patients receiving ART within 30 days of HIV infection demonstrated a sharper and long-lasting decay in the HIV reservoirs [128]. This suggests that initiating ART as early as possible may have long-term benefits in controlling viral reservoirs. However, sustained viral replication in GALT was observed in patients receiving

suppressive ART [113, 129, 130]. Furthermore, low levels of ARVs in HIV reservoirs, especially in lymphoid tissues, were found to allow persistent viral reproduction and the development of drug resistance [131, 132]. The limited penetration of ARVs into these viral sanctuaries is believed to be one of the main barriers to eradicating HIV. Delivery of ARVs to these difficult-to-penetrate HIV reservoirs, especially to MLNs, may lead to substantial improvement in treatment outcomes of HIV.

1.3. Antiretroviral therapy (ART)

1.3.1. Overview

In 1985, a thymidine analogue, known as azidothymidine or zidovudine (AZT), was found to inhibit the replication of HIV by blocking viral reverse transcriptase [133]. AZT was then used as a monotherapy in treating people with HIV infection. Long-term use of AZT has been shown to improve the survival of HIV/AIDS patients and reduce the incidence of opportunistic infections [134]. However, AZT resistance occurred in patients receiving prolonged therapy and led to treatment failure [135-138]. In the early 1990s, dual therapy combining two nucleoside reverse transcriptase inhibitors (NRTIs) was implemented to treat HIV-infected patients. Despite the effective viral suppression, recovered $CD4^+$ T cell counts and improved survival rate [139, 140], dual NRTIs combination failed to control HIV infection efficiently [141]. Therefore, highly active antiretroviral therapy, also known as combination antiretroviral therapy, consisting of three or more different classes of antiretroviral drugs, was introduced in the mid-1990 [141]. This approach significantly improved

the treatment outcomes and is recognised as the most promising strategy for treating HIV-infected people and reducing drug resistance [142-146]. To date, 34 ARVs within nine classes have been approved by the FDA for clinical use [147]: (1) attachment inhibitor; (2) CCR5 antagonist; (3) post-attachment inhibitor (PAI); (4) fusion inhibitor (FI); (5) integrase strand transfer inhibitor (INSTI); (6) non-nucleoside reverse transcriptase inhibitor (NNRTI); (7) NRTI; (8) protease inhibitor (PI); (9) pharmacokinetic enhancer (PE). Each class of ARVs targets specific stages of the HIV life cycle described in section **1.1.2** (**Figure 1-1**). This PhD work focuses on targeting PI and INSTI to mesenteric lymphatics through intestinal lymphatic transport to reduce or eliminate HIV reservoirs.

1.3.2. PIs and tipranavir (TPV)

1.3.2.1. HIV protease and its inhibitors

HIV protease drives the maturation of HIV by cleaving provirus polypeptides into functional proteins. It has been reported that immature viral particles containing inactive HIV proteases cannot complete the life cycle to become infectious virions [148]. Thus, the essential role of HIV protease makes it a promising target for antiretroviral drugs [149, 150]. HIV protease belongs to the aspartic protease family [151] and is a symmetric homodimer [152]. This homodimer assembles two identical monomers of 99 amino acids [152, 153]. Each monomer contains an asp25 catalytic residue at the substrate-binding site. Asp25 residue is essential in the proteolytic cleavage of Gag and GagPol precursor

polypeptides of HIV [151]. Gag polypeptide encrypts six viral structure proteins: matrix, capsid, nucleocapsid, docking protein p6, and two spacer proteins, p2 and p1. GagPol polypeptide encodes some structural proteins: matrix, capsid, p2, nucleocapsid, and the transframe protein, and enzymes: protease, reverse transcriptase and integrase. The proteolytic cleavage of Gag and GagPol polyproteins can produce corresponding proteins and enzymes [154].

HIV protease initiates proteolytic cleavage by asp25 deprotonating a water molecule to generate a hydroxide ion. The nucleophilic hydroxide ion attacks the substrate on the cleavage site to form a tetrahedral transition state peptide. The transition state peptide will rearrange the structure and break down into functional viral proteins [155]. PIs were developed as uncleavable 'transition state' peptide substrates that compete with viral polypeptides at the active site of HIV protease [156, 157]. All peptidic PIs have a hydroxyethylene core to react with the asp25 residue [155]. Once the PIs are at the active site, the hydroxyethylene core will construct a hydrogen bonding network within catalytic regions of HIV protease [158], disrupting the interaction between viral polypeptide substrates and HIV protease. Although PIs have shown robust antiretroviral activity [159-162], the therapeutic effects were limited by drug resistance [163]. HIV mutates the amino acid sequences in or near the substrate binding site, where the PIs compete with the viral peptide substrates. In addition, these amino acid mutations can occur on viral polypeptide substrates. The mutated viral polypeptide can react with the altered substrate binding site of drug-resistance proteases [154].

Since most peptidomimetic PIs have similar structural backbones, some mutations can affect multiple PIs [164].

1.3.2.2. TPV

In 2005, FDA approved TPV (APTIVUS®) to treat highly experienced HIV-infected patients with multiple-PI resistance [165]. TPV is the first non-peptidic protease inhibitor designed based on the structure of coumarin (**Figure 1-2**) [166]. The central backbone of TPV is a dihydropyrone ring [167]. It binds to the active site of HIV protease with fewer hydrogen bonds than peptidomimetic PIs [168], resulting in higher flexibility to adjust to amino acid mutations [169, 170]. Furthermore, TPV has a strong hydrogen bond to the highly conserved amino acid residue asp30 [171], which is less likely to be changed during the viral mutations. Therefore, TPV has a high genetic barrier to drug resistance.

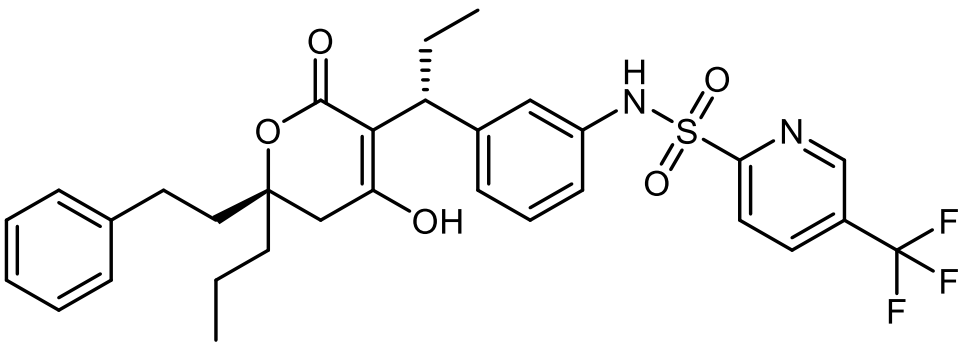

Figure 1-2. Structure of TPV.

In preclinical studies, TPV has a moderate absolute oral bioavailability (~30%) after oral administration in a lipid-free 0.01M sodium hydroxide solution to rats [172]. Limited absolute oral bioavailability was found in other preclinical species (6.5-7.7% in dogs, 11% in mice and 9.9% in

rabbits) [173]. The absolute oral bioavailability of TPV in the human population has not been reported, probably due to the limited solubility in intravenous formulations [173]. It is believed that the moderate to low oral bioavailability in preclinical species is attributed to limited intestinal absorption. Since TPV is a substrate for P-glycoprotein (P-gp) and is mainly metabolised by cytochrome P450, these factors contribute to the poor absorption of TPV [174]. Ritonavir (RTV) is a P-gp and CYP3A4 inhibitor often used as a booster for ARVs and, more recently, for anti-COVID-19 agents [175]. In an open-label study, co-administration of TPV and a low dose of RTV substantially increased the systemic exposure of TPV in healthy volunteers [176].

Formulating a self-emulsifying drug delivery system (SEDDS) with TPV in a soft gelatin capsule doubled the oral bioavailability in treatment-experienced HIV-infected patients compared to a hard-filled capsule [177]. The SEDDS used in formulating TPV comprised dehydrated alcohol, polyoxyl 35 castor oil, propylene glycol, and mono/diglyceride of capric acids/caprylic acids [178]. Polyoxyl 35 castor oil is a non-ionic surfactant used as an emulsifying and solubilising agent in pharmaceutical preparations of lipophilic drugs [179]. Moreover, polyoxyl 35 castor oil can modulate the activity of P-gp in the intestine and improve the absorption of drugs which are substrates for P-gp [180, 181]. Capric acid (C10) and caprylic acid (C8) are medium-chain fatty acids which would not contribute to CM production and subsequent intestinal lymphatic transport. Therefore, the increased oral bioavailability of SEDDS-formulated TPV might be due to improved intestinal absorption.

Administration of TPV with a high-fat meal has been reported to increase systemic absorption two-fold in healthy volunteers [182], which suggests the post-prandial effects promote the production of CM and subsequent intestinal lymphatic transport of TPV. The adverse effects following the administration of TPV are mostly gastrointestinal-related symptoms, while lethal side effects such as intracranial haemorrhage and hepatotoxicity were also occasionally reported [183].

1.3.3. INSTIs and dolutegravir (DTG)

1.3.3.1. HIV preintegration complex (intasome) and its inhibitors

After the reverse transcription of HIV DNA in the host cytoplasm, viral integrases will aggregate on the end of viral DNA to form an intasome. The intasome will then migrate into the host cell nucleus. Integrases will remove two nucleotides from the end of viral DNA to generate free hydroxyl groups at 3' ends, called '3'-end processing'. The free 3'-OH groups of viral DNA can trap the host DNA and drive the strand transfer [184]. As catalyst cofactors, two metal ions are included in the intasome active site during the strand transfer [185]. Inserting the viral DNA into the host DNA strand is an irreversible and central event that turns host cells into permanent viral carriers [186]. INSTIs were developed to prevent this event. The antiretroviral activity of INSTIs is attributed to the two functional moieties in their structure. One is the di-keto acid, which acts as the pharmacophore for chelating the two metal ion cofactors in the active site of HIV protease [187]. The other is the halogenated benzyl

moiety, which can displace viral DNA from the intasome to block the 3' end processing [188-191]. Various pharmacological compounds were described as integrase inhibitors in the 1990s [192]. The first generation of INSTIs, raltegravir (RAL) and elvitegravir (EVG), were approved by FDA in 2007 and 2012, respectively. Unfortunately, drug-resistant variants are against the first generation of INSTIs [193-196]. HIV alters the residues of integrase (mostly on Y143, Q148 and N155) to counteract the first-generation INSTIs [197]. For example, a Y143 pathway has been identified that is specific to RAL. Since viral residue Y143 directly forms a π–π stacking interaction with the oxadiazole ring of RAL, the mutants changed the residue on this position to interrupt the interaction with the drug [198]. Therefore, the second generation of INSTIs, including DTG, was developed to overcome drug resistance [199-201]. The second-generation INSTIs have several fundamental changes in comparison to the first-generation INSTIs:

1. The backbone of the di-keto acid pharmacophore is replaced from monocyclic or bicyclic to tricyclic, resulting in more connection to the integrase residues.
2. A longer linker is introduced to bridge the pharmacophore backbone and halogenated benzyl group. The long amide carbonyl linker allows the halobenzyl group to be inserted deeper into the active site of HIV integrase and increases the torsional flexibility to adjust to mutations.
3. The mono-halogen-substituted benzyl analogue was replaced by two-halogen-substituted benzyl analogues. It has been reported

that benzyl analogues substituted with two halogens have higher antiretroviral activity than those substituted with one halogen [191].

1.3.3.2. DTG

DTG is a tricyclic carbamoyl pyridine INSTI (**Figure 1-3**) [202]. It has potent antiretroviral activity with a protein-adjusted 90% inhibitory concentration (IC_{90}) of 64 ng/mL [203] and a high genetic barrier to drug resistance [204]. The robust potency and genetic barrier to resistance are attributed to its structural differences from the first-generation INSTIs. DTG is not affected by the Y143 pathway as it does not have an oxadiazole group [205]. Furthermore, in DTG, the linker bridging the halobenzyl and hydrophobic groups allows a deeper insertion and stable configuration position in the active site of integrase [206]. Therefore, DTG has a slower (5-40 times slower) dissociation rate from viral intasome than the first generation of INSTIs [207]. In clinical trials, DTG showed remarkable viral suppression and increased recovery of $CD4^+$ T cells from depletion in ART-naïve, ART-experienced HIV-infected adults and paediatric patients [208]. In 2013, DTG was approved by FDA to treat HIV-infected patients. According to WHO guidelines, DTG-based regimens are recommended as the first-line ART for HIV-infected adult and adolescent patients and have conditional recommendations for infants and children [209]. More recently, a dual combination of DTG and lamivudine (3TC) has shown non-inferior antiretroviral efficacy compared to three or more drug combination regimens [210-213]. In 2019, FDA

approved this combination of DTG and 3TC (DOVATO) for treating HIV-infected people.

However, rare treatment-emergent resistance to DTG has been reported [214-217]. The emergence of drug resistance could due to poor adherence and HIV disease factors, such as suboptimal levels of ARV in viral reservoirs. Poor adherence may be due to adverse effects or missed or delayed doses. Traditional combination ART involves three or more different classes of ARVs, leading to a higher incidence of adverse effects. Too frequent dosing could also lead to poor adherence. Therefore, some studies have been devoted to exploring long-acting formulations of ARVs. Sillman et al. developed an intramuscular (IM) administered long-acting slow-release system of DTG by an alkyl ester prodrug approach combined with an intramuscular (IM) nano-formulation [218]. Following the IM administration of nano-formulated myristoylated prodrug of DTG (NMDTG) to mice, the plasma concentration of released DTG was above PA-IC_{90} (64 ng/mL) for 56 days. Furthermore, NMDTG showed an extended protective effect against HIV-1 for at least 28 days in humanised mice. In non-human primates, IM administration of a single dose of NMDTG maintained the plasma concentration of released DTG above PA-IC_{90} for 35 days [219]. Deodhar et al. prepared nano-formulated myristoylated, stearoylated (M2DTG), behenoylated (M3DTG) prodrugs of DTG and a C18 carbon chain conjugated with two DTG on either side (M4DTG). These nanocrystal prodrugs were administered IM to rats and mice. M2DTG was found to maintain the plasma concentration of released DTG above PA-IC_{90} for 308 and 367 days in

rats and mice, respectively, suggesting an ultra-long antiretroviral activity for a yearly dose [220]. These injectable formulations of DTG have shown promising results in prolonging the dosing interval and facilitating adherence.

Current efforts to deliver antiretroviral drugs to lymph nodes are mainly through subcutaneous or IM injection of nano-formulated drugs or prodrugs [201, 218, 219, 221-223]. Although the nano-scale formulations are preferentially taken up by lymphatics rather than drained into blood vessels, only local lymph nodes near the injection sites can be targeted. Oral administration is the most preferred route for delivering ARVs to the central HIV reservoirs in MLNs and other deep lymphatic reservoirs, such as retroperitoneal lymph nodes. In addition, orally taking drugs with an extended dosing interval could have higher patient compliance as it is non-invasive and simple.

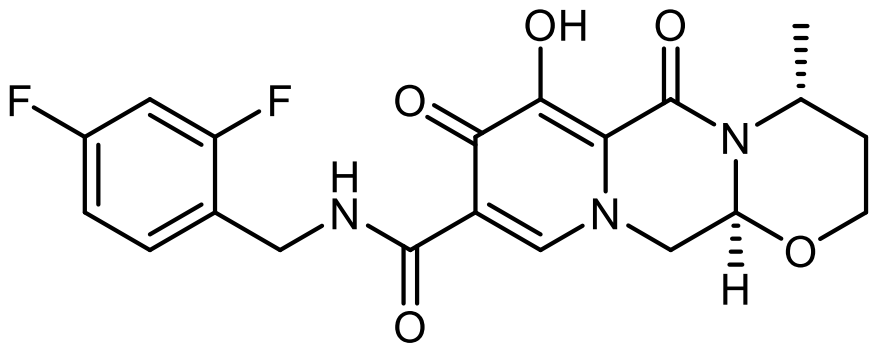

Figure 1-3. Structure of DTG.

1.4. Intestinal lymphatic transport for drug delivery

1.4.1. Prerequisites of intestinal lymphatic transport of orally administered drugs

Charman et al. proposed two critical factors for substantial intestinal lymphatic transport of orally administered drugs: long-chain triglyceride (LCT) solubility greater than 50 mg/mL [224] and the partition coefficient (Log P) more than 4.7 [224, 225]. These criteria successfully predicted intestinal lymphatic transport in some cases when drugs were co-administered with lipids or in the presence of food [226]. For example, dichlorodiphenyltrichloroethane (DDT) possesses the required physicochemical properties (log P 6.19 and LCT solubility at 97.5 mg/mL). The intestinal lymphatic system transported 33% of the DDT dose following co-administration with peanut oil to rats [224]. Halofantrine (log P 8.5 and LCT solubility >200 mg/mL) had 20% of the administered dose recovered in the intestinal lymph when administered in a micellar system to rats [227]. However, the threshold of LCT solubility above 50 mg/mL for intestinal lymphatic transport has been challenged. Several studies demonstrated that some compounds do not meet this threshold but have intestinal lymphatic transport [228, 229]. In this work, TPV has appropriate experimental log P at 6.9, but low LCT solubility (5.9 ± 0.3 mg/mL). DTG is a non-lipophilic compound (experimental log P 2.2) and limited LCT solubility (0.015 ± 0.002 mg/mL). Both TPV and DTG seem not to meet the prerequisite of intestinal lymphatic transport when administered orally.

1.4.2. Lipid digestion and absorption in the intestine

Intestinal lymphatic transport is an alternative absorption route for highly lipophilic molecules, dietary lipids, lipid-soluble vitamins and xenobiotics in the GI tract [230]. In contrast to portal vein absorption, intestinal lymphatic transport avoids hepatic first-pass metabolism. Furthermore, it exploits the inherent lipid digestion process to deliver drugs to systemic blood through lymphatic circulation. Lipids digestion takes place in the stomach and small intestine with the contributions of a number of enzymes. The first digestive event is carried out by gastric lipase in the stomach. Gastric lipases partially hydrolyse dietary triglyceride (TG) (10-30%), releasing free fatty acids and diacylglycerides [231]. Digested products and undigested lipids are then transferred to the duodenum for further digestion. At the same time, digested products stimulate the secretion of bile salts and pancreatic lipases, which are essential enzymes for lipids digestion. Bile salts emulsify lipids into droplets, and pancreatic lipases digest TG at 1- and 3- positions to release two free fatty acids and a 2-monoglyceride [232, 233]. These digested products are merged into amphiphilic micelles, which will diffuse across the unstirred water layer to the border of enterocytes. Micelles and lipidic substances accumulate near the apical membrane of enterocytes [234]. The concentration gradient drives the passive diffusion of these lipidic materials from the intestinal lumen into enterocytes. In enterocytes, short- and medium-chain fatty acids ($C < 12$) are drained by portal blood flow, while long-chain fatty acids ($C \geq 12$) are re-synthesised to TG in the

endoplasmic reticulum [235]. TGs assemble with cholesterol, cholesterol ester, phospholipids and apolipoproteins to form chylomicrons (CM).

1.4.3. The role of CM in the intestinal lymphatic transport of highly lipophilic drugs

CM are the largest lipoproteins with the lowest density compared to other lipoproteins and responsible for transporting dietary lipids from the enterocytes to the systemic circulation through the lymphatic system. They are produced in enterocytes and then secreted into the intestinal lymphatic system. In the lymphatic lacteal, CM joins the lymph draining from the GI system to form chyle, which will flow into MLNs. The chyle then leaves the MLNs and enters the systemic circulation *via* the thoracic duct at the junction of the left jugular and subclavian veins [236]. Highly lipophilic drugs are believed to be incorporated into the TG-rich core during or after the CM assembly. Drug-CM is then transported through the intestinal lymphatic system [237]. Some studies suggest that lipophilic drugs could also interact with surface components of the CM rather than being incorporated into the TG-rich core [228, 238, 239]. The detailed mechanisms of drug association with CM remain unclear.

The intestinal lymphatic transport of highly lipophilic drugs shares the same pathway as the absorption of dietary lipids. It has been reported that the association of drug molecules with CM is critical in determining the extent of drug absorption through the intestinal lymphatic system [224, 237]. Since LCT is the main component of the core of CM, it is reasonable to expect that drugs with high LCT solubility can substantially associate

with CM. However, Gershkovich and Hoffman demonstrated that LCT solubility was only moderately correlated with the degree of association of lipophilic compounds with CM (R^2 = 0.55) and lymphatic bioavailability in rats (R^2 = 0.55) [237]. Instead, they found that the degree of association of lipophilic compounds with CM strongly correlates with intestinal lymphatic transport in rats (R^2 = 0.94). In a subsequent study, Log $D_{7.4}$, rather than Log P, was determined as the most important physicochemical property affecting drug affinity to CM [238]. Other physicochemical properties of drugs, including the degree of ionisation (Log P – Log $D_{7.4}$), polar surface area, number of H-acceptors and H-donors, density, molar volume, and freely rotatable bonds, were also found to impact the affinity to CM. Thus, an *in silico* model was established based on these physicochemical properties to predict the association of drug molecules with CM for assessing the potential of intestinal lymphatic transport.

1.4.4. Approaches for intestinal lymphatic transport of orally administered drugs

Intestinal lymphatic transport and targeting could benefit many diseases, including gastrointestinal cancer, autoimmune diseases and HIV infection. However, this pathway is not feasible for most drugs without chemical modification. Not all drugs possess the required physicochemical properties to associate with CM, a critical step during the process [237]. Furthermore, although highly lipophilic drugs usually have a high affinity to CM, limited water solubility could restrict their

absorption in the intestine. Therefore, drug delivery approaches, including lipid-based formulations and lipophilic ester prodrug systems, have been proposed to overcome these obstacles and enhance intestinal lymphatic transport and targeting of orally administered drugs.

1.4.4.1. Lipid-based formulation

Oral administration of drugs with a high-fat meal was reported to increase oral bioavailability [182, 240-242]. This could be attributed to the post-prandial effects caused by dietary lipids, especially LCT, promoting intestinal lymphatic transport and portal absorption of administered drugs. The post-prandial effects include prolonging gastric emptying time, stimulating the secretion of bile salts and pancreases, increasing contact of drugs with enterocyte membrane, changing the luminal environment to improve drugs dissolution and solubilisation, and facilitating the CM production [237, 243-248]. Lipid-based formulations have been profoundly used to improve the luminal solubility and intestinal lymphatic bioavailability of lipophilic drugs [230, 249]. Based on a lipid formulation classification system, lipid formulations are classified into four types [250]. Briefly, type 1 formulation is pure lipids or oils; type 2 formulation contains oils and water-insoluble surfactants; type 3 formulation has oils, surfactants and cosolvents; and type 4 formulation is oil-free but contains water-soluble surfactants and cosolvents. This PhD work has chosen a type 1 formulation containing LCT as our administration vehicle. LCT-containing formulations have been used extensively to facilitate the

intestinal lymphatic transport of highly lipophilic drugs or prodrugs by our and other groups [229, 239, 251-261].

1.4.4.2. Lipophilic ester prodrug system

Although LCT-based formulations can facilitate intestinal lymphatic transport, it is only feasible for highly lipophilic drugs with high LCT solubility and substantial affinity to CM. Non-lipophilic compounds are primarily absorbed through the portal vein rather than the intestinal lymphatic system after oral administration, as they are unlikely to associate with CM [237, 238]. Furthermore, the flow rate of intestinal capillary blood is 500-fold faster than intestinal lymph, which results in the preferred portal absorption route for most non-lipophilic drugs [262]. Therefore, chemical modifications are needed to improve the association of non-lipophilic drugs with CM and promote their targeting of the intestinal lymphatic system. Lipid moieties, including fatty acid, glyceride, and phosphoglyceride, are commonly used to synthesise lipophilic ester or amide prodrugs for improved oral bioavailability and intestinal lymphatic transport [229, 253, 256, 263-278]. These lipid moieties have similar characterisations to natural lipids and can take benefits from the physiological lipid digestion process, allowing drugs to be targeted to specific active sites [279].

TG-mimic prodrugs are designed based on the TG absorption mechanism described in section **1.4.2**. The parent drug is placed at the 2-position of the TG structure. When the pancreatic lipase hydrolysis takes place at the 1- and 3-positions of the drug-conjugated TG, the

parent drug will remain at the 2-position of the glycerol backbone. Drug-glycerol is re-esterified with long-chain fatty acids to TG in enterocytes, which will then be incorporated into CM for intestinal lymphatic transport [230]. On the other hand, fatty acid prodrugs can optimise parent drugs' physicochemical properties to increase the affinity to CM and subsequent intestinal lymphatic absorption. The lymphatically-absorbed prodrugs will release the parent drugs through the enzymatic cleavage in the lymph or plasma.

Esterifying drugs with lipophilic moieties can generate lipophilic ester prodrugs. Based on the conjugated moiety, there are different types of ester prodrugs, including simple alkyl esters, activated esters, and biomimetic lipid esters. Elz et al. have proposed that the triglyceride-mimetic prodrug approach is the core prodrug technology and is superior to simple alkyl esters [275]. They stated that simple alkyl esters are vulnerable to presystemic metabolism. Furthermore, the extent of intestinal lymphatic transport of simple alkyl esters relies on passive uptake by CM, while bio-mimetic prodrugs, such as TG-mimetic prodrugs, are designed to participate in lipid digestion actively. Han et al. compared the intestinal lymphatic transport of the alkyl ester prodrug and TG-mimetic prodrug of mycophenolic acid (MPA), an immunomodulatory agent, in rats [277]. Although the alkyl ester has improved the intestinal lymphatic transport of MPA 13-fold, the TG-mimetic prodrug showed a more promising result with a 90-fold increase in MPA transport through the intestinal lymphatic system. Hu et al. chemically modified testosterone by linking a monoglyceride moiety with a self-immolation

group [276]. The glyceride prodrug of testosterone increased systemic exposure up to 90-fold compared to the currently marketed product testosterone undecanoate (a simple alkyl ester) in rats. Another biomimetic prodrug approach is phospholipid-mimetic prodrugs. Dahan et al. investigated the oral absorption of a phospholipid prodrug of valproic acid [253]. After oral administration with LCT solution, intestinal lymphatic transport of the phospholipid prodrug of valproic acid contributed to 60% of oral bioavailability.

Our group has previously successfully achieved mesenteric lymphatic targeting of drugs with low or negligible affinity to CM using a simple alkyl or activated ester prodrug approach combined with an LCT-based formulation approach [229, 256]. Lee et al. attempted to target an anticancer drug, bexarotene, with lipophilic esters, including simple alkyl esters, a TG-mimetic ester, and activated esters [256]. Although TG-mimetic ester had a higher affinity to CM than the simple alkyl ester, it did not lead to substantial levels of parent drug bexarotene in MLNs and mesenteric lymph following oral administration in LCT formulation to rats. In contrast, the simple alkyl ester of bexarotene was delivered to mesenteric lymph but did not efficiently release bexarotene in the mesenteric lymphatic system. The activated ester of bexarotene showed significant lymphatic transport and more efficient release of parent drug in the MLNs compared to the TG-mimetic and simple alkyl ester prodrugs. To note, the activated ester approach is to insert a heteroatom (O or S) at the beta or gamma position of the acyl moiety to increase the sensitivity of the carboxyl esters to the action of the plasma and lymph

carboxylesterase [280]. The concentrations of bexarotene in the MLNs following oral administration of simple alkyl ester, TG-mimetic ester, and activated ester were increased by 6.4-, 6.7-, and 17-fold, respectively, compared to oral administration of unmodified bexarotene. Qin et al. have utilised a simple alkyl and activated ester prodrug approach to target lopinavir (LPV) to mesenteric lymphatics [229]. LPV is an HIV PI with no affinity to CM, requiring chemical modification to associate with CM for intestinal lymphatic transport. Although the alkyl ester prodrug of LPV has substantial intestinal lymphatic transport, it did not efficiently release the parent drug LPV in the lymph, MLNs, and plasma. Therefore, an activated ester prodrug was then introduced. Oral administration of the activated ester prodrug in LCT formulation increased the levels of released LPV in the mesenteric lymph and MLNs 10.3-fold and 6.8-fold, respectively, compared to the simple alkyl ester prodrug. In these cases, the activated esters approach seems to outperform the simple alkyl esters and the TG-mimetic esters in mesenteric lymphatic targeting.

1.5. Hypothesis and aims

Although ART brings HIV patients back to near-normal life, adherence and adverse effects remain important limitations. Furthermore, latent HIV reservoirs expose patients to rebound viremia risk when interrupted by antiretroviral treatment. Poor penetration of ARVs to HIV reservoirs is believed to be one of the main barriers to achieving a cure. MLNs are the largest lymphoid aggregates throughout the body. Many immune $CD4^+$ T cells are housed in this anatomical compartment. However, MLNs are a hard-to-penetrate reservoir for ARVs. Therefore, it is an ideal sanctuary for HIV and an important target for the delivery of ARVs. Intestinal lymphatic transport is a pathway which could overcome the pharmacokinetic barrier and deliver highly lipophilic drugs or prodrugs to MLNs. This PhD hypothesises that the LCT-based formulations approach alone or combined with the lipophilic ester prodrug approach could achieve high levels of highly lipophilic drugs or prodrugs in HIV reservoirs in MLNs.

In this study, two antiretroviral agents, TPV and DTG, are selected as model drugs. TPV is a lipophilic drug that has a moderate association with CM, while DTG is a hydrophilic drug with a negligible affinity to CM. In view of the different physicochemical properties between TPV and DTG, this study was conducted by two different approaches:

1. Targeting of lipophilic drug TPV to MLNs by means of intestinal lymphatic transport using an LCT-based formulation approach.

2. Design and synthesis of lipophilic ester prodrugs of hydrophilic drug DTG to increase the affinity to CM, followed by co-formulating with LCT-based formulation to target DTG to MLNs by means of intestinal lymphatic transport.

The specific objectives of this work are described as follows:

Chapter 3.

1. Screening of drug candidates by *in silico* prediction of the association of HIV PIs with CM.
2. *In vitro* and *ex vivo* assessments of TPV for its intestinal lymphatic transport potential by experimental association assay with artificial and natural CM.
3. *In vivo* pharmacokinetics assessment of TPV in rats.
4. *In vivo* biodistribution assessment of TPV in mesenteric lymph and MLNs in rats.

Chapter 4.

1. Design of lipophilic ester prodrugs of DTG based on *in silico* prediction of drug-CM association.
2. Chemical synthesis and characterisation of designed prodrug candidates.
3. *In vitro* and *ex vivo* assessments of synthesised prodrugs for their intestinal lymphatic transport potential by experimental association assay with artificial and natural CM.

4. Evaluation of the stability and biotransformation of prodrugs to DTG in bio-relevant media.
5. Assessment of the solubility of prodrugs in LCT (sesame and olive oils).
6. *In vivo* pharmacokinetics assessment of DTG and its prodrug candidate in rats.
7. *In vivo* biodistribution assessment of DTG and its prodrug candidate in mesenteric lymph, MLNs and other HIV reservoirs in rats.
8. *In vitro* lipolysis of DTG prodrug candidate.

2. MATERIALS AND METHODS

2.1. Materials

Tipranavir (TPV) was extracted from Aptivus® soft capsules (250 mg of TPV, Boehringer Ingelheim GmbH, Germany) as described below in section **2.2.1**. Dolutegravir (DTG) sodium (CAS: 1051375-19-9) was purchased from Chemshuttle (California, USA). Cannabidiol (CBD, >98%, CAS: 13956-29-1) was purchased from THC Pharm GmbH (Frankfurt, Germany). Acyl chloride (lauroyl chloride, myristoyl chloride, palmitoyl chloride, stearoyl chloride and oleoyl chloride), methanol-*d*4, DMSO-d_6, Intralipid®, Dulbecco's phosphate buffered saline (DPBS), propylene glycol, serum triglyceride determination kit, esterase from porcine liver crude, porcine pancreatin powder (8 × USP specifications), tris maleate, potassium bromide, phosphate-buffered saline tablets (PBS, P4417-100TAB), ethylenediaminetetraacetic acid (EDTA), sodium chloride (NaCl), sodium hydroxide (NaOH) pellet, sodium fluoride (NaF), anhydrous N,N-dimethylformamide (DMF), sesame oil and olive oil were all purchased from Merck Life Science (Gillingham, UK). Calcium chloride ($CaCl_2$) was purchased from Alfa Aesar (Lancashire, UK). Linoleoyl chloride was bought from Tokyo Chemical Industry (Oxford, UK). Sodium taurocholate hydrate (NaTc), L-alpha-phosphatidylcholine from egg yolk, sodium phosphate monobasic (NaH_2PO_4) were purchased from Scientific Laboratory Supplies (Nottingham, UK). Costar Spin-X centrifuge tube filters, HPLC grade methyl tertiary butyl ether (MTBE), ethyl acetate, n-hexane, acetonitrile (ACN), ammonium acetate, ammonium formate crystal and formic acid were purchased from Fisher

Scientific (Leicestershire, UK). Polyethylene glycol 400 (PEG-400) was bought from VWR international LTD (Leicestershire, UK). Rat plasma (pooled male Sprague Dawley rat plasma, K3EDTA), dog plasma (pooled male Beagle plasma, K3EDTA) and mouse plasma (pooled male CD-1 (ICR) mouse plasma, K3EDTA) were bought from Sera Laboratories International Ltd (West Sussex, UK). HPLC-grade water was obtained from PURELAB® ultra system (ELGA LabWater, UK). Other experiment agents and solvents were obtained from commercial sources with HPLC grade or higher level.

2.2. Chemistry methods

2.2.1. Extraction of TPV

An Aptivus® soft capsule (containing 250 mg of TPV) was dispersed in 5 mL of warm water at 37°C. Liquid-liquid extraction was then performed 3 times using 20 mL of dichloromethane. The pooled organic fractions were washed with brine (30 mL) and dried with anhydrous Na_2SO_4, and then filtered. The crude product was purified by column chromatography using ISOLUTE SPE columns (Flash Silica II 5g/25mL) (Biotage, Hengoed, UK) and monitored by thin layer chromatography (TLC) plate and liquid chromatograph-tandem mass spectrometry (LC-MS/MS). The purified eluents were pooled and evaporated .The final product (10 mg) was dissolved in methanol-*d*4 for NMR characterization. The details of chemical characterization methodologies of purified TPV is described in section **2.2.3**. The full characterization of extract and purified TPV can be

found in **Appendix 1.** Characterization of tipranavir extracted from Aptivus® soft capsules.

2.2.2. The design and synthesis of ester prodrugs of DTG

The prodrugs of DTG were designed by substituting the 7-hydroxyl group with different carbon-length fatty acids to generate alkyl esters with increased lipophilicity, and improved predicted association with chylomicrons (CM). An established multiple physiochemical properties-based *in silico* model (described in section **2.3.1**) was used to predict the association of compounds with CM [281]. Prodrugs with moderate to high predicted affinity to CM (> 20%) were selected as drug candidates for synthesis and taken forward to subsequent studies. The esterification of DTG was based on a previously reported methodology with slight modifications [218]. Briefly, the corresponding fatty acid acyl chloride (4.4 mmol) was mixed with DTG sodium (1.1 mmol) in anhydrous DMF (3mL) and stirred under N_2 at 0°C overnight. The product formation was monitored by wither TLC plate and/or LC-MS/MS. After complete conversion, the mixture was filtered and purified by reverse phase chromatography (PuriFlash® PuriFlash 4100, Interchim Inc, CA, US) using a 50 µm particle size C18 column (IR-50C18-F0012, Interchim Inc, CA, US) with a gradient of acetonitrile/water from 50:50 to 90:10 (**Table 2-1)**. The collected fractions, containing the pure product were pooled and evaporated. A sample of the final compound (10 mg) was dissolved in DMSO-d_6 for NMR characterization. The details of chemical

characterisation methodologies of purified compounds are described in section **2.2.3**. The schematic presentation of general synthesis principles and all synthesised prodrugs structures are shown in **Figure 2-1**.

.

Table 2-1. Reverse phase gradient program.

Reverse phase gradient program [a]		
Column volume (CV) [b]	**Solvent A [c] (%)**	**Solvent B [d] (%)**
Pre-equilibration (3 CV)	**50**	**50**
0	**50**	**50**
3	**90**	**10**
30	**90**	**10**

[a] Flow rate: 20 mL/min
[b] Column volume: 19 mL
[c] Solvent A: acetonitrile
[d] Solvent B: water

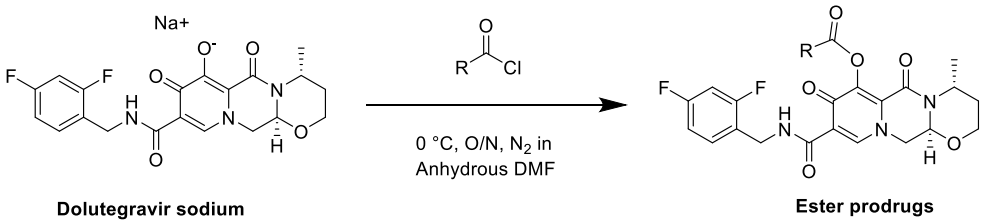

Dolutegravir sodium **Ester prodrugs**

Ester prodrugs

1: R = $(CH_2)_{10}CH_3$, MW = 601.68

2: R = $(CH_2)_{12}CH_3$, MW = 629.73

3: R = $(CH_2)_{14}CH_3$, MW = 657.79

4: R = $(CH_2)_{16}CH_3$, MW = 685.84

5: R = $(CH_2)_7CH{=}CH(CH_2)_7CH_3$, MW = 683.82

6: R = $(CH_2)_7CH{=}CHCH_2CH{=}CH(CH_2)_4CH_3$, MW = 681.81

Figure 2-1. Chemical synthesis and structures of DTG and its ester prodrugs.

2.2.3. Characterisation of compounds

The following methodologies were used to characterise compounds described in **Chapter 3** and **4**. TLC was performed for monitoring compounds by using silica gel 60 Å F254 plates (Merck, Darmstadt, Germany). The LC-MS/MS system used for monitoring compounds consisting of a Shimadzu UFLCXR module equipped with an Applied Biosystems API 2000. An analytical C18 Gemini-NX column (50 mm × 2 mm I.D.) with a particle size of 3 µm (Phenomenex, Macclesfield, UK) was used at 40°C to accomplish separations. All compounds were monitored at UV wavelength 220 nm (channel 2) and 254 nm (channel 1) using short and long gradient programs (**Table 2-2**). ^{1}H and ^{13}C NMR spectra were obtained using Bruker 400 Ultrashield Spectrometry at 400 and 100 MHz, respectively, at ambient temperature. Chemical shifts (δ) are reported as parts per million (ppm) relative to methanol-d_4 (^{1}H, δ = 3.31 ppm; ^{13}C, δ = 49.00 ppm) for purified TPV described in **Chapter 3** and DMSO-d_6 (H, δ = 2.50 ppm; ^{13}C, δ = 39.52 ppm) for DTG and synthesised prodrugs described in **Chapter 4** [282]. ^{1}H NMR results were presented as follows: chemical shift, integration, multiplicity (s = singlet, d = doublet, t = triplet, q = quartet, p = pentet, m = multiplet) and coupling constants (*J*) were recorded in Hz. TopSpin 4.0.8 software was used to process the spectra. High-resolution mass spectrometry was performed for further characterisation of purified products using a Bruker MicroTOF II with electrospray (ESI). Reagents and solvents were purchased from Merck Life Science (Gillingham, UK), Tokyo Chemical Industry (Oxford, UK) and Fisher Scientific (Leicestershire, UK).

Table 2-2. Short- and long-gradient programs of LC-MS/MS.

Short-gradient program[$]			Long-gradient program[$]		
Time (min)	**Solvent A[*] (%)**	**Solvent B[&] (%)**	**Time (min)**	**Solvent A[*] (%)**	**Solvent B[&] (%)**
Pre-equilibration (1 min)	**95**	**5**	**Pre-equilibration (1.5 minutes)**	**95**	**5**
0	**95**	**5**	**0**	**95**	**5**
2	**2**	**98**	**8**	**2**	**98**
4	**2**	**98**	**10**	**2**	**98**
4.5	**95**	**5**	**10.5**	**95**	**5**
5.5	**95**	**5**	**11.5**	**95**	**5**

[*] Solvent A: 0.1% formic acid in water
[&] Solvent B: 0.1% formic acid in acetonitrile
[$] Flow rate: 0.5 mL/min

2.3. Association with artificial CM-like emulsion and plasma-derived CM

2.3.1. *In silico* model for the prediction of the association with CM

A previously established physicochemical properties-based computational model [281] was used to screen the potential affinity of protease inhibitors (PIs) (**Chapter 3**) and DTG and its prodrugs (**Chapter 4**) to CM. All physicochemical properties (**Table 2-3**) of analysed compounds used in *in silico* model were calculated using ACD/I-Lab (Advanced Chemistry Development Inc., Toronto, ON, Canada).

Table 2-3. Physiochemical properties used in *in silico* model [281].

Parameter
Log $D_{7.4}$
Log P – Log $D_{7.4}$
polar surface area
H-acceptors
H-donors
Density
Molar volume
Freely rotatable bonds

2.3.2. Preparation of protein-free artificial CM-like emulsion (Intralipid®)

Intralipid® 20% (Merck Life Science, Gillingham, UK) was measured for triglyceride (TG) concentration by a TG enzymatic kit (Sigma Aldrich, Dorset, UK) based on manufacturer's instructions utilising a plate reader (BIO-TEK FL600™, BIO-TEK INSTRUMENTS, INC. Vermont, USA). Dulbecco's phosphate buffered saline (DPBS) was then used to dilute

Intralipid® to generate a 1 mg/mL concentration of TG emulsion as previously described [229, 254, 281].

2.3.3. Isolation of human plasma-derived CM

The following protocol was used to generate the CM association results described in **Chapter 3**.

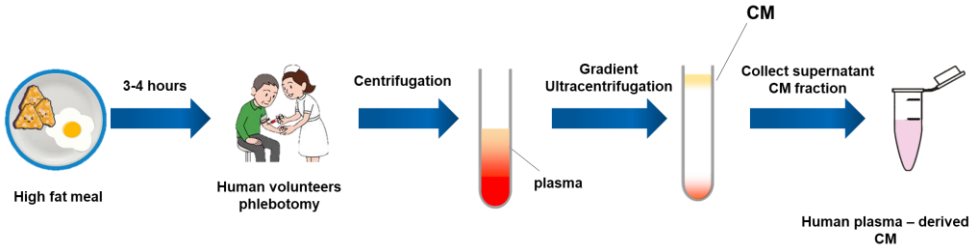

Figure 2-2. Isolation of human plasma-derived CM.

The protocol for isolation of human plasma-derived CM emulsion was approved by the Faculty of Medicine and Health Sciences Research Ethics Committee, Queens Medical Centre, Nottingham University Hospitals (Ethics reference number: BT12102015). The isolation of human plasma-derived CM was performed as previously described [229, 254, 256] (**Figure 2-2**). Healthy male volunteers between the age of 28–33 years old and body mass index (BMI) of 18.5–25.0 were enrolled in the study. Participants receiving prescribed or over-the-counter medicines within 1 week before the study were excluded from the enrolment. On the day of the study, high-fat meal (equivalent to full English breakfast) was provided to volunteers. Within the interval of 3 to 4 h following the meal, 50 mL of blood was withdrawn using K2-EDTA tubes (Vacutainer® Blood Collection Tubes, Fischer Scientific, Loughborough, UK), and plasma was obtained by centrifugation (1,160

g, 15°C, 10 minutes). CM isolation was performed based on the previous reports [254, 256, 283]. Briefly, 4 mL of plasma was mixed with 0.57 g potassium bromide (KBr) to achieve a density of 1.1 mg/mL. A density gradient was built on the top of the plasma layer with densities of 1.006 (2mL), 1.019 (2 mL) and 1.063 (2.5 mL) g/mL in a polyallomer ultracentrifuge tube using a 3 mL syringe with bent needle (23G × 1 in.). The samples were then ultracentrifuged (SORVALL Discovery 100SE; TH-641 rotor, 268,350 *g*, 15°C, 35 minutes). The upper layers containing CM fractions were collected into 1.5 mL Eppendorf tubes using glass Pasteur pipettes. TG concentration of collected CM emulsion concentration was determined by the TG enzyme kit and diluted with DPBS to generate TG concentration of 1 mg/mL. The human plasma-derived CM emulsion was kept in 4°C for up to 24 h until the association assay.

2.3.4. Production of rat plasma-derived CM

The following protocol was used to generate the CM association results described in **Chapter 4**.

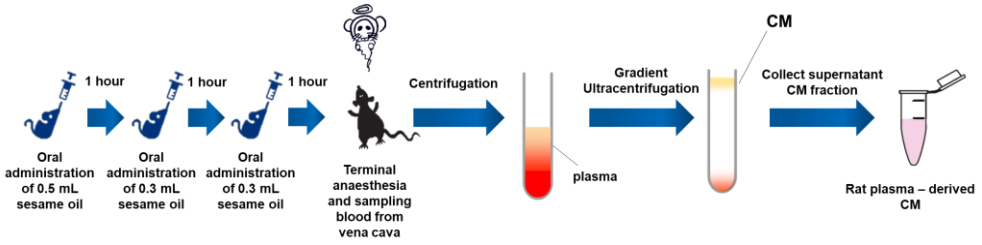

Figure 2-3. Isolation of rat plasma-derived CM.

The protocol for isolation of rat plasma-derived CM emulsion was approved by the Home Office in accordance with the Animals [Scientific

Procedures] Act 1986. Male Sprague Dawley rats (Charles River Laboratories, UK) weighing 275-300 g were used in this experiment. The rats were housed in Bio Support Unit, University of Nottingham in a controlled-temperature environment with 12 h light/dark cycles and were allowed free access to food and water. Rat plasma-derived CM were separated as previously described with slight modifications [254] (**Figure 2-3**). Rats were fasted with free access to water overnight prior to the experiment. On the day of the study, rats were orally administered with 0.5 mL of sesame oil. Two additional doses of 0.3 mL of sesame oil were given at each one-hour interval following the first dose. One hour after the last dose, rats were anaesthetized (terminal anaesthesia) with 2.5% isoflurane and 10 mL of blood was withdrawn from vena cava. Plasma was obtained by centrifugation (1,160 *g*, 15°C, 10 minutes). CM isolation was performed as described in section **2.3.3**. The collected rat plasma-derived CM emulsion was measured for TG concentration and diluted to 1 mg/mL with DPBS. The rat plasma-derived CM were kept in 4°C for up to 24 hours until the association assay.

2.3.5. CM association assay

The following protocol was used to generate the CM association results described in **Chapter 3** and **4**.

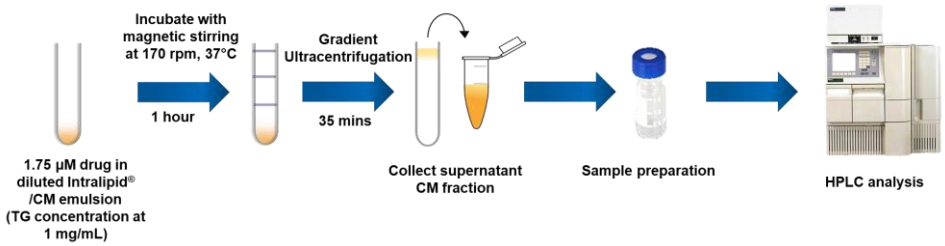

Figure 2-4. Chylomicron association assay.

The experiments for the uptake of tested compounds by the artificial CM-like emulsion and natural CM were based on previously described methodology with minor modifications [229, 254, 256, 283] (**Figure 2-4**). The stock solutions of tested compounds were prepared in a mixture of propylene glycol-ethanol (99:1, *v*/*v*) (**Chapter 3**) or 100% DMSO or propylene glycol-ethanol (97:3, *v*/*v*) (**Chapter 4**) at the concentration of 0.1 mg/mL. Stock solutions were spiked into 2 mL (**Chapter 3**) or 1 mL (**Chapter 4**) of artificial or natural CM emulsions (1 mg/mL of TG) to generate the final concentration of 1.75 µM of tested compounds in the experimental media. The emulsions were then incubated at 37°C with magnetic stirring at 170 rpm for 1 hour. Following the incubation, the experimental emulsion was transferred to a polyallomer ultracentrifuge tube and the density was adjusted to 1.1 g/mL by adding an appropriate amount of KBr. The density gradient was then built by layering the density solutions at volumes as described in **Table 2-4**. After the density gradient was built, the samples were ultracentrifuged at 268,350 *g* for 35 minutes at 15°C (SORVALL® TH-641 rotor, Thermo Fisher Scientific, UK), and the supernatant CM fraction was collected and processed for HPLC analysis.

Table 2-4. The volume of density solutions loaded into 1 mL and 2 mL of incubation media.

Density solution (g/mL)	Loading volume (mL)	
	1mL incubation media	2mL incubation media
1.006	2	2
1.019	4	2.5
1.063	4	3

2.4. Stability of DTG and its release from prodrugs in biorelevant conditions

The following protocol was used to generate the stability and biotransformation results described in **Chapter 4**. The stability of DTG and its release from the prodrugs were assessed in plasma (mimicking the environment of mesenteric lymph), fasted state simulated gastric fluid (FaSSGF, pH = 3.9 [284]) with pepsin (0.1 mg/mL) [285] and fasted state simulated intestinal fluid (FaSSIF, pH = 6.5) with added esterase enzyme (20 IU/mL) [229, 256]. FaSSGF and FaSSIF were prepared as described in **Table 2-5** and **Table 2-6**, respectively [285, 286]. The media was pre-heated at 37°C for 5 minutes. The stability/biotransformation assay was initiated by spiking stock solution of tested compounds into media to generate a final concentration at 10 µM or in cases of poor solubility, 5 µM. The reaction mixtures were incubated at 37°C and shaken at 200 rpm on a thermo-controlled orbital incubator (Thermo Scientific MaxQ4000, Waltham, MA, USA) for up to 2 hours. A hundred microliter of incubation media was sampled at pre-determined time points and immediately spiked into 300 µL cooled acetonitrile to terminate the reaction. The samples were analysed for the levels of DTG and prodrugs

concentrations by means of HPLC as described in section **2.8.2.2**. All experiments were performed in triplicates.

Table 2-5. The preparation of FaSSGF [285].

FaSSGF* (500 mL)		
Content	Concentration	To 500 mL
NaTc	80 uM	21.5 mg
Lecithin	20 uM	7.6 mg
NaCl	34.2 mM	1000.0 mg
Pepsin	0.1mg/mL	just before the study
* Adjust pH to 3.9 by titrating 0.1M HCl		

Table 2-6. The preparation of FaSSIF [286].

FaSSIF* (500 mL)		
Content	Concentration (mM)	To 500 mL DDW (g)
NaTc	3 mM	0.807 g
Lecithin	0.75 mM	0.286 g
NaOH (pellets)	8.7 mM	0.174 g
NaH2PO4	28.65 mM	1.977 g
NaCl	105.9 mM	3.093 g
Esterase	20 IU/mL	just before the study
* Adjust pH to 6.5 by titrating 0.1M NaOH		

2.5. Long-chain triglyceride (LCT) solubility

The following protocol was used to generate the LCT solubility results described in **Chapter 3** and **4**. The LCT solubilities of tested compounds were assessed by adding excessive amount of compounds (more than 5 mg) to sesame oil (**Chapter 3** and **4)** or olive oil (**Chapter 4**) (100 µL) and stirring using a magnetic stirrer at 37°C for 72 h. Following the incubation, the mixture was spin-filtered using Costar Spin-X centrifuge tube (Fisher Scientific, Loughborough, UK) at 2,400 *g* for 20 minutes. The filtrates were firstly diluted 10-fold with acetone, then further diluted 10-fold with ethanol, followed by a 100-fold dilution with acetonitrile. The diluted samples were analysed for compounds concentrations by means of HPLC. All measurements were performed in triplicates for each tested compound.

2.6. *In vitro* lipolysis

2.6.1. Preparation of pancreatic lipase/colipase

Fasted state incomplete digestion buffer was prepared by dissolving Tris maleate (50mM), NaCl (150mM) and $CaCl_2$ (5mM) in water and adjusting to pH 6.8 at 37°C using a pH-stat titrator (T50 Graphix, Mettler Toledo Inc,). Porcine pancreatin powder was stir-mixed with incomplete digestion buffer (1:5, *w/v*) for 15 minutes at room temperature. The mixture was centrifuged at 1600 *g*, 5°C for 15 minutes. The supernatant containing pancreatin extract was collected and placed on the ice for lipolysis assay.

2.6.2.*In vitro* lipolysis

The following protocol was used to generate the lipolysis results described in **Chapter 4**. Fasted state complete digestion buffer was prepared by adding sodium taurocholate (5mM) and L-α-phosphatidylcholine (1.25mM) into incomplete digestion buffer and adjusting pH to 6.8 at 37°C using the pH-stat titrator. The lipolysis model used in this study was based on previously described methodology with minor modifications [257, 260, 287, 288]. A reaction vessel containing 35.5 mL complete digestion buffer was attached to the pH-stat titrator and pre-warmed to 37°C. Tested formulations were freshly prepared by dissolving tested compounds in fresh LCT vehicle (sesame oil) at the concentration of 8.15 mg/mL (prodrug 5) and 8.13 mg/mL (prodrug 6), respectively. Eighty microliter of tested formulations was incubated with pre-warmed complete digestion buffer at 37°C and stirred for 15 minutes, following by addition of 3.5 mL pancreatin extract to initiate the lipolysis reaction. Sodium hydroxide solution (1M) was used as the titrant to maintain the pH of experimental medium at 6.8 throughout the whole reaction. The termination of lipolysis was determined by a titration rate of 1M NaOH falling below 3 µL/min. After the lipolysis reaction was completed, the mixture was transferred to a polyallomer ultracentrifuge tube and ultracentrifuged at 268,350 *g* (SORVALL® TH-641 rotor, Thermo Fisher Scientific, UK) for 90 minutes at 37°C. The supernatant lipid fraction, middle micellar fraction and sediment were kept in -80°C until analysis by means of HPLC.

2.7. Animal studies

2.7.1. Animals

The protocols for pharmacokinetics and biodistribution experiments in this study were reviewed and approved by the University of Nottingham Ethical Committee in accordance with the Animals [Scientific Procedures] Act 1986. Male Sprague Dawley rats (Charles River Laboratories, UK) weighing 275–300 g were housed in Bio Support Unit, University of Nottingham in a controlled-temperature environment with 12 h light/dark cycles and were allowed free access to food and water.

2.7.2. Preparation of formulations

2.7.2.1. Formulations of TPV

The following protocol was used to prepare formulations for the pharmacokinetics and biodistribution studies described in **Chapter 3**. Lipid-free solution formulations for intravenous (IV) bolus and oral gavage administration were prepared by dissolving TPV in propylene glycol/sterile water/ethanol (70:20:10, *v*/*v*/*v*) vehicle to achieve concentrations at 1 mg/mL and 5 mg/mL, respectively. For oral LCT-based formulation, TPV was dissolved in sesame oil at a concentration of 5 mg/mL. The vials containing the LCT-based formulation were filled with nitrogen and protected from light and air to avoid oxidation of the sesame oil. The orally administered dose of lipids to rats was 1 mL/kg.

2.7.2.2. Formulations of DTG and prodrugs

The following protocol was used to prepare formulations for the pharmacokinetics and biodistribution studies described in **Chapter 4**. Sodium salt form of DTG was used in pharmacokinetics and biodistribution studies. The administration doses of IV and oral groups were 1.05 mg/kg and 5.25 mg/kg of DTG sodium (equivalent to 1 mg/kg and 5 mg/kg of DTG, respectively). Lipid-free formulations for IV and oral gavage administration were prepared by dissolving DTG sodium in a mixture of polyethylene glycol 400 (PEG 400)/non pyrogenic water/ethanol (70:20:10, *v*/*v*/*v*) to achieve concentrations at 1.05 mg/mL and 5.25 mg/mL, respectively. Sesame oil was used as LCT-based formulation in this study. Due to limited solubility of DTG sodium in LCT, sesame oil (1 mL/kg) was administered immediately before drug administration in oral LCT-based group. The doses of prodrug 5 in pharmacokinetics and biodistribution studies were 1.63 mg/kg (1 mL/kg of 1.63 mg/mL solution in propylene glycol/ethanol/non pyrogenic water (80:10:10, *v*/*v*/*v*)) for IV bolus administration (equivalent to 1 mg/kg of DTG) and 8.15 mg/kg (1 mL/kg of 8.15 mg/mL solution in sesame oil) for oral gavage administration (equivalent to 5 mg/kg of DTG). Prodrug 6 was orally administered at a dose of 8.13 mg/kg (1 mL/kg of 8.13 mg/mL solution in sesame oil) (equivalent to 5 mg/kg of DTG) to rats. The vials containing the LCT-based formulation were filled with nitrogen and protected from light and air to avoid oxidation of the sesame oil. The orally administered dose of lipids to rats was 1 mL/kg.

2.7.3. Pharmacokinetic studies

2.7.3.1. Pharmacokinetic studies of TPV

The following protocol was used to generate the pharmacokinetics results described in **Chapter 3**. Right jugular vein cannulation surgery was performed under general gaseous anaesthesia (2.5% isoflurane in oxygen) as previously described [229, 254, 256]. Following the surgery, the animals were allowed to recover for 2 nights. Animals were then fasted for up to 16 h prior to the drug administration with free access to water. Rats were divided into 3 treatment groups: IV bolus administration of TPV at a dose of 1 mg/kg, oral gavage administration of TPV at a dose of 5 mg/kg in lipid-free or LCT-based formulations, followed by 1 mL of water for facilitating the emulsification of oil. Blood samples were collected from the cannula at pre-determined time points (pre-administration, 5 and 15 minutes, 0.5, 1, 2, 4, 8, 12, 18 and 24 h following IV bolus administration; and 1, 2, 3, 4, 5, 6, 8, 10, 12, 18 and 24 h following oral gavage administration) into EDTA containing (1.5M) tubes. Blood samples were centrifuged at 1,160 *g* at 10°C for 10 minutes to obtain plasma. The levels of TPV in the plasma were determined by means of HPLC as described in section **2.8.2.1**.

2.7.3.2. Pharmacokinetic studies of DTG and prodrugs 5 and 6

The following protocol was used to generate the pharmacokinetics results described in **Chapter 4**. All animal preparation procedures

(jugular vein cannulation surgery, recovery period and fasting time) were the same as described in section **2.7.3.1**. For pharmacokinetic study of DTG, rats were divided into 3 treatment groups: IV bolus administration of DTG sodium at a dose of 1.05 mg/kg (equivalent to 1 mg/kg of DTG) through jugular vein cannula, and oral gavage administration of DTG sodium at a dose of 5.25 mg/kg (equivalent to 5 mg/kg of DTG) with and without LCT (representing LCT-based and lipid-free formulation), followed by 1 mL of water for facilitating the emulsification of oil. Following the administration, blood samples were collected from jugular vein cannula at pre-determined time points (pre-administration, 5, 15, 30 minutes, 1, 2, 4, 6, 9, 14 and 24 hours for IV group; and pre-administration, 30 minutes, 1, 2, 3, 4, 5, 6, 9, 14 and 24 hours for oral lipid-free and LCT-based groups) into EDTA containing (1.5M) tubes. In the pharmacokinetic study of prodrug 5, rats were divided into 2 treatment groups: IV bolus administration of prodrug 5 at a dose of 1.63 mg/kg (equivalent to 1 mg/kg of DTG) and oral gavage administration of prodrug 5 at a dose of 8.15 mg/kg (equivalent to 5 mg/kg of DTG) in LCT-based formulation, followed by 1 mL of water for facilitating the emulsification of oil. Blood was sampled at pre-determined time points (pre-administration, 5, 15, 30 minutes, 1, 2, 4, 8, 12, 24, 36 and 48 hours for IV bolus group; and pre-administration, 30 minutes, 1, 2, 3, 4, 6, 8, 12, 24, 36 and 48 hours for oral LCT-based group). Prodrug 6 was administered to rats *via* oral gavage at a dose of 8.13 mg/kg (equivalent to 5 mg/kg of DTG) in LCT-based formulation. Blood sampling time points were the same as the oral groups of prodrug 5. EDTA (1.5M) was used

as an anticoagulant for DTG studies, and sodium fluoride (NaF, 10 mg/mL) was used as an anticoagulant and esterase inhibitor for prodrug experiments [256, 289, 290]. All blood samples were gently mixed and centrifuged (1,160 *g*, 10°C, 10 minutes) to separate plasma, which was kept in -80°C until analysis. At the end of the pharmacokinetic study, rats were euthanized by CO_2 inhalation and death was confirmed by cervical dislocation. Tissues were then harvested and stored at -80°C until analysis. All biological samples were analysed by means of HPLC as described in section **2.8.2.2**.

2.7.3.3. Pharmacokinetic analysis

Pharmacokinetic parameters generated from plasma concentration-time profiles were calculated by non-compartmental analysis using Phoenix WinNonlin 6.3 software (Pharsight, Mountain View, CA, USA). The oral absolute bioavailability (F_{oral}) was calculated based on the following equation:

$$F_{oral}\,(\%) = \frac{AUC_{oral}}{AUC_{IV}} \times \frac{Dose_{IV}}{Dose_{oral}}$$

2.7.4. Biodistribution studies

2.7.4.1. Biodistribution studies of TPV

The following protocol was used to generate the biodistribution results described in **Chapter 3**. Animals were fasted up to 16 h prior to the drug administration. LCT-based and lipid-free formulations of TPV were prepared as described in **2.7.2.1** and administered by oral gavage at a

dose of 5 mg/kg. Following the administration of TPV, the rats were euthanized at predetermined time points according to the time of maximum plasma concentrations observed in pharmacokinetic study (2 and 3 h following administration, $t_{max\text{-}1h}$ and t_{max}). The mesenteric lymph samples were collected from the superior mesenteric lymph duct with the aids of an assistant immediately after confirming the death of the animals. Briefly, the dead rat was laid on back and the abdominal tissues were exposed. The gut (small intestine and colon) was moved aside to expose deep tissues. A suture was tightened at the cisterna chyli to block the lymph flow. The superior mesenteric lymph duct can be then identified as a white duct with sufficient milky lymph fluid. A needle (25G x 1.6 mm) was bent to 60-90 degree and equipped to a 1 mL syringe. The needle and syringe were rinsed by EDTA (1.5M) before collecting lymph sample. Lymph sample collection was initiated by inserting the bent needle into the superior mesenteric lymph duct and withdrawing the lymph fluid while the assistant held and squeezed the gut (including the small intestine and colon).The lymph sample was put into an eppendorf tube contained 1 µL EDTA (1.5M) and stored on ice. The mesenteric lymph nodes (MLNs) were also collected as previously described [255, 291]. All biological samples were kept at - 80°C until analysis for TPV levels by means of HPLC as described in section **2.8.2.1**.

2.7.4.2. Biodistribution studies of DTG and prodrug 5

The following protocol was used to generate the biodistribution results described in **Chapter 4**. Rats were fasted overnight before the study up

to 16 hours as described above. DTG sodium was administered by oral gavage to rats at a dose of 5.25 mg/kg (equivalent to 5 mg/kg of DTG) in lipid-free solution formulation (as described in section **2.7.2.2**) with or without sesame oil (representing LCT-based and lipid-free formulation), followed by 1 mL water. Prodrug 5 was administered by oral gavage to rats at a dose of 8.15 mg/kg (equivalent to 5 mg/kg of DTG) solubilised in sesame oil, followed by 1 mL water. Rats were euthanized at pre-determined time points (2, 4 and 8 hours following the administration) by CO_2 inhalation. The mesenteric lymph fluid samples were collected as described in the section **2.7.4.1**. The MLNs, brain, testes, liver, spleen, thymus, duodenum and duodenum juice, ascending colon, small intestine contents and faeces in colon were harvested and kept in -80°C until analysis.

2.7.4.3. Distribution of compounds into CM of rat mesenteric lymph *in vivo*

The following protocol was used to generate the biodistribution results described in **Chapter 3 and 4**. The rat lymph samples generated from biodistribution studies were diluted with PBS to 1 mL (**Chapter 4**) or 2 mL (**Chapter 3**) emulsion, followed by the density gradient ultracentrifugation for separating of CM as described in section **2.3.5**. The supernatant CM fraction and each density layer (lipoprotein fractions and lipoprotein-free fraction) were collected and analysed by means of HPLC.

2.8. Bioanalytical procedures

2.8.1. Instruments

The HPLC-UV system consisting of a Waters Alliance 2695 separations module coupled with Waters 996 photodiode array detector was used for analysis of all biological samples.

2.8.2. Analytical conditions

2.8.2.1. HPLC analytical condition for the determination of TPV in biological samples

The following HPLC analytical condition was used to generate part of the experimental results described in **Chapter 3**. The analytical conditions used for the initial screening of affinity of PIs to artificial CM are described in **Table 2-7.** The autosampler was maintained at 5°C and the column temperature was 45°C. Chromatographic separation was performed using Waters Atlantis C18 4.6 × 150 mm, 5 µm particle size column (Elstree, Herts, UK) equipped with a 2 × 4 mm, 3 µm particle size guard column (Phenomenex, Macclesfield, UK). The mobile phase was composed of ammonium acetate buffer (10 mM, pH adjusted to 4.2 with glacial acetic acid) and ACN in a ratio of 20:80 (v/v) with a 0.4 mL/min flow rate. The assay for determination of TPV was validated for the selectivity, sensitivity and linearity in rat plasma as described in section **2.8.2.3**. The analytes were monitored at 263 nm for TPV and 220 nm for CBD. Data were recorded and analysed using Empower™ 2 software.

Table 2-7. Analytical conditions of the initial screening of affinity of PIs to artificial CM. An HP Agilent 1100 HPLC system was used for analysis of samples. Chromatographic separation was performed using C18 column equipped with C8 guard column at 40°C. Five microliters of samples were injected. Analytes were analyzed in positive ion mode, fragmented with electrospray ionization mass spectrometer (ESI-MS/MS) API-2000 (SCIEX), quantified by multiple reaction monitoring (MRM).

Gradient program[$]		
Time (min)	**Solvent A[*] (%)**	**Solvent B[&] (%)**
0	**80**	**20**
1	**15**	**85**
3	**15**	**85**
3.1	**0**	**100**
6.0	**0**	**100**
6.1	**80**	**20**
10	**80**	**20**

[$] Flow rate: 0.3 mL/min.
[*] Solvent A: 2.5mM ammonium acetate buffer with 10% methanol (pH 3.6 ± 0.2).
[&] Solvent B: 2.5mM ammonium acetate buffer with 90% methanol (pH 6.6 ± 0.2).

2.8.2.2. HPLC analytical conditions for the determination of DTG and its prodrugs in biological samples

The following HPLC analytical condition was used to generate part of the experimental results described in **Chapter 4**. The same HPLC system was used for determination of DTG and its prodrugs in biological samples. The autosampler and the column temperature was maintained at 5°C and 40°C, respectively. Chromatographic separations of DTG and prodrugs were achieved by Waters XTerra MS C18 4.6 x 150 mm, 5 µm particle size column (Waters, Cheshire, UK) equipped with a 2 x 4 mm, 3 µm particle size guard column (Phenomenex, Macclesfield, UK). Complete chromatography conditions for all tested compounds are shown in **Table 2-8**. The assay for determination of DTG was validated for the selectivity, sensitivity and linearity in rat plasma as described in section **2.8.2.3**. The data was collected and processed by Empower^{TM} 2 software.

Table 2-8. HPLC bioanalytical conditions for DTG and prodrugs

Compounds	Mobile phase		Flow rate (mL/min)	Internal standard (IS)	UV wave length (nm)		Reconstitute solvent [b]
	Buffer [a]	Acetonitrile			Compound		ACN
DTG and prodrug 2	Gradient 1 [c]		0.8	CBD [f]	258	211	50%
Prodrug 1	Gradient 2 [d]		0.8	CBD [f]	258	211	50%
Prodrug 3, 4, 5 and 6	Gradient 3 [e]		0.8	CBD [f]	258	211	50%

[a] Buffer: 10mM ammonium formate buffer (adjust to pH = 3 with formic acid).
[b] Reconstitute solvent is presented as the percentage of acetonitrile in HPLC grade water.
[c] Gradient 1: 35% Acetonitrile from 0-8 min, gradually increase to 85% from 8-11 min, maintain at 85% from 11-21 min, gradually decrease to 35% from 21-24 min, maintain at 35% from 24-30 min.
[d] Gradient 2: 35% Acetonitrile from 0-8 min, gradually increase to 70% from 8-11 min, maintain at 70% from 11-24 min, gradually decrease to 35% from 24-27 min, maintain at 35% from 27-33 min.
[e] Gradient 3: 35% Acetonitrile from 0-8 min, gradually increase to 90% from 8-11 min, maintain at 90% from 11-31 min, gradually decrease to 35% from 31-34 min, maintain at 35% from 34-40 min.
[f] CBD: Cannabidiol.

2.8.2.3. The validation of HPLC-UV methods of TPV and DTG

The bioanalytical HPLC-UV methods used for generating part of results in Chapter **3** and **4** were validated for selectivity, sensitivity and linearity in rat plasma according to the US Food and Drug Administration (FDA) guidelines for bioanalysis [292].

Selectivity

The chromatograms of blank plasma samples were compared with plasma samples spiked with TPV and DTG to assess the selectivity of current bioanalytical assay in six validation runs [292]. The selectivity was evaluated in rat plasma samples obtained from the animal experiments.

Sensitivity

The validation of sensitivity was performed by determination of the LLOQ of TPV and DTG spiked into plasma samples with the accuracy and precision meeting the acceptance criteria of RE and RSD ≤ 20% in intra- and inter-day analyses [292].

Linearity

Calibration curves of TPV and DTG were constructed as described in section **2.8.3.1** and **2.8.3.2**, respectively. A blank sample (plasma without spiking compounds) was included in each validation run. Calibration curves (the peak ratio between TPV or DTG and the internal standard against nominal concentration) were fitted by least-squares linear regression analysis using a weighted factor (1/X).

2.8.3. Sample preparation procedures for HPLC analysis

2.8.3.1. Preparation of biological samples of TPV

The following protocol was used to generate part of the experimental results described in **Chapter 3**. The stock solutions of TPV and CBD (internal standard, IS) were prepared at the concentration of 1 mg/mL in ACN and kept at - 20°C. Working standard solutions of TPV were prepared by diluting the stock solution with ACN in a series of concentrations of 50, 100, 250, 500, 1,000, 5,000, 10,000, 50,000, 100,000 and 150,000 ng/mL. CBD stock solution was diluted with ACN to generate working solution at a concentration of 100 µg/mL. For the preparation of calibration curve samples, aliquots of 117 µL blank rat plasma were mixed with 13 µL TPV working solutions in a borosilicate glass culture tubes (Fischer Scientific, UK). Thirteen microliters IS working solution was spiked into 130 µL sample, followed by protein precipitation with 390 µL of ice-cold ACN (-20°C). Liquid-liquid extraction was then performed using 5 mL MTBE and vortex-mixing for 5 minutes. Samples were centrifuged at 1,160 *g* (Eppendorf Centrifuge 5810R, Stevenage, UK) at 10°C for 10 minutes. The upper organic layer was then transferred to a fresh tube and evaporated to dryness under nitrogen gas at 40°C (Techne DRI-Block type DB-3D, Cambridge, UK). The dry residue was reconstituted with 130 µL of ACN-water (1:1, v/v) followed by vortex-mixing for 5 minutes. Following a brief centrifugation (1,160 *g*, 10°C for 1 minute), 90 µL of the clear solution was injected into HPLC system. All biological samples (plasma, chylomicron emulsion, lymph and tissues homogenates) generated from pharmacokinetic and

biodistribution studies underwent the same procedure as described above.

2.8.3.2. Preparation of biological samples of DTG and prodrugs

The following protocol was used to generate part of the experimental results described in **Chapter 4**. The stock solution of DTG was prepared at the concentration of 1 mg/mL in DMSO. Prodrugs and CBD (internal standard, IS) were dissolved in ACN to generate stock solutions at 1 mg/mL. All stock solutions were kept at -20°C. Working solutions of DTG and prodrugs were prepared by diluting stock solutions with ACN to achieve concentrations of 100, 250, 500, 1000, 5000, 10000, 50000, 100000, 200000 and 250000 ng/mL. CBD stock solution was diluted by ACN to 50 µg/mL to obtain IS working solution. Calibration curve samples were prepared by mixing 10 µL of working solutions of the prodrugs and 10 µL IS working solution with 100 µL blank biorelevant media. Three hundred µL of ice-cold ACN was added for protein precipitation. Following one minute vortex-mixing, liquid-liquid extraction was performed by adding 3 mL MTBE and vortex-mixing for 5 minutes. Samples were then centrifuged at 1,160 *g*, 10°C for 10 minutes. The upper organic layer was collected and evaporated to dryness under nitrogen gas at 40°C. The residue was reconstituted with 100 µL ACN-water mixture (1:1, v/v) and vortex-mixed for 5 minutes. Following a brief centrifugation, 60 µL of clear solution was injected into HPLC system. All biological samples (plasma, lymph, CM emulsion, FaSSIF and tissue

homogenates) generated from *in vitro*, *ex vivo* and *in vivo* studies underwent the same sample processing procedure described above. The original formulations of *in vivo* studies were used to prepare the calibration curves for determination the drug levels in plasma or tissue samples.

2.8.3.3. Assessment of the stability of DTG prodrugs in rat plasma

The stability of DTG prodrugs in rat plasma was validated by mimicking the time frame of pharmacokinetic study. The assessment initiated by spiking the stock solution of prodrugs (in acetonitrile) into NaF-rat plasma (10 mg/mL). For the validation of prodrug 5, samples were kept on ice for 5 minutes, followed by a centrifugation (3000 *g*, 4°C, 3 minutes) to mimic the procedure of blood collection and plasma separation during pharmacokinetic study. The plasma samples were then stored on the ice for another one hour, and then transferred to -80°C for 24 hours (overnight) to simulate the storage conditions of samples during pharmacokinetic study. For the validation of prodrug 6, plasma samples were placed on ice for 5 minutes and immediately centrifuged (3000 *g*, 4°C, 3 minutes). After the centrifugation, a volume of 300 µL ice-cold ACN (-20°C) was immediately added to the samples for protein precipitation. Samples were then processed for HPLC analysis. All experiments were performed in triplicates (results were presented as mean ± SD).

2.8.3.4. Homogenization of tissue samples

This procedure was used for preparing tissue samples harvested from *in vivo* studies described in **Chapter 3** and **4**. Tissues were collected at the end point of the pharmacokinetics and biodistribution studies and kept at -80°C until analysis. On the day of the analysis, tissues were thawed on ice then weighed. HPLC-grade water was added to tissues (1:3, *w*/*v*) obtained from *in vivo* studies after administration of TPV, DTG sodium and prodrug 5. HPLC-grade water solubilised with NaF (14 mg/mL) was added to tissues generated from *in vivo* studies following administration of DTG prodrug. Tissues samples were homogenised (POLYTRON® PT 10-35 GT, Kinematica AG, Luzern, Switzerland) on ice bath. The homogenates were kept on ice until sample preparation for HPLC analysis.

2.8.3.5. Assessment of the stability of DTG prodrug 5 in MLNs

Stock solution of prodrug 5 was spiked into the blank homogenates of MLNs (tissue:HPLC-grade water, 1:3, *w*/*v*) and kept on ice for 5 minutes then placed on dry ice for 1 hour. The samples were then transferred to -80°C for overnight (24 hours). The treated samples were thawed on ice and appropriate amount of NaF was added to achieve 10 mg/mL of NaF, followed by homogenisation on the ice for 30 seconds. The prepared homogenates were ready for sample preparation as described in section **2.8.3.2** and the HPLC condition is described in section **2.8.2.2.** The reference sample was freshly prepared on the day of the study for

comparing the recovery of prodrug 5. The validation samples were prepared in triplicates (results were presented as mean ± SD).

2.9. Statistical analysis

One-way ANOVA followed by Tukey's or Dunnett's multiple comparisons tests, two-way ANOVA followed by Sidak or Dunnett multiple comparison tests, or two-tailed unpaired t-test were used where appropriate. All values were expressed as mean ± standard deviation (SD). A significant difference was stated when a *p* value was below 0.05. The statistical analyses were performed using GraphPad Prism version 7.04 (GraphPad Software, Inc., San Diego, CA, USA).

3. ORAL ADMINISTRATION OF TIPRANAVIR WITH LONG-CHAIN TRIGLYCERIDE RESULTS IN MODERATE INTESTINAL LYMPH TARGETING BUT NO EFFICIENT DELIVERY TO HIV-1 RESERVOIR IN MESENTERIC LYMPH NODES

The work in this chapter has been published in a peer-review journal: Chu, Y., Qin, C., Feng, W., Sheriston, C., Khor, Y., Medrano-Padial, C., Watson, B., Chan, T., Ling, B., Stocks, M., Fischer, P., Gershkovich, P. (2021). Oral administration of tipranavir with long-chain triglyceride results in moderate intestinal lymph targeting but no efficient delivery to HIV-1 reservoir in mesenteric lymph nodes. *International Journal of Pharmaceutics*, 602: p. 120621

3.1. Introduction

Since the first detection of HIV-1 infection cases in the 1980s, HIV/AIDS pathophysiology and treatments have been studied and developed for decades. The introduction of combination antiretroviral therapy (cART) led to successful treatment in many cases [143, 293] and dramatically improved the morbidity and mortality of HIV-1 infection [160]. However, numerous studies demonstrated that HIV-1 remains replication-competent in patients undergoing cART treatment with undetectable plasma viral loads [54-56]. This could be due to the establishment of latent HIV-1 reservoirs in cells and various tissues at the initial stage of the infection [294, 295]. It is believed that the poor penetration of

antiretroviral agents to such HIV reservoirs limits the ability of the drugs to eliminate the virus. The mesenteric lymph and mesenteric lymph nodes (MLNs) are one of the main HIV-1 reservoirs with the highest viral load reported [296] and SIV reservoirs in the nonhuman primate models [297-299]. Therefore, an effective delivery of antiretroviral drugs to mesenteric lymphatic system can contribute to eradication of HIV-1 from this important reservoir.

Most orally administered drugs following absorption from the gastrointestinal tract gain access to the systemic circulation through portal vein with a potential for hepatic first-pass metabolic loss. However, for some highly lipophilic compounds administered with lipids, intestinal lymphatic system rather than hepatic portal blood is the main route to enter the systemic blood circulation [224, 300, 301]. During the intestinal lymphatic absorption of drugs, chylomicrons (CM) play a crucial role as they transport drugs to the lymph lacteals rather than blood capillary by forming drug-CM complexes in the enterocytes [302]. A strong correlation between the intestinal lymphatic absorption and the affinity of drugs to CM has been established [237]. It is known that dietary lipids stimulate the assembly of CM [303]. We have previously shown that long-chain triglyceride (LCT)-based formulation can not only facilitates the intestinal lymphatic absorption but also leads to extremely high concentration of drugs within the mesenteric lymph and MLNs [254, 304]. This suggests that intestinal lymphatic absorption pathway substantially increases the concentration of drugs in mesenteric lymph and MLNs [305]. However, only highly lipophilic compounds with high affinity to CM

could be delivered to the intestinal lymphatic system by LCT-based formulation approach. For other compounds, prodrug approach combined with LCT-based formulation was required in order to achieve substantial intestinal lymphatics targeting [306, 307].

Several studies have demonstrated that in many cases drug combination regimens that include protease inhibitor (PI) show greater benefits of HIV-1 treatment compared to monotherapy or combination regimens without PIs [160, 293, 308, 309]. Moreover, boosted PIs have been successfully used in monotherapy and showed non-inferiority compared to cART [310]. Although PIs are gradually fading from the mainstream of HIV-1 treatment in recent years, they are still an important component of many recommended cART regimens. For instance, a raltegravir (RAL) backbone regimen is recommended as the preferred first-line regimen for neonates. In addition, ritonavir (RTV)-boosted PIs are suggested to be incorporated in a NRTI-based therapy as a preferred second-line regimen for patients with failed dolutegravir (DTG)-based treatment [288]. Targeted delivery of PIs to mesenteric lymphatic system, including mesenteric lymph and MLNs, may potentially lead to more effective treatment by increasing the exposure of this HIV-1 reservoir to PIs.

Since the association of drugs with CM determines the extent of intestinal lymphatic absorption, an *in silico* model was previously established based on multiple physiochemical properties to predict the degree of CM association of drugs [238]. In this study, PIs were assessed for their potential of intestinal lymphatic targeting using this computational model. Although four PIs showed predicted CM association *in silico*, further

experimental results indicated that tipranavir (TPV) is the only candidate which has affinity to artificial and natural CM *in vitro* and *ex vivo*. TPV is a non-peptidic PI which has high genetic barrier to drug resistance and is active for both wild and multidrug-resistant HIV-1 strains [311, 312]. Furthermore, it is a second-line agent reserved for HIV-1 infected patients previous treatment failure [313]. However, box warnings for intracranial hemorrhage and hepatotoxicity substantially constrain the actual clinical use of TPV [314]. It has been proposed that Intestinal lymphatic targeting, if successful, can potentially result in lower total required dosage, which could eventually limit these life-threating adverse effects of this compound. Accordingly, it has been hypothesized in this work that based on its physiochemical [167, 315], TPV may have substantial intestinal lymphatic absorption if it is co-administered with LCT vehicle (**Figure 3-1**). Therefore, the aim of this study was to assess the feasibility of LCT-based formulation approach for targeting TPV to HIV-1 reservoirs within the MLNs and mesenteric lymph.

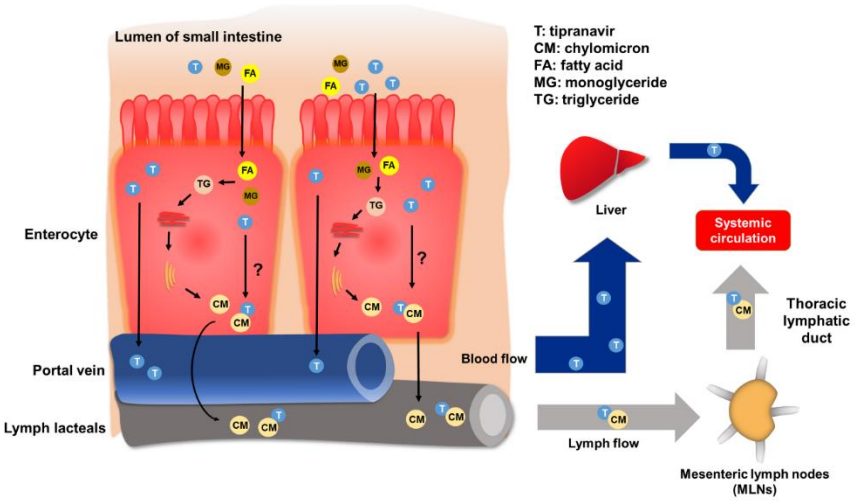

Figure 3-1. The schematic presentation of intestinal lymphatic transport of TPV following oral administration with the presence of lipids.

3.2. Experimental design

In silico prediction is described in section **2.3**. The *in vitro* and *ex vivo* assessments of the affinity to chylomicrons are described in section **2.5**. Formulation preparation is described in section **2.8.2.1**. Pharmacokinetics and biodistribution studies are described in sections **2.8.3.1** and **2.8.4.1**, respectively. The scheme of the study is shown in **Figure 3-2**.

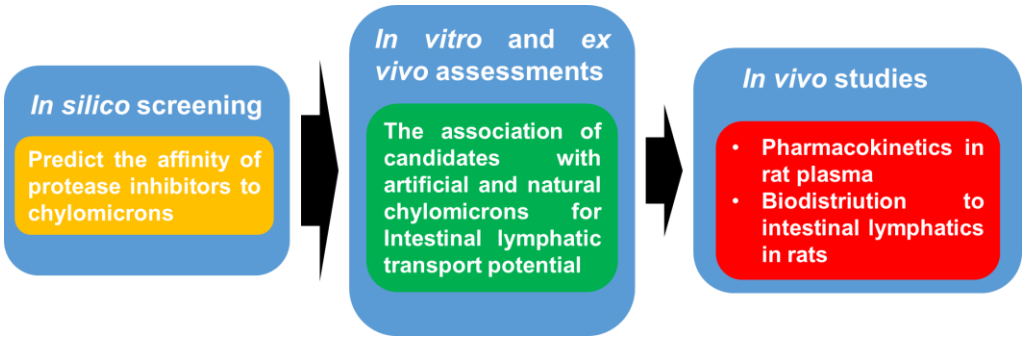

Figure 3-2. The workflow of experimental design for targeting TPV to mesenteric lymphatic system.

3.3. Results

3.3.1. The validation of bioanalytical method

3.3.1.1. Selectivity

The chromatograms of blank plasma samples were compared with plasma samples spiked with tipranavir (TPV) at a lower limit of quantification (LLOQ) to assess the selectivity of the current bioanalytical assay in six validation runs [292]. The selectivity was evaluated in rat plasma samples obtained from animal experiments. The current bioanalytical assay showed good selectivity as TPV peaks were

efficiently separated from endogenous peaks in plasma samples (**Figure 3-3**).

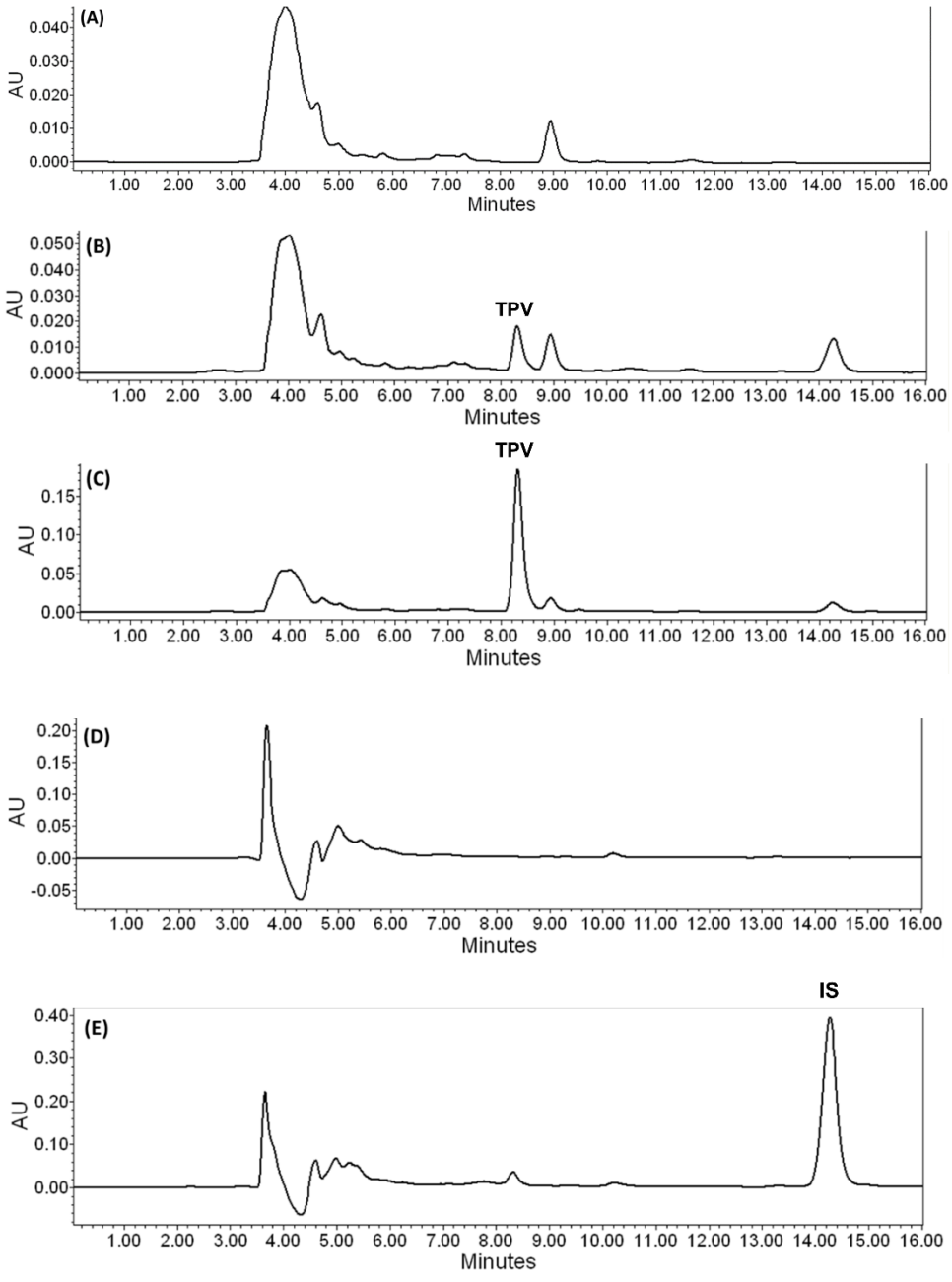

Figure 3-3. Representative chromatograms of (A) blank rat plasma sample at λ = 263 nm; (B) rat plasma spiked with 500 ng/mL TPV at λ = 263 nm; (C) rat plasma spiked with 5000 ng/mL TPV at λ = 263 nm; (D) blank rat plasma sample at λ = 220 nm; (E) rat plasma spiked with 10000 ng/mL of the IS at λ = 220 nm. IS, internal standard; TPV, tipranavir.

3.3.1.2. Sensitivity

The validation of sensitivity was performed by determination of the LLOQ of TPV spiked into plasma samples with the accuracy and precision meeting the acceptance criteria of RE and RSD ≤ 20% in intra- and inter-day analyses [292]. In this assay, the LLOQ was determined to be 5 ng/mL (**Table 3-1**).

Table 3-1. Intra- and inter-day validation results for LLOQ determination of TPV in plasma.

Nominal concentration level	*Intra-day (n = 6)*		*Inter-day (n = 6)*	
	Accuracy (RSE, %)	Precision (RSD, %)	Accuracy (RSE, %)	Precision (RSD, %)
LLOQ (5 ng/mL)	13.02	4.98	5.62	7.95

3.3.1.3. Linearity

A calibration curve of TPV with the range of 5-15000 ng/mL was constructed as described in section **2.8.3.1**. A blank sample (plasma without spiked TPV and the internal standard) was included in each validation run. Calibration curves (the peak ratio between TPV and the internal standard against nominal concentration) were fitted by least-squares linear regression analysis using a weighted factor (1/X). This assay was linear for TPV with a correlation coefficient (r^2) over 0.99 in all calibration curves.

3.3.2. Assessment of intestinal lymphatic targeting potential of tipranavir (TPV)

Association of drugs with chylomicrons (CM) in enterocytes plays a crucial role in the intestinal lymphatic targeting. To investigate the potential of intestinal lymphatic targeting of different protease inhibitors (PIs), the affinity of PIs to CM was predicted using a previously established *in silico* model (**Table 3-2**) [238]. Of the 10 PIs assessed *in silico*, ritonavir (RTV), nelfinavir (NFV), lopinavir (LPV) and TPV showed mild to moderate (>10 %) potential for association with CM (**Figure 3-4A**). However, when these selected candidates were screened *in vitro* for association with artificial CM-like emulsion (Intralipid®), the only PI that showed measurable experimental association with Intralipid® at the initial screening was TPV. The association values of TPV with artificial and natural human plasma-derived CM are summarized in **Figure 3-4B**. Although TPV has low triglyceride (TG) solubility (5.9 ± 0.3 mg/mL), the association of TPV with artificial lipid particles and natural CM was substantial (31.6% and 66.7%, respectively), suggesting a potential for intestinal lymphatic targeting when administered orally with lipids. Interestingly, the affinity of TPV for the human CM was significantly higher than for artificial lipid particles ($p < 0.0001$).

Table 3-2. Physicochemical properties of protease inhibitors, and *in silico* prediction of association with CM [281].

Compound	cLog $D_{7.4}$	cLog P – cLog $D_{7.4}$	PSA	H-acceptors	FRB	Density (g/cm^3)	Molar volume (cm^3)	H-donors	Predicted association with CM (%)
SQV	3.99	0.06	166.75	11	13	1.211	553.8	6	6.08
RTV	4.81	0	202.26	11	18	1.239	581.7	4	13.63
INV	3.32	0.03	118.03	9	12	1.25	491	4	6.92
NFV	5.1	0.06	127.2	7	10	1.22	463.1	4	17.65
APV	2.68	0	139.57	9	12	1.3	387.8	4	1.02
LPV	5.88	0	120	9	15	1.163	540.4	4	50.8
ATV	4.13	0.02	171.22	13	18	1.178	597.9	5	8.51
FPV	-3.96	5.88	195.91	12	14	1,4	416.3	5	0
TPV	7.04	0.1	113.97	7	12	1.313	458.9	2	57.15
DRV	2.5	1.44	148.8	10	12	1.34	408.4	4	0.33

SQV, saquinavir; RTV, ritonavir; INV, indinavir; NFV, Nelfinavir; APV, amprenavir; LPV, lopinavir; ATV, atazanavir; FPV, fosamprenavir; TPV, Tipranavir; DRV, darunavir.

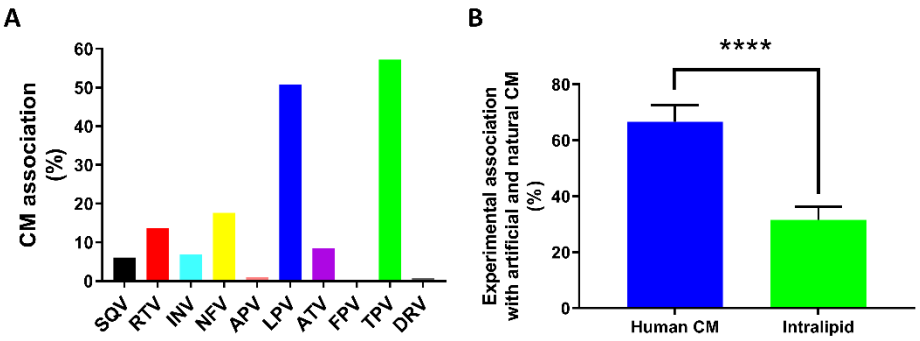

Figure 3-4. The predicted CM association of tested PIs and the experimental CM association of TPV. **(A)** The screening for CM association of PIs using in silico model. **(B)** Association of TPV with artificial CM-like emulsion (Intralipid®, n = 22) and human CM (n=9), mean ± SEM. ****, $p < 0.0001$.

3.3.3. Plasma pharmacokinetics of TPV following intravenous bolus (IV), and oral administration in lipid-free and long-chain triglyceride (LCT)-based formulations

Pharmacokinetic profiles of TPV were assessed following single IV and oral gavage administrations in LCT-based and lipid-free formulations in rats. The plasma concentration-time profiles of TPV are presented in **Figure 3-5**. **Table 3-3** summarizes the pharmacokinetic parameters derived from these pharmacokinetic profiles. Both oral groups share similar area under the curve (AUC_{inf}). The absolute oral bioavailability of lipid-free group is similar to the LCT-based group (36% and 44%, respectively). Furthermore, the TPV reaches similar maximum plasma concentration (C_{max}) when administered with or without lipids.

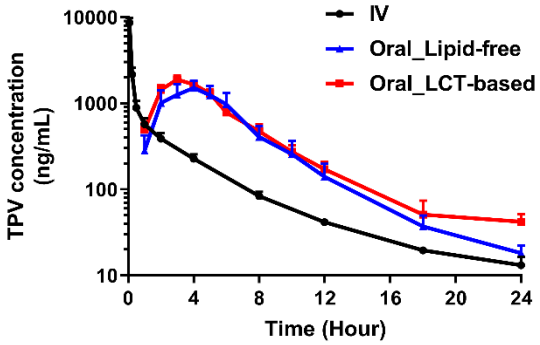

Figure 3-5. Plasma concentration-time pharmacokinetic profiles of TPV following IV (1 mg/kg, n = 5) and oral administration in lipid-free and LCT-based formulations (5 mg/kg, n = 3 for lipid-free group and n=6 for LCT-based group), mean ± SEM.

Table 3-3. Pharmacokinetic parameters of TPV following IV (1 mg/kg, n = 5) and oral administrations in lipid-free and LCT-based formulations (5 mg/kg, n = 3 for lipid-free group and n = 6 for LCT-based group), mean ± SEM. One-way ANOVA followed by Tukey's multiple comparison post-hoc analysis and two-tailed unpaired t-test was used to assess statistical difference among groups.

Route of administration	IV (n=5)	Oral	
		LCT-based (n=6)	Lipid-free (n=3)
AUC_{inf} (h*ng/mL)	4,873 ± 577	10,618 ± 1,093	8,733 ± 771
C_0 (ng/mL)	17,586 ± 1828	-	-
C_{max} (ng/mL)	-	1,937 ± 204	1,916 ± 98
$t_{1/2}$ (h)	5.21 ± 0.51	4.11 ± 0.4	3.57 ± 0.73
CL (mL/h/kg)	273 ± 45	-	-
V_{ss} (mL/kg)	903 ± 204	-	-
F_{oral} (%)	-	44 ± 4	36 ± 3

3.3.4. Biodistribution of TPV to the mesenteric lymph and MLNs following oral administration

The drug distribution to the mesenteric lymphatic system at plasma t_{max} time point and one hour prior to t_{max} (t_{max-1h}) was assessed following oral administration of TPV in LCT-based and lipid-free formulations to rats. The concentrations of TPV in plasma, lymph fluid and MLNs of LCT-based group at t_{max-1h} and t_{max} are shown in **Figure 3-6A-B**. The levels of TPV in mesenteric lymph were three-fold higher compared to plasma at both t_{max-1h} and t_{max} following oral administration. This suggests that the intestinal lymphatic transport plays a certain role in the absorption of TPV following oral administration with LCT. The concentrations of TPV in mesenteric lymph nodes (MLNs) and plasma of lipid-free group at t_{max-1h} and t_{max} are shown in **Figure 3-6C-D**. To note, mesenteric lymph is translucent and invisible without oral administration of lipids and therefore could not be collected for this group. The levels of TPV in plasma were comparable to MLNs at both time points in lipid-free group, as well as in LCT-based group.

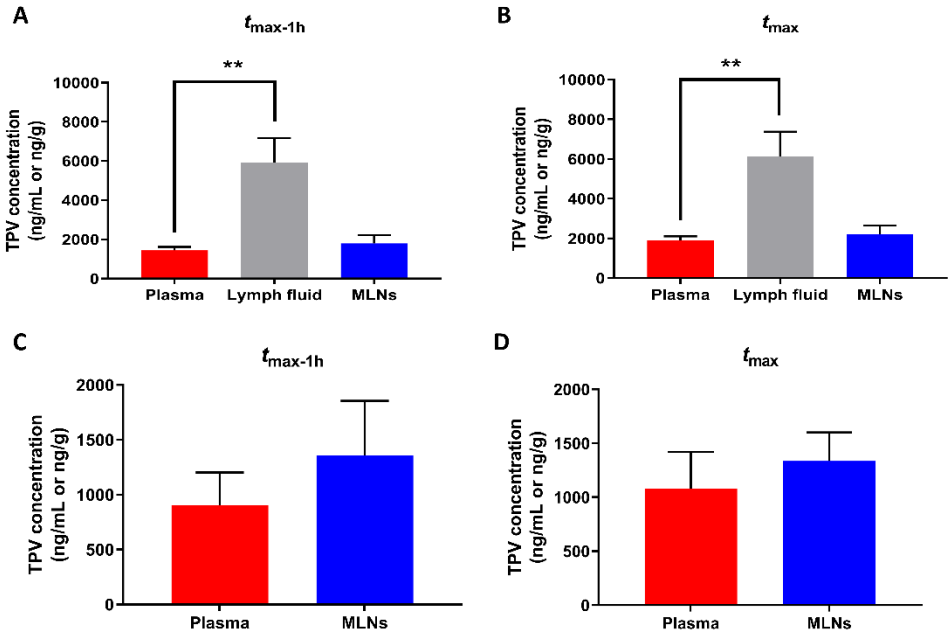

Figure 3-6. Distribution of TPV to plasma (obtained from pharmacokinetic study), mesenteric lymph fluid and MLNs following oral administration of TPV (5 mg/kg) in LCT-based (fresh sesame oil) and lipid-free formulations to rats. **(A)** Concentration of TPV in plasma (n=5), lymph fluid and MLNs (n=8 for both groups) two hours (one-hour prior to t_{max}, (t_{max-1h})) following oral administration of TPV in LCT-based formulation. **(B)** Concentration of TPV in plasma (n=5), lymph fluid and MLNs (n=9 for both groups) three hours (t_{max}) following oral administration of TPV in LCT-based formulation. **(C)** Concentration of TPV in plasma and MLNs (n=4 for each group) at t_{max-1h} following oral administration of TPV in lipid-free formulation. **(D)** Concentration of TPV in plasma and MLNs (n=4 for each group) at t_{max} following oral administration of TPV in lipid-free formulation. One-way ANOVA followed by Dunnett's multiple comparisons was used for statistical analysis for (A) and (B). Two-tailed unpaired t-test was used for statistical analysis for (C) and (D). All values are expressed as mean ± SEM. **, $p < 0.01$.

3.3.5. Distribution of TPV into lipoproteins in rat mesenteric lymph

The association of TPV with lipoproteins in rat mesenteric lymph fluid is shown in **Figure 3-7**. In order to investigate the interaction between CM and TPV during the intestinal lymphatic transport, we isolated CM from mesenteric lymph samples by density gradient ultracentrifugation and measured the concentration of TPV in lipoprotein and lipoprotein-free fractions. We found that at least 35% of TPV were associated with lipoproteins (CM and very low density lipoprotein (VLDL)) in mesenteric lymph fluid following oral administration in LCT-based formulation to rats.

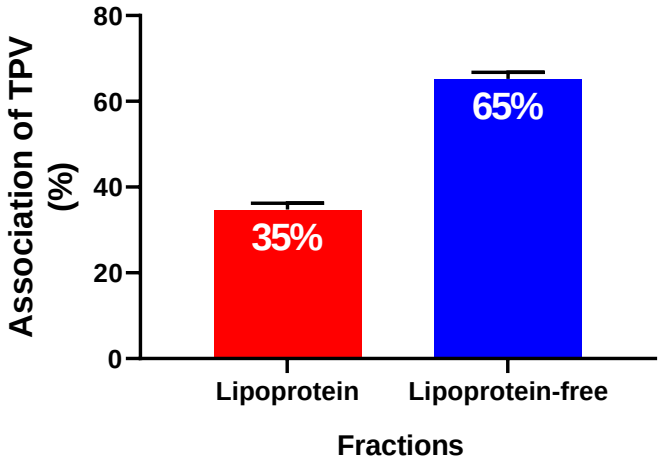

Figure 3-7. The association of TPV with lipoproteins in rat mesenteric lymph fluid at t_{max} (3h) following oral administration in LCT-based formulation. The collected volume of lymph fluid samples were between 49 – 95 µL. Lipoprotein fractions includes CM fraction and other density layers; lipoprotein-free fraction is the bottom layer with density at 1.1 g/mL.

3.4. Discussion

The latent HIV-1 reservoirs, including anatomical and cellular viral reservoirs, represent a substantial barrier for eradication of the virus [316]. The poor penetration of antiretroviral drugs to HIV-1 reservoirs limits the therapeutic efficacy and could be one of the reasons for difficulty to achieve functional cure [113, 317]. Mesenteric lymph nodes (MLNs) are believed to be the largest HIV-1 reservoir [318]. In this work, protease inhibitors (PIs) were assessed for their potential to be delivered to the HIV-1 reservoir in mesenteric lymphatic system. Since tipranavir (TPV) is the only candidate that showed experimental association with chylomicrons (CM), in this work we have attempted to deliver TPV to viral reservoir within the mesenteric lymphatic system using long-chain triglyceride (LCT)-based formulation approach.

3.4.1.1. Assessment of intestinal lymphatic targeting potential of TPV

Delivering PIs or other antiretroviral drugs to difficult-to-penetrate viral reservoirs, especially mesenteric lymphatic system, could result in better treatment outcomes of HIV-1 infection. Intestinal lymphatic targeting is potentially a promising approach as it can not only increase the plasma exposure to antiretroviral drugs, but also efficiently deliver the drugs to viral reservoirs within the mesenteric lymph and MLNs [301]. Since association of drugs with CM in the enterocytes is a key step in the intestinal lymphatic targeting of drugs, in the current study, FDA-approved PIs [319] were screened *in silico* for their predicted affinity to

CM based on their physicochemical properties [238]. We found that ritonavir (RTV), nelfinavir (NFV), lopinavir (LPV) and TPV showed mild to moderate potential for association with CM based on *in silico* prediction (**Figure 3-4A**). NFV was excluded from further assessment as it has been withdrawn from clinical use due to high-level genotoxic drug contamination found in 2007 [320, 321] and the marketing authorization in the European Union has been terminated since 2013 [322]. Remaining compounds were then further screened for their experimental association with Intralipid®. Intralipid® is an artificial lipid-rich emulsion which has similar compositions and particle size to CM with the exception of absence of apolipoproteins on the surface of artificial particles. It has been extensively used as a surrogate for natural CM in our previous studies [238, 254, 306]. Despite *in silico* prediction results, TPV was the only compound that had measurable experimental affinity to artificial emulsion (31.6%) and was therefore suitable for the next level of assessment with human plasma-derived CM. Interestingly, the association of TPV with natural CM was substantially higher (66.7%) compared to artificial emulsion (**Figure 3-4B**). This was an unusual phenomenon, as for vast majority of assessed compounds in the past the association is driven by solubility in triglyceride (TG) and lipophilicity, and is therefore similar for artificial emulsion and natural CM [238, 254, 306, 307]. This probably indicates that TPV's affinity to CM is driven, at least partially, by a different mechanism from most other assessed compounds, which are widely believed to associate with the lipophilic CM core [300, 323]. It is likely that surface apolipoproteins (which are present

on natural CM but not on artificial emulsion) play an important role in association of TPV with natural plasma-derived CM. Recently, drugs' affinity to the interfacial region and the surface apolipoproteins have been reported to play a certain role [228, 238]. In addition, previously proposed LCT solubility above 50 mg/mL threshold [224] has been recently suggested as not an absolute requirement for intestinal lymphatic transport [228]. In this study, the LCT solubility of TPV was measured to be far below the 50 mg/mL, but substantial association with artificial CM-like emulsion and even more so with natural plasma-derived human CM were still observed.

3.4.1.2. Plasma pharmacokinetics of TPV following intravenous bolus, oral administration in lipid-free and LCT-based formulation

LCT vehicle is known to facilitate the transport of highly lipophilic drugs through the intestinal lymphatic system [324, 325]. In this study, sesame oil was used as LCT-based formulation. It was demonstrated in multiple works that sesame oil is a powerful vehicle for facilitation of intestinal lymphatic transport of lipophilic compounds [304, 306, 307]. Moreover, we have recently shown that sesame oil is superior to pre-digested artificial formulations in promoting intestinal lymphatic transport of cannabidiol [326]. Although previous reports suggest that administration of TPV with a high-fat meal could enhance the oral bioavailability in humans [327, 328], our results showed similar oral bioavailability of TPV with and without co-administration of LCT vehicle in rats (**Table 3-3**). To

the best of our knowledge there are no previous reports about the effect of LCT-based formulations on oral bioavailability of TPV in rats. One study reported oral bioavailability of TPV in rats of 30 % (similar to the finding in our work) following administration with lipid-free formulation, but co-administration of lipids was not assessed in that work [329].

3.4.1.3. Biodistribution of TPV to mesenteric lymph fluid and MLNs following oral administration in LCT-based formulation

Although the LCT-based formulation showed no beneficial effect on the oral bioavailability of TPV, our results suggest that TPV indeed has some intestinal lymphatic absorption following oral administration with LCT, as suggested by about 3-fold higher concentrations of the drug in mesenteric lymph fluid compared to plasma (**Figure 3-6A-B**). However, despite the substantial affinity to CM (**Figure 3-4B**) and moderate intestinal lymphatic absorption, LCT-based formulation approach alone was not sufficient for effective delivery of TPV to MLNs, as the concentration of the drug in MLNs were similar to plasma in both LCT-based and lipid-free formulation groups (**Figure 3-6B, D**). It should be emphasized that MLNs rather than lymph fluid are the primary reservoirs of HIV-1. Therefore, for the eradication of the virus from these reservoirs, the antiretroviral drugs should be efficiently delivered primarily to MLNs, while lymph fluid has secondary importance [277, 296, 330]. Our previous studies showed that LCT-based formulation approach alone could achieve very high concentrations of some drugs in MLNs [304],

while for other less lipophilic compounds a combined approach of chemical lipophilic prodrug modification with LCT-based formulation was required for efficient MLNs targeting [306, 307]. Thus, a combination of both prodrug and LCT-based formulation approaches looks like a more promising way forward for targeting TPV and other PIs to viral reservoirs within the mesenteric lymphatic system compared to LCT-based formulation only.

3.5. Conclusion

In this study, tipranavir (TPV) was found to be the only compound with experimental affinity to chylomicrons (CM) among other screened protease inhibitors (PIs). Long-chain triglyceride (LCT)-based formulation approach results in 3-fold higher concentrations of TPV in mesenteric lymph compared to plasma. However, despite substantial association with CM and considerable drug concentration in mesenteric lymph, the levels in MLNs, the primary viral reservoir, were similar to the concentrations in plasma. Therefore, LCT-based formulation approach alone does not lead to effective targeting of TPV to HIV-1 reservoirs in MLNs. Future efforts should be directed to a combined lipophilic prodrugs/lipid-based formulation approach to target TPV, other PIs and potentially other classes of antiretroviral agents to viral reservoirs within the mesenteric lymphatic system.

4. DEVELOPMENT OF LIPOPHILIC ESTER PRODRUGS OF DOLUTEGRAVIR FOR INTESTINAL LYMPHATIC TRANSPORT

The work in this chapter has been published in a peer-review journal: Chu, Y., Wong, A., Chen H., Ji, L., Qin, C., Feng, W., Stocks, M. J., Gershkovich, P. (2023). Development of lipophilic ester prodrugs of dolutegravir for intestinal lymphatic transport. *European Journal of Pharmaceutics and Biopharmaceutics*. Online ahead of print.

4.1. Introduction

The combination of antiretroviral therapy (ART) with two or more antiretroviral drugs (ARV) is widely used for the treatment of HIV infection [17, 145, 210, 212, 331-338]. However, despite viral suppression in the blood, replicate-competent HIV is still found in patients receiving long-term ART [54, 339]. The establishment of viral reservoirs during the early stages of infection has been reported in HIV-infected individuals and simian immunodeficiency virus (SIV) infected nonhuman primates [55, 59, 340]. These viral reservoirs constitute a substantial systemic viral burden [103], resulting in the recurrence of viremia after the cessation of ART [341-346]. Gut-associated lymphoid tissue (GALT), in particular mesenteric lymph nodes (MLNs), is an important site of immune response and one of the major anatomical HIV reservoirs [104, 105, 115, 347-349]. In SIV-infected rhesus macaques on suppressive ARVs, latent viral reservoirs in MLNs were reported to be larger than other lymphoid tissues and lymph nodes [350, 351]. However, suboptimal levels of ARVs

in difficult-to-penetrate reservoirs, including MLNs, lead to the persistence of HIV reservoirs and sustained viral replication [132, 352-355]. Efficient targeting of ARVs to MLNs could reduce this important HIV reservoir and bring us closer to a functional cure.

A core-shell nanoparticle coated with α4β7 monoclonal antibody was developed to achieve co-delivery of ARVs and monoclonal antibody to HIV reservoirs in GALT [356]. The α4β7 integrin is a critical receptor for homing of T cells to intestine and is believed to be a binding site of HIV for cell-to-cell transmission [357]. However, this strategy is under development and more studies are needed. Intestinal lymphatic transport is a widely used approach for targeting nano-materials, lipophilic drugs or their prodrugs to MLNs [229, 230, 255-257, 260, 358]. High lipophilicity (log $D_{7.4}$ > 5) [281] and long-chain triglyceride (LCT) solubility above 50 mg/mL are thought to be the most important physicochemical properties for intestinal lymphatic transport of drugs [359]. The affinity of drugs to chylomicrons (CM) was reported to exhibit a linear correlation with the *in vivo* intestinal lymphatic transport [283]. CM are the largest lipoproteins responsible for the absorption of dietary lipids *via* intestinal lymphatics. Since lipids can promote the production of CM and subsequent intestinal lymphatic transport of drugs, lipid-based formulations, especially LCT-based, have been used to target drugs to mesenteric lymph and MLNs [229, 252, 255, 256, 274, 360]. We previously reported that efficient targeting of HIV protease inhibitors (PIs) to MLNs requires a combination approach of lipophilic prodrugs and long-chain triglyceride (LCT)-based formulation [229] rather than an LCT-based formulation approach alone

[360]. Therefore, a combination approach of chemical modifications and LCT-based formulation is needed to target not highly lipophilic ARVs to MLNs.

Dolutegravir (DTG) is a second-generation integrase strand transfer inhibitor (INSTI). It is currently the preferred option in most first-line ART regimens [132, 210, 213, 337, 361] due to its potent antiretroviral activity (protein-adjusted 90% inhibitory concentration (PA-IC_{90}) of 64 ng/mL) and high genetic barrier to drug resistance [208]. Since DTG is not a lipophilic compound (clog P is 0.05 [362]), it is unlikely to have substantial intestinal lymphatic transport following oral administration. Therefore, this study aims to develop a lipophilic ester prodrug system of DTG formulated with an LCT-based vehicle to target DTG to HIV reservoir in MLNs. To this end, a number of simple alkyl ester prodrugs were designed based on *in silico* prediction affinity to CM [281] and synthesised. Synthesised prodrugs were screened for their intestinal lymphatic transport potential by previously reported *in vitro* and *ex vivo* assessments [229, 256, 283, 287, 363]. The most promising prodrug candidate was then assessed *in vivo* for systemic pharmacokinetics and MLNs targeting of DTG in rats. The lipophilic prodrug approach combined with LCT-based formulation for targeting active DTG to mesenteric lymph and MLNs is presented in **Figure 4-1**.

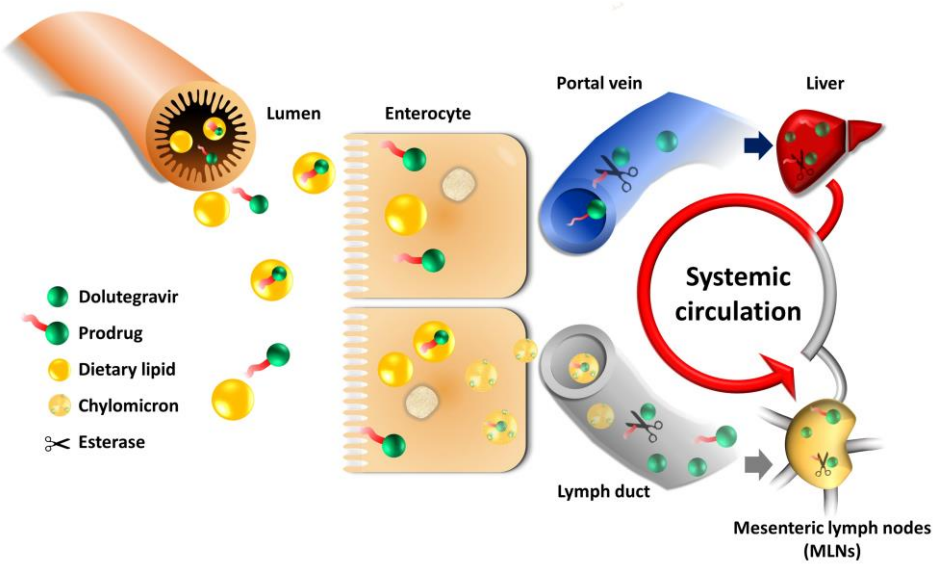

Figure 4-1. Schematic presentation of intestinal lymphatic transport of lipophilic prodrugs.

4.2. Experimental design

The design and synthesis of alkyl ester prodrugs of DTG are described in section **2.2.2**. The synthesised prodrugs were further assessed for their intestinal lymphatic transport potential and biotransformation in biorelevant media *in vitro* and *ex vivo* which are described in section **2.3**, **2.4**, and **2.5**, respectively. DTG and the most promising prodrugs were then assessed in pharmacokinetics (section **2.7.3.2**) and biodistribution (section **2.7.4.2**) studies in rats. The workflow of experimental design is shown in **Figure 4-2**.

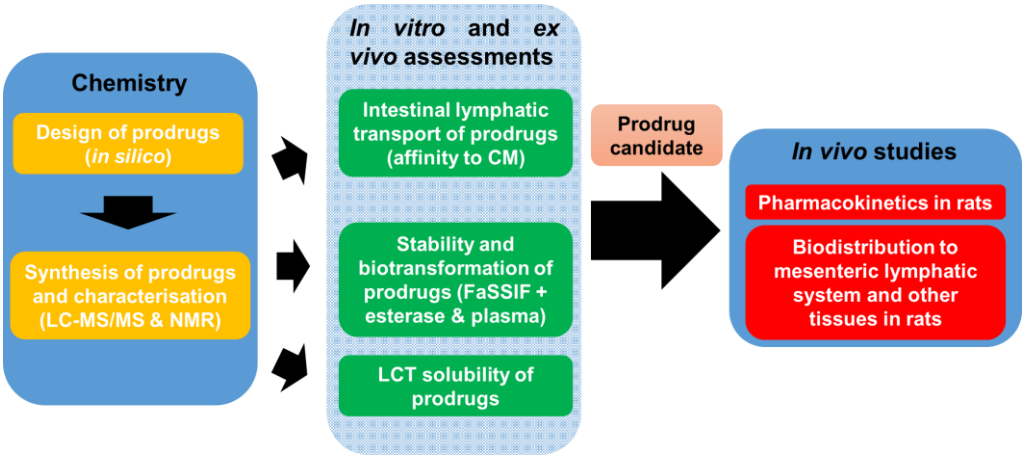

Figure 4-2. The workflow of experimental design of lipophilic ester prodrug approach for targeting DTG to mesenteric lymphatic system. CM, chylomicrons; FaSSIF, fast stated simulated fluid; LCT, long-chain triglyceride.

4.3. Results

4.3.1. Validation of HPLC bioanalytical method for the determination of DTG

4.3.1.1. Selectivity

The chromatograms of blank plasma samples were compared with DTG-spiked plasma samples for selectivity validation in six validation performances [292]. The current HPLC bioanalytical assay exhibited good selectivity as DTG peaks were separated from background peaks in blank plasma (**Figure 4-3**).

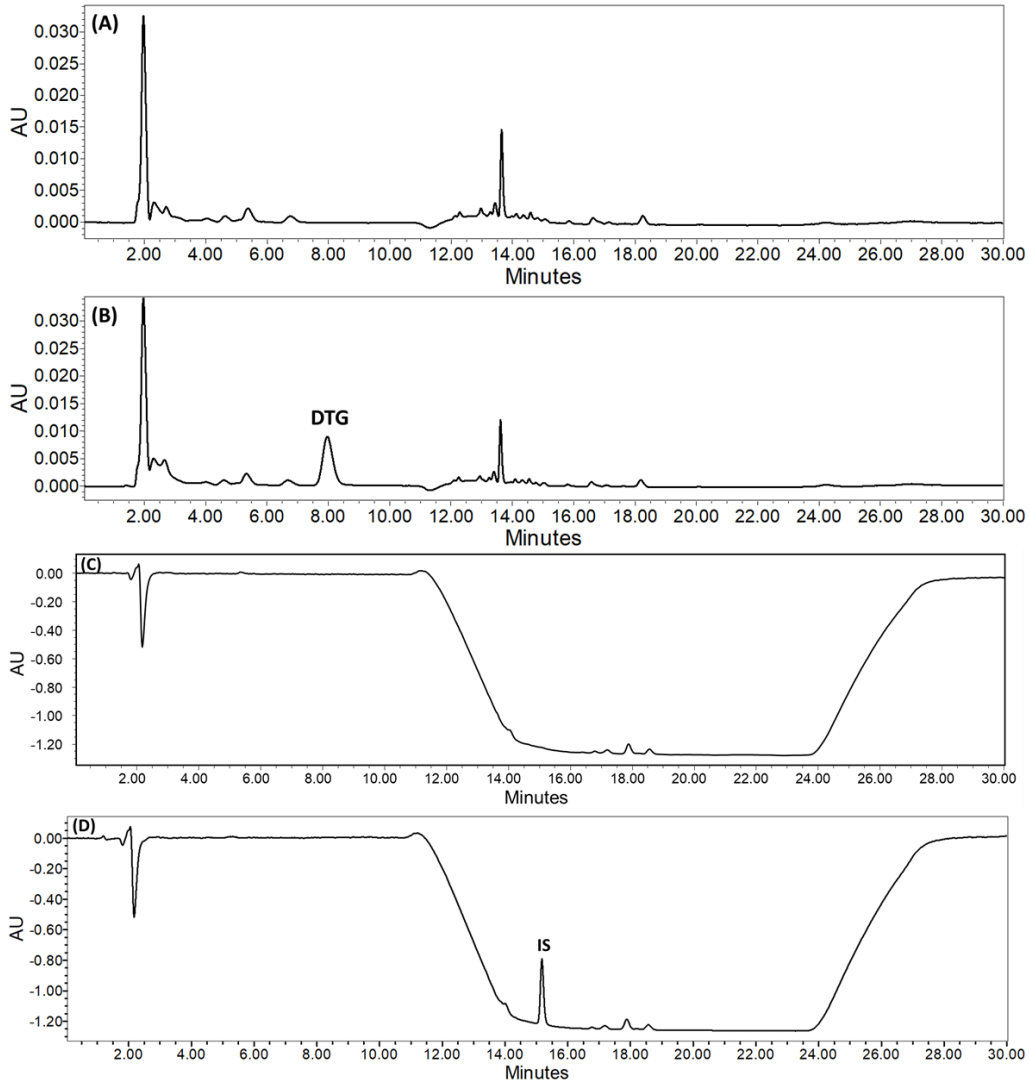

Figure 4-3. Representative chromatograms of (A) blank rat plasma sample at λ = 258 nm; (B) rat plasma spiked with 1000 ng/mL DTG at λ = 258 nm; (C) blank rat plasma sample at λ = 211 nm; (D) rat plasma spiked with 5000 ng/mL of the IS at λ = 211 nm. IS, internal standard; DTG, dolutegravir.

4.3.1.2. Sensitivity

The sensitivity of the bioanalytical method was validated by determining the LLOQ of DTG-spiked plasma samples. The LLOQ of DTG was found to be 10 ng/mL in this HPLC method (**Table 4-1**). The accuracy and precision of intra- and inter-day analyses met the acceptance criteria of RE and RSD ≤ 20% [292].

Table 4-1. Intra- and inter-day validation results for LLOQ determination of DTG in plasma.

Nominal concentration level	*Intra-day (n = 6)*		*Inter-day (n = 6)*	
	Accuracy (RSE, %)	Precision (RSD, %)	Accuracy (RSE, %)	Precision (RSD, %)
LLOQ (10 ng/mL)	3.06	8.74	12.41	2.39

4.3.1.3. Linearity

The linearity of the bioanalytical method was validated by fitting a calibration curve of DTG built with the range of 10-25000 ng/mL (described in section **2.8.3.2**) using least-squares linear regression analysis with a weighted factor (1/X). A blank plasma sample was included in each performance. This HPLC method showed good linearity for determining DTG with a correlation coefficient (r^2) over 0.99 in all calibration curves.

4.3.1.4. Stability of DTG prodrugs in rat plasma and MLNs

Prodrugs 5 and 6 were assessed their stability in rat plasma by mimicking the sampling procedure of pharmacokinetic study described in section **2.8.3.3**. Prodrug 5 has 92.4 ± 9.8% and prodrug 6 has 97.4 ± 5.2%

remaining in the plasma following the corresponding simulation. Prodrug 5 was assessed its stability in MLNs by mimicking the tissue homogenisation procedure described in section **2.8.3.5**. After the simulation, 95.8 ± 2.6% of prodrug 5 remained in this condition.

4.3.2. Prodrugs design, synthesis and structural characterisation

Physicochemical parameters of prodrugs used for *in silico* prediction of association with chylomicrons (CM), as well as predicted affinity of prodrugs to CM were calculated using ACD/I-Lab (Advanced Chemistry Development Inc., Toronto, ON, Canada) and listed in **Table 4-2**. A series of prodrug with different fatty acids was designed and predicted for their affinity to CM by the *in silico* model. Prodrugs conjugated with 12-, 14-, 16- and 18-carbon length fatty acid were selected for synthesis due to their moderate to high predicted association with CM. The description of synthetic reactions and the chemical structures of prodrugs are shown in **Figure 2-1.** Chemical synthesis and structures of DTG and its ester prodrugs. The full characterization of synthesised prodrugs can be found in **Appendix 2.** Characterisation of ester prodrugs of dolutegravir. Prodrugs 1-4 are conjugated with saturated fatty acid, while prodrugs 5 and 6 are conjugated with unsaturated oleic (C18:1) and linoleic acid (C18:2), respectively.

Table 4-2. Physicochemical properties of DTG and its prodrugs, and *in silico* prediction of association with CM [281].

Compounds	cLog $D_{7.4}$	cLog P – cLog $D_{7.4}$	PSA	H-acceptors	FRB	Density (g/cm^3)	Molar volume (cm^3)	H-donors	Predicted association with CM (%)
DTG	0.05	0.18	99.18	8	3	1.53	273.7	2	0.034
1	5.2	0	105.25	9	15	1.27	472.2	1	22.88
2	6.08	0	105.25	9	17	1.24	504.2	1	51.63
3	6.82	0	105.25	9	19	1.22	536.3	1	78.31
4	7.96	0	105.25	9	21	1.2	568.3	1	94.14
5	6.76	0	105.25	9	20	1.21	561.6	1	84.71
6	6.37	0	105.25	9	19	1.22	554.9	1	76.97

4.3.3. Association with artificial and natural CM

The affinity of DTG and prodrugs 1-6 to artificial and rat plasma-derived CM is summarized in **Figure 4-4**. Unmodified DTG showed, as predicted, no affinity to CM, while all prodrugs showed moderate to high affinity to CM. Interestingly, as the saturated fatty acid chain length increased in compounds 1-4, the association of prodrugs with CM decreased. After introducing double bonds on the long chain fatty acid in prodrugs 5 and 6, the association with CM increased with the number of double bonds introduced, suggesting the degree of unsaturation on pro-moiety correlated with drug-CM association performance.

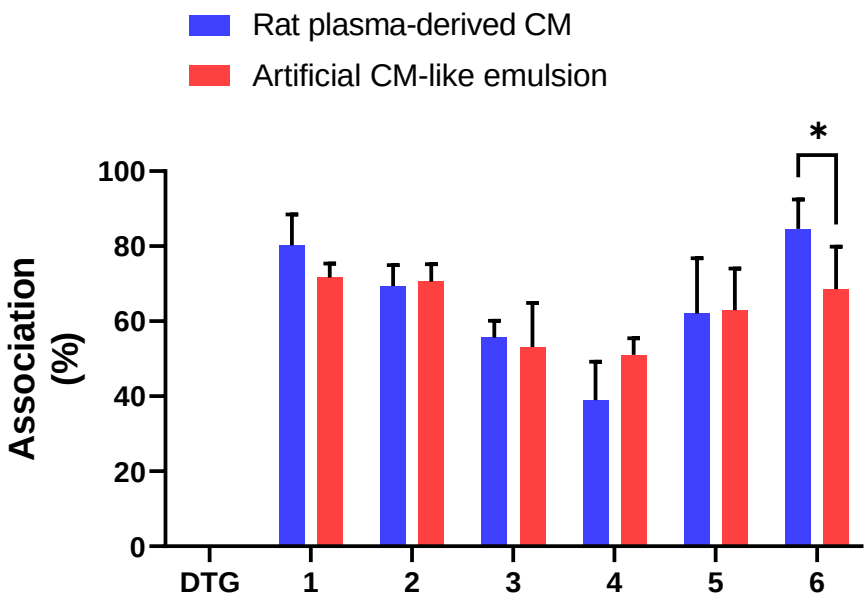

Figure 4-4. Association of DTG and its prodrugs with rat plasma-derived CM and artificial CM-like emulsion, representing the potential for intestinal lymphatic transport (n=5). Two-tailed unpaired t test was used for statistical analysis. All results are presented as mean ± SD, n=5. *, $p < 0.05$.

4.3.4. The stability of DTG and biotransformation of prodrugs in biorelevent media

The hydrolysis half-lives of DTG and its prodrugs in fasted state simulated intestinal fluid (FaSSIF) plus esterase enzyme (20 IU/mL) and plasma (mouse, rat and dog) are shown in **Figure 4-5**. Due to high stabilities, the half-lives of catabolism of unmodified DTG in FaSSIF and plasma could not be calculated. The half-lives of prodrugs catabolism in FaSSIF increased with the extension of the length of fatty acid (prodrugs 1-4) and decreased when the number of double bonds increased (prodrugs 5-6). A similar trend can also be observed in plasma of all tested species. All prodrugs, were more stable in FaSSIF than in plasma. Parent drug DTG was efficiently released from all prodrugs in plasma (**Figure 4-6**). Unmodified DTG was very stable in simulated rat fasted state gastric fluid (FaSSGF) (pH 3.9) complemented with 0.1 mg/mL pepsin at least for 60 minutes. The stability of prodrugs 2 and 5 in FaSSGF were 406 ± 37 and 805 ± 460 minutes, respectively, suggesting both prodrugs are stable in gastric environment (**Figure 4-7**). The half-lives of hydrolysis of prodrugs in FaSSIF and plasma are available in **Appendix 2.** Characterisation of ester prodrugs of dolutegravir **Figure A3-1**.

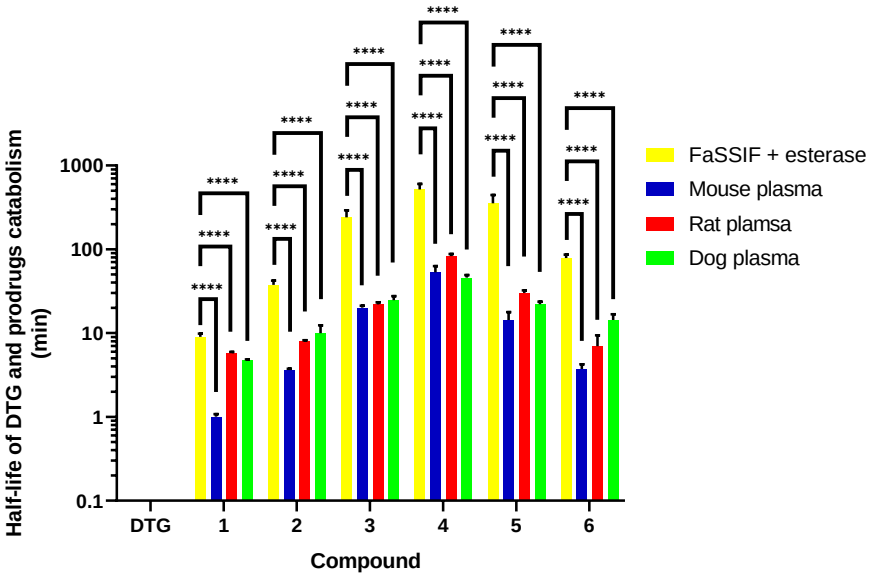

Figure 4-5. The half-lives of DTG and prodrugs catabolism in FaSSIF + esterase, mouse, rat and dog plasma. Due to the high stabilities in FaSSIF and plasma, the half-life of DTG cannot be calculated. All results are presented as mean ± SD, n = 3. One-way ANOVA followed by Dunnett's multiple comparison test was used for statistical analysis. ****, $p < 0.0001$. Additional statistical analysis for comparison of hydrolysis half-lives in FaSSIF and plasma between different prodrugs is available in **Appendix 3.** Half-life of hydrolysis of prodrugs in FaSSIF and plasma. **Figure A3-2**.

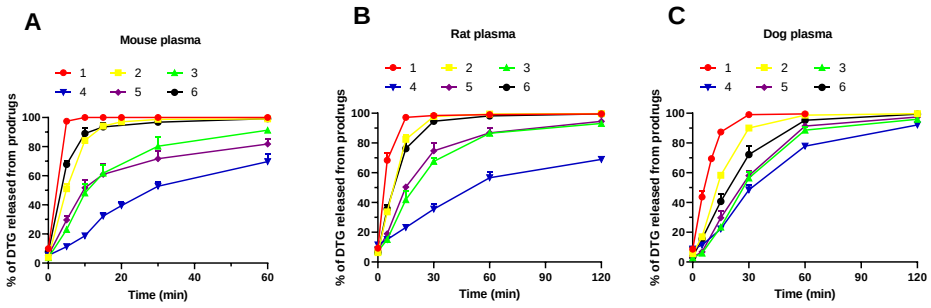

Figure 4-6. The release profiles of DTG from corresponding prodrugs in **(A)** mouse, **(B)** rat, and **(C)** dog plasma. All results are presented as mean ± SD, n = 3.

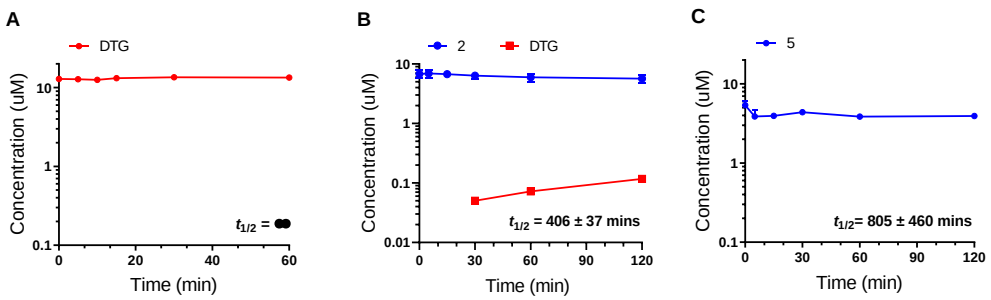

Figure 4-7. Stabilities of DTG, prodrugs 2 and 5 in rat fasted state simulated gastric fluid (FaSSGF, pH 3.9) with pepsin (0.1 mg/mL) activity. **(A)** DTG, **(B)** prodrug 2 and **(C)** prodrug 5. All results are presented as mean ± SD, n = 3.

4.3.5. Long-chain triglyceride (LCT) solubility

The solubilities of DTG and prodrugs in sesame and olive oils are summarized in (**Table 4-3**). DTG has very low solubility of 0.015 ± 0.002 mg/mL and 0.029 ± 0.004 mg/mL in sesame and olive oils, respectively. All saturated prodrugs (1-4) exhibited solubility of no more than 5 mg/mL in both oils. However, unsaturated fatty acid esters 5 and 6 showed significantly higher solubility of 49.1 ± 0.8 mg/mL and 40.4 ± 2.1 mg/mL in sesame oil, and 42.5 ± 1.5 mg/mL and 42.5 ± 5.4 mg/mL in olive oil, respectively, compared to unsaturated esters. Taking together the results of CM affinity, kinetics of DTG released in FaSSIF and plasma, and especially LCT solubility, prodrug 5 was selected as the most promising candidate for subsequent *in vivo* studies in rats.

Table 4-3. The solubility of DTG and its prodrugs in sesame and olive oils. All results are presented as mean ± SD, n = 3.

	DTG	1	2	3	4	5	6
Sesame oil (mg/mL)	**0.015 ± 0.002**	**1.2 ± 0.12**	**2.2 ± 0.09**	**2.2 ± 0.08**	**3.2 ± 0.3**	**49.1 ± 0.8[a]**	**40.4 ± 2.1[b]**
Olive oil (mg/mL)	**0.029 ± 0.004**	**1.1 ± 0.06**	**1.6 ± 0.07**	**4.5 ± 0.06**	**5.1 ± 0.05**	**42.5 ± 1.5[c]**	**42.5 ± 5.4[d,e]**

One-way ANOVA followed by Dunnett's multiple comparison test was used for statistical analysis.
[a] ****, $p < 0.0001$ compared to DTG and other prodrugs in sesame oil group.
[b] ****, $p < 0.0001$ compared to DTG and other prodrugs in sesame oil group.
[c] ****, $p < 0.0001$ compared to DTG and other prodrugs in olive oil group.
[d] ****, $p < 0.0001$ compared to DTG and other prodrugs in olive oil group.
[e] No significant difference compared to prodrug 5 in olive oil group.

4.3.6. Pharmacokinetics of DTG and prodrugs 5 and 6

The pharmacokinetic profiles of DTG and selected prodrugs in plasma were generated following intravenous (IV) bolus and oral gavage administration in lipid-free and LCT-based formulations in rats (**Figure 4-8A-B**). Pharmacokinetic parameters of DTG and prodrugs 5 and 6 were calculated based on the plasma concentration-time profiles and summarized in **Table 4-4**. The absolute oral bioavailability of DTG did not show a significant difference between lipid-free (57 ± 17%) and LCT-based (69 ± 19%) groups.

On the other hand, prodrug 5 showed an efficient release profile of active DTG following an IV bolus administration (**Figure 4-8C**). Although prodrug 5 itself was only detectable in plasma up to 24 hours after the IV bolus administration, the levels of released DTG were detectable in the systemic circulation for more than 48 hours. The AUC_{inf} of DTG following IV bolus administration of prodrug 5 is comparable to the AUC_{inf} after IV bolus administration of unmodified DTG at equivalent dose (**Table 4-4**). This suggests a complete or near complete biotransformation of prodrug 5 to active DTG *in vivo* in rats. After oral administration of prodrugs 5 in LCT-based formulation, only DTG can be detected in systemic blood (**Figure 4-8D**). This could be due to the rapid conversion of orally administered prodrug 5 in hepatic circulation or rat mesenteric lymph after intestinal lymphatic uptake. Furthermore, the elimination half-life of released DTG was significantly increased following oral administration of prodrug 5 (13.71 ± 3.56 hours) compared to oral administration of unmodified DTG with lipids (6.45 ± 0.5 hours) (**Table 4-4**). However, the

absolute oral bioavailability of released DTG following oral administration of prodrug 5 (5.4 ± 1.8%) was substantially lower than after oral administration of unmodified DTG with (69 ± 19%) or without (57 ± 17%) lipids at equivalent dose (**Table 4-4**).

We conducted a preliminary pharmacokinetic study of oral administration of prodrug 6 in LCT-based formulation to compare the oral bioavailability with prodrug 5. Results showed that although the oral bioavailability of release DTG (9.6 ± 4.4%) after oral administration of prodrug 6 in LCT-based formulation was higher in comparison to prodrug 5, it is still profoundly lower than oral administration of unmodified DTG with or without lipids at equivalent dose (**Table 4-4**).

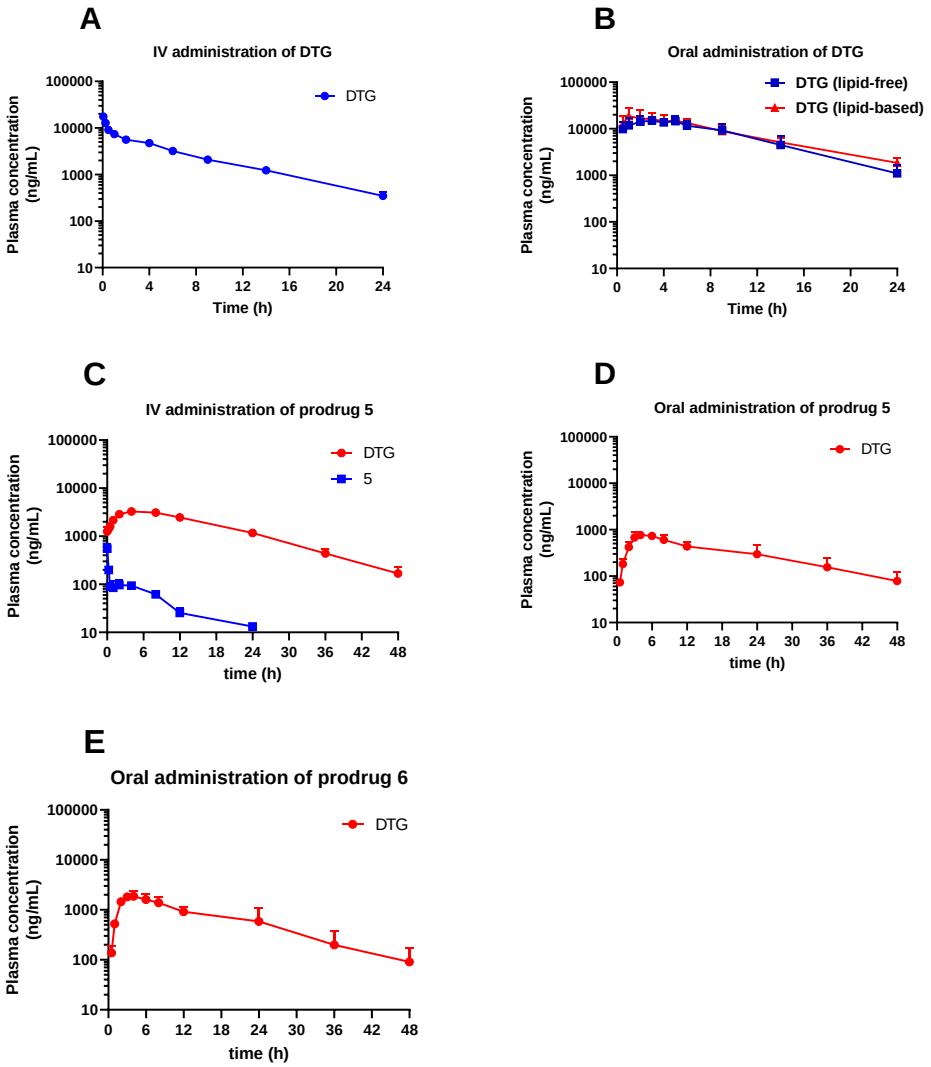

Figure 4-8. Plasma concentration-time profiles of DTG and prodrugs 5 and 6 in rats. **(A)** IV bolus of DTG sodium (1.05 mg/kg, n=4); **(B)** oral gavage administration of DTG sodium (5.25 mg/kg) in lipid-free formulation (n = 4) and with lipids (n = 6); **(C)** IV bolus of prodrug 5 (1.63 mg/kg, n = 4); **(D)** oral gavage administration of prodrug 5 (8.15 mg/kg, n = 7) in LCT-based formulation; **(E)** oral gavage administration of prodrug 6 (8.13 mg/kg, n = 2) in LCT-based formulation. All values are presented as mean ± SD.

Table 4-4. Pharmacokinetic parameters of DTG following administration of DTG and prodrugs 5 and 6 to rats. All results are presented as mean ± SD.

	PK parameters of DTG following administration of DTG			PK parameters of DTG following administration of prodrug 5		PK parameters of prodrug 5 following administration of prodrug 5		PK parameters of DTG following administration of prodrug 6
Route of administration	i.v. (n=4)	Oral		i.v. (n=4)	Oral	i.v. (n=4)	Oral	Oral
		Lipid-free (n=4)	LCT-based (n=6)		LCT-based (n=7)		LCT-based (n=7)	LCT-based (n=2)
AUC_{inf} (h*ng/mL)	60730 ± 11348	172978 ± 50856	210804 ± 58839	69619 ± 7039	16357 ± 5482	1287 ± 145	-	31442 ± 14368
C_0 (ng/mL)	17865 ± 1319	-	-	-	-	591 ± 172	-	-
C_{max} (ng/mL)	-	16519 ± 4196	21514 ± 7518	3296 ± 147	850 ± 142	-	-	1896 ± 430
$t_{1/2}$ (h)	5.37 ± 0.77	5.14 ± 0.98	6.45 ± 0.50	9.09 ± 1.10	13.71 ± 3.56***	7.3 ± 1.0	-	8.66 ± 0.60**
V_{ss} (mL/Kg)	120 ± 7	-	-	-	-	1292 ± 72	-	-
CL (mL/h/Kg)	17 ± 4	-	-	-	-	128 ± 14	-	-
F_{oral} (%)	-	57 ± 17	69 ± 19	-	5.4 ± 1.8****	-	-	9.6 ± 4.4**

AUC_{inf}, area under the curve from time zero to infinity; C_0, concentration extrapolated to time zero; C_{max}, maximum observed concentration; $t_{1/2}$, half-life; V_{ss}, volume of distribution at steady state; CL, clearance; F_{oral}, absolute oral bioavailability.

Unpaired two-tailed test was used for statistical analysis, all values are presented as mean ± SD.

**, p < .0.01 compared to DTG oral LCT-based group.

***, $p < 0.001$ compared to DTG oral LCT-based group.

****, $p < 0.0001$ compared to DTG oral LCT-based group.

4.3.7. Biodistribution of DTG and prodrug 5

The biodistribution profiles of DTG at 2, 4 and 8 hours following oral administration of unmodified DTG with and without lipids are shown in **Figure 4-9A-B**. In both lipid-free and LCT-based groups, the concentrations of DTG in mesenteric lymph and MLNs were lower than in serum at each time point. However, DTG's levels in MLNs and other tissues were higher than protein binding-adjusted IC_{90} (PA-IC_{90}) (64 ng/mL). Following oral administration of prodrug 5 in LCT-based formulation, the distribution of released DTG and intact prodrug 5 in mesenteric lymph, MLNs and other tissues were analysed at the same time points as for unmodified DTG administration (**Figure 4-10A-B**). At 2 hours following oral administration of prodrug 5, the concentration of released DTG was two-fold higher in mesenteric lymph than in serum, suggesting mesenteric lymphatic targeting of prodrug 5 and release of active drug within the lymphatic system (**Figure 4-10B**). High concentrations of prodrug 5 were found in small intestine contents and in faeces in the colon following oral administration of prodrug 5 (**Figure 4-11**). The drug concentration ratio in tissues to serum was previously used to estimate the efficiency of tissue distribution of drugs [364, 365]. Orally administered prodrug 5 increased the lymph-to-serum and MLNs-to-serum ratio of DTG concentration up to 9.4-fold and 4.8-fold, respectively, in comparison to unmodified DTG (**Figure 4-12**). This suggests that orally administered prodrug 5 increased the selectivity for targeting of DTG to mesenteric lymphatics.

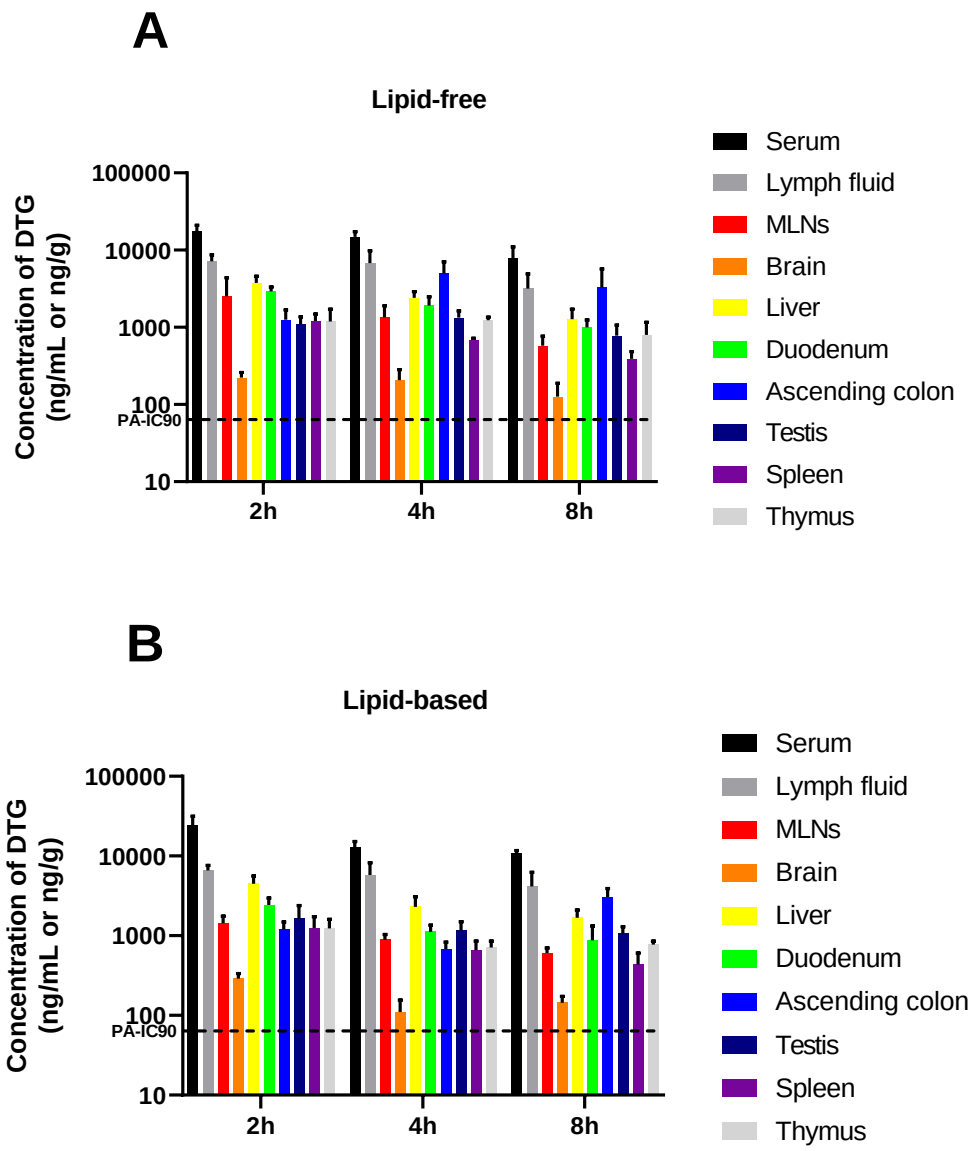

Figure 4-9. Biodistribution of DTG at 2, 4 and 8 hours following oral administration of DTG sodium (at an equivalent dose of 5 mg/kg of DTG) **(A)** in lipid-free formulation and **(B)** with lipids. All results are presented as mean ± SD, n=4. PA-IC_{90} = 64 ng/mL.

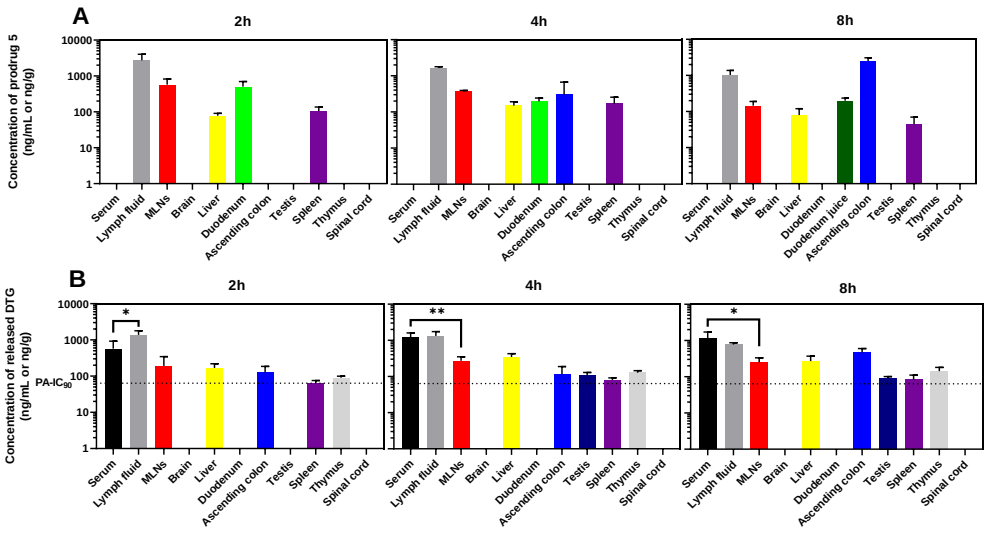

Figure 4-10. Biodistribution of **(A)** prodrug 5 and **(B)** DTG at 2, 4 and 8 hours following oral administration of prodrug 5 (at an equivalent dose of 5 mg/kg of DTG) in LCT-based formulation. All results are presented as mean ± SD, n=4. PA-IC_{90} = 64 ng/mL. *, $p < 0.05$; **, $p < 0.01$.

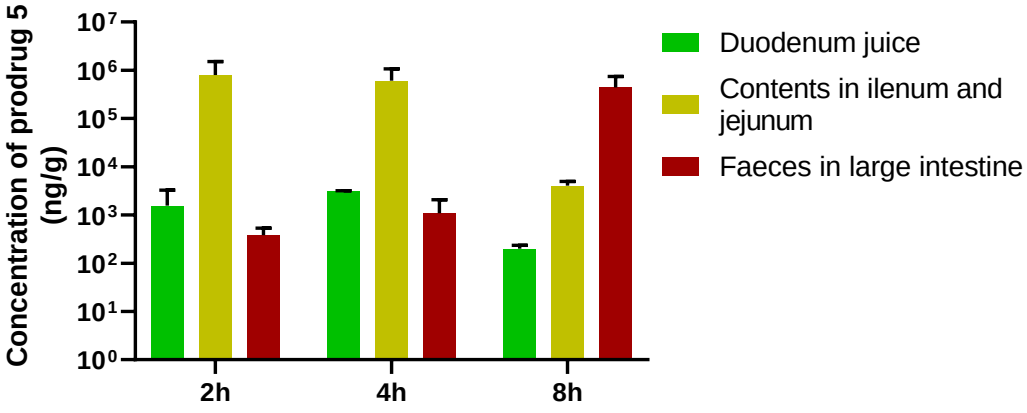

Figure 4-11. Concentrations of prodrug 5 in duodenum juice, contents in ileum and jejunum and faeces in large intestine at 2, 4 and 8 hours following oral administration of prodrug 5 (at an equivalent dose of 5 mg/kg of DTG) in LCT-based formulation. All results are presented as mean ± SD, n=4.

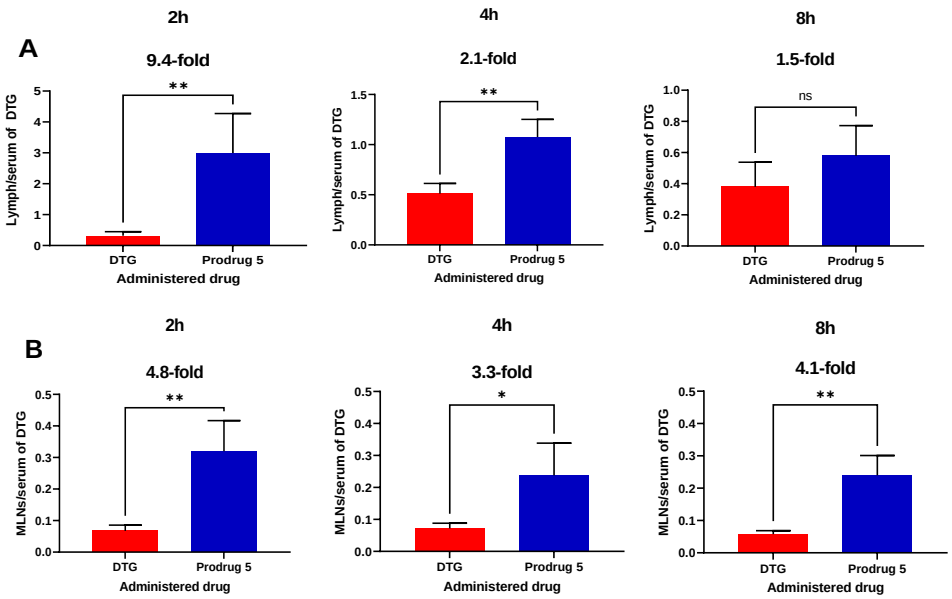

Figure 4-12. (A) Lymph to serum and **(B)** MLNs to serum ratio of the concentration of DTG following oral administration of unmodified DTG or prodrug 5 in LCT-based formulation. All results are presented as mean ± SD, n = 4. Unpaired two-tailed t test was used for statistical analysis. ns, no significant; *, $p < 0.05$; **, $p < 0.01$.

4.3.8. *In vivo* distribution of DTG and prodrug 5 into rat CM in mesenteric lymph

The association of DTG or prodrug 5 with rat CM in mesenteric lymph *in vivo* was assessed by isolating CM from mesenteric lymph samples. DTG was undetectable in CM fraction and mostly distributed into CM-free fraction in rat mesenteric lymph following oral administration of unmodified DTG in lipid-free formulation (**Figure 4-13**). On the other hand, 62% of prodrug 5 were associated with CM in rat mesenteric lymph following oral administration of prodrug 5 in LCT-based formulation, while no released DTG was detected in either CM or CM-free fraction (**Figure 4-14**).

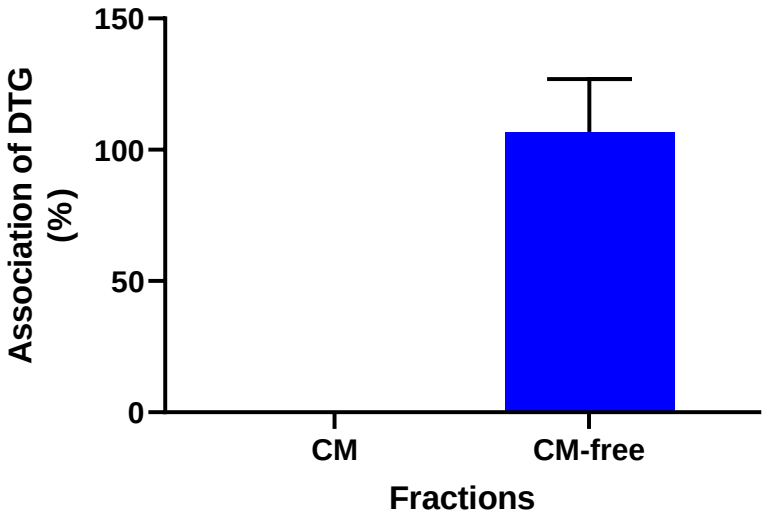

Figure 4-13. The association of DTG with CM in rat mesenteric lymph following oral administration in lipid-free formulation. The loaded volume of lymph fluid samples for ultracentrifugation were 30 µL. CM fraction is the supernatant fraction; CM-free fraction include each density layer (1.006, 1.019, 1.063 and 1.1 g/mL). All results are presented as mean ± SD, n = 5.

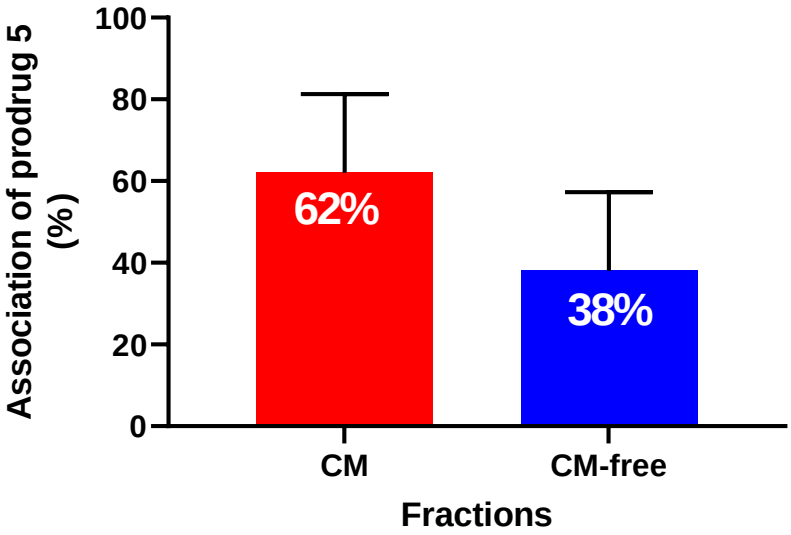

Figure 4-14. The association of prodrug 5 with CM in rat mesenteric lymph following oral administration in LCT-based formulation. The loaded volume of lymph fluid samples for ultracentrifugation were between 16-50 µL. CM fraction is the supernatant fraction; CM-free fractions include each density layer (1.006, 1.019, 1.063 and 1.1 g/mL). All results are presented as mean ± SD, n = 3.

4.3.9. Intraluminal processing of prodrug 5 and 6

Following results of unexpectedly low systemic exposure of DTG after oral administration of prodrug 5, the mechanism of small intestine lumen processing of prodrug 5 formulated in LCT-based vehicle was investigated by an *in vitro* lipolysis system. The results of intraluminal post-lipolysis distribution of prodrug 5 are shown in **Figure 4-15A**. Following the lipolysis of sesame oil formulation, around 5.8% of prodrug 5 dose was found in micellar layer (assuming the readily absorbed fraction). More than 90% of prodrug 5 was distributed into unprocessed lipid or precipitated into sediment fraction, indicating poor availability for absorption.

Since prodrug 6 was also low oral bioavailable following oral administration in LCT formulation, it was assessed for its intestinal absorption by means of *in vitro* lipolysis (**Figure 4-15B)**. Following the lipolysis reaction, only 12.1% of prodrug 6 dose was found in micellar fraction. The majority of prodrug 6 dose were distributed into lipid or sediment fraction, indicating low intestinal absorption. Interestingly, the levels of prodrugs 5 and 6 distributed in the micellar fraction *in vitro* (5.8% and 12.1%, respectively) (**Figure 4-15**) were very close to their oral bioavailability *in vivo* (5.4% and 9.6%, respectively) (**Table 4-4**).

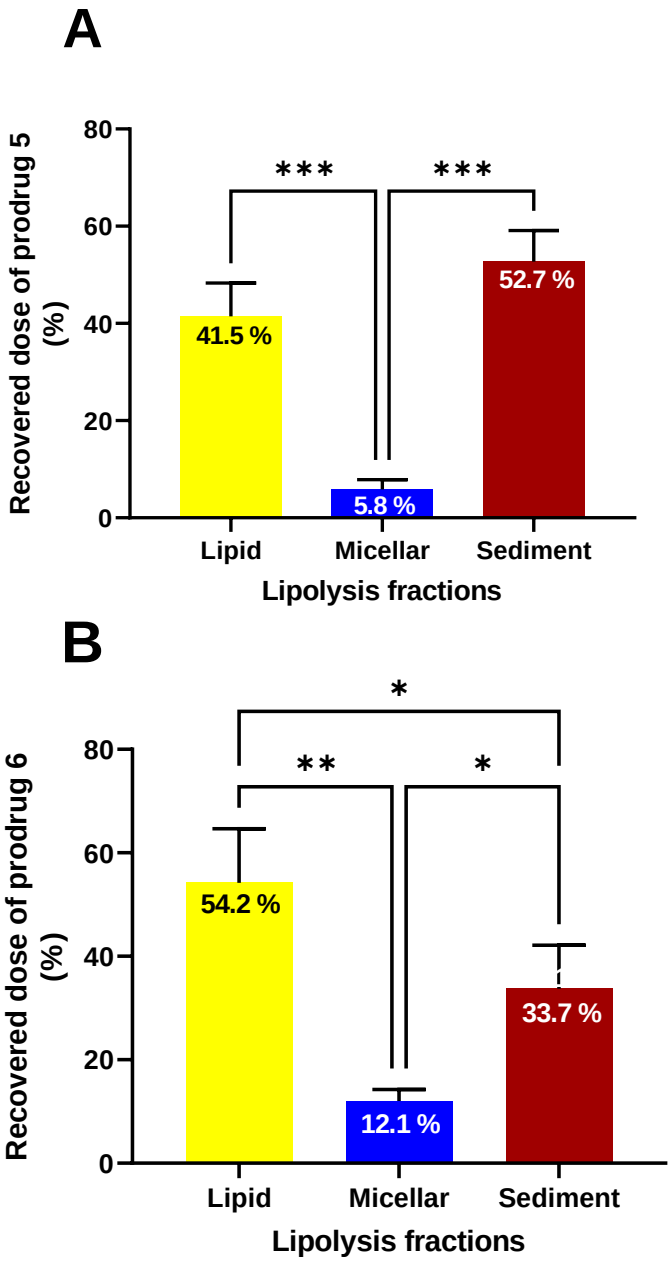

Figure 4-15. Distribution of prodrugs 5 and 6 in the lipid, micellar and sediment fractions after lipolysis of 80 µL of LCT-based formulation containing **(A)** prodrug 5 at a concentration of 8.15 mg/mL and **(B)** prodrug 6 at a concentration of 8.13 mg/mL. All results are presented as mean ± SD, n = 3. One-way ANOVA followed by Tukey multiple comparisons was used for statistical analysis. *, $p < 0.05$; **, $p < 0.01$; ***, $p < 0.001$. DTG levels were undetectable in all fractions.

4.4. Discussion

The establishment of latent cellular and anatomical viral reservoirs is one of the major obstacles to achieving a cure for HIV infection. Mesenteric lymph nodes (MLNs) are one of the most important and largest reservoirs of HIV [104]. Poor penetration of drugs into these reservoirs is an important limitation of current ART regimens [132]. A combination approach of lipophilic prodrugs and long-chain triglyceride (LCT)-based formulation was reported to be efficient for targeting HIV protease inhibitors (PIs) to MLNs [229] rather than an LCT-based formulation-only approach [360]. This work aimed to develop a lipophilic ester prodrug system coupled with LCT-based formulation to achieve targeting of HIV integrase inhibitor dolutegravir (DTG) into HIV reservoirs in MLNs through intestinal lymphatic transport.

4.4.1. The affinity of DTG prodrugs to chylomicrons (CM)

The degree of intestinal lymphatic transport of drugs was reported in multiple studies to have a strong correlation with their affinity to CM [248, 366]. DTG is not a highly lipophilic compound (cLog P = 0.5 [362]) and has negligibly predicted and no detected experimental association with CM (**Table 4-2** and **Figure 4-4**). We previously reported that increasing the lipophilicity of compounds by lipophilic ester prodrug approach can dramatically increase the affinity to CM [229, 256]. Therefore, highly lipophilic alkyl ester prodrugs of DTG were designed. Based on the predicted affinity value to CM, six prodrugs were synthesised for further experimental assessments (**Table 4-2**). All synthesised prodrugs

showed a moderate to high experimental association (30-70%) with artificial and natural CM (**Figure 4-4**), indicating a high potential for intestinal lymphatic transport. Interestingly, there was a decrease in the affinity of prodrugs to CM when the saturated alkyl chain was increased above C12. Similar results were observed in our previous studies [229, 256]. It has been proposed that an interplay between specific physicochemical properties, such as lipophilicity and molecular weight, leads to a limited window favouring higher affinity to CM [229].

4.4.2. The stability and biotransformation of DTG prodrugs in biorelevant media

In order to efficiently deliver active drugs to the intestinal lymph and MLNs, the ideal lipophilic prodrug has to be stable in the intestinal lumen, but rapidly enzymatically degraded in the lymph fluid following uptake into the intestinal lymphatic system. Therefore, prodrugs were assessed for their stability in a fasted state simulated intestinal fluid (FaSSIF) supplemented with esterase activity, representing the environment of the intestinal lumen and plasma (a surrogate of lymph [229, 256]). The esterase used in this study was extracted from porcine liver and mainly contains carboxylesterases [367]. Carboxylesterases are present in the liver and gastrointestinal tract [368] and have been used as additional enzymes in assessing the stability of ester prodrugs in FaSSIF, as they are responsible for the metabolism of compounds containing ester groups (including carboxyl esters) [229, 256, 363]. All prodrugs exhibited good stability in the conditions mimicking the intestinal environment

(**Figure 4-5**) and rapid DTG release profiles in plasma of all tested species (**Figure 4-6)**, suggesting that the current prodrug system based on simple alkyl esters has the potential to deliver active DTG to intestinal lymph and MLNs efficiently. It is worth noting that only 'activated ester' prodrugs achieved the outcome of good stability in the intestine but rapid release in the plasma in our previous studies [229, 256]. However, in the case of DTG prodrugs, the 'activated ester' approach does not seem to be necessary as this outcome is achieved with simple alkyl esters.

4.4.3. The solubility of DTG prodrugs in LCT

The solubility of prodrug candidates in LCT was assessed in sesame and olive oils. As both sesame and olive oils are mainly composed of triglycerides containing unsaturated long-chain fatty acid of oleic and linoleic acids, they were reported to efficiently promote the intestinal lymphatic transport of lipophilic compounds [260]. The results indicate that the solubility of prodrugs (**Table 4-3**) was more related to the degree of saturation of conjugated alkyl esters than the chain length of the conjugate (**Figure 2-1**). Taken together, the results of CM affinity, stability and DTG released in FaSSIF and plasma, and especially LCT solubility, prodrug 5 was selected as the most promising candidate for subsequent *in vivo* studies in rats.

4.4.4. Pharmacokinetics of DTG and prodrugs 5 and 6

A good oral bioavailability (75.6%) was previously reported following oral administration of DTG in a lipid-free formulation to rats [369]. This study

also observed similar results (**Table 4-4**). The oral bioavailability of DTG did not show significant differences between lipid-free (57±17%) and LCT-based groups (69±19%), which is in accordance with its negligible affinity to CM (**Figure 4-4**) and undetectable DTG in lipoprotein fraction in rat mesenteric lymph following oral administration in lipid-free formulation (**Figure 4-13**). On the other hand, the absolute systemic oral bioavailability of DTG was quite low following the oral administration of prodrugs 5 and 6 (**Table 4-4**). This result was surprising, as lipophilic prodrug systems designed for intestinal lymphatic targeting were previously reported to also improve the systemic oral bioavailability of the parent drug, or at least comparable to the parent drug [229, 256, 370, 371]. Notably, prodrugs 5 and 6 themselves were not detected in plasma after oral administration. Furthermore, the prolonged terminal slope of released DTG in plasma was observed following oral administration of either prodrugs 5 or 6, suggesting flip-flop kinetics. It is likely that prodrugs were taken up into MLNs through intestinal lymphatic transport and then slowly released active DTG into the lymph and, subsequently, the systemic circulation.

4.4.5. Biodistribution of DTG and prodrug 5 in the mesenteric lymphatic system and other reservoirs

The results showed similar concentrations of DTG between lipid-free and LCT-based groups in systemic blood, mesenteric lymph, MLNs and other viral reservoirs following oral administration of unmodified DTG (**Figure 4-9**). This suggests that lipids do not affect the absorption and distribution

of unmodified DTG. It should be noted that the levels of DTG were lower in MLNs and all other tissues in comparison to serum, indicating that MLNs and other reservoirs were not selectively targeted when unmodified DTG was orally administered (**Figure 4-9**). After oral administration of prodrug 5, it was indeed targeted to the intestinal lymphatic system and efficiently released active DTG within 2 hours (**Figure 4-10**). We found that 62% of prodrug 5 were associated with CM in mesenteric lymph, suggesting that the intestinal lymphatic transport of prodrug 5 was driven by drug-CM association (**Figure 4-14**). The lymph-to-serum and MLNs-to-serum ratios of concentration of DTG were substantially increased up to 8.4-fold and 4.8-fold, respectively, following oral administration of prodrug 5 compared to oral administration of unmodified DTG **(Figure 4-12**). This suggests that the lipophilic prodrug system can improve the selectivity of targeting of DTG to the mesenteric lymph and MLNs. However, although oral administration of prodrug 5 was shown to selectively target DTG to mesenteric lymphatics, the levels of prodrug 5 and released DTG in MLNs and other tissues were limited by low systemic bioavailability. It was hypothesised that the low oral bioavailability of DTG might be due to the low extent of absorption of the prodrug from the intestinal lumen. This hypothesis was further tested by collecting and analysing the duodenum juice, contents in the ileum and jejunum, and faeces in the colon following the oral administration of prodrug 5. Results showed extremely high concentrations of prodrug 5 in the upper and lower parts of the intestinal tract (**Figure 4-11**). This was surprising, as in our and other groups previous reports, highly lipophilic

drugs and prodrugs were well absorbed and exhibited enhanced systemic bioavailability with high concentrations in mesenteric lymph, MLNs and plasma following oral administration with LCT-based formulations [229, 255, 256, 259, 274, 287, 366, 372-375]. To shed light on the intraluminal processing of prodrug 5 in the presence of LCT, *in vitro* lipolysis studies were conducted.

4.4.6. *In vitro* lipolysis of LCT-based formulation of prodrugs 5 and 6

The LCT-based formulation containing prodrugs 5 and 6 was evaluated by an *in vitro* lipolysis model. This model is commonly used to aid in designing and developing the lipidic delivery systems of oral drugs as it simulates the process of lipid digestion in the small intestine [257, 287, 373]. During lipolysis in the small intestine, triglycerides are hydrolysed into 2-monoglyceride and fatty acids by pancreatic lipase. The lipid breakdown products, bile salts and co-formulated drugs form mixed micelles [376, 377]. Following lipolysis, lipid and sediment phases are considered not readily absorbed fractions, while the aqueous micellar phase represents the fraction readily available for intestinal absorption [378]. The results showed that half of the dose of prodrug 5 precipitated during the lipids digestion process (**Figure 4-15A**). Similar rapid precipitation of lipophilic drugs during lipolysis has been previously reported [379, 380]. It was previously suggested that the physicochemical properties of the compound might affect the nature of the precipitated form (amorphous or crystalline) [378, 381]. The high

amount of precipitated prodrug 5 and limited distribution into micellar fraction could explain high levels of unabsorbed prodrug 5 in the intestinal tract contents (**Figure 4-11**) and low oral bioavailability of DTG following oral administration of prodrug 5 (**Table 4-4**), respectively. Around 5.8% of the prodrug 5 dose was recovered in micellar fraction available for absorption. This number, in fact, is very close to the absolute bioavailability of DTG following oral administration of prodrug 5 (5.4%). Although the role of membrane permeability cannot be completely ruled out, the distribution of prodrug 5 into the micellar fraction seems to be a good predictor of the oral bioavailability of DTG when administered orally to rats in the form of prodrug 5. Similar results were observed in the case of prodrug 6. After the *in vitro* lipolysis, 12.1% prodrug 6 was recovered in the micellar fraction, which is close to 9.6% of oral bioavailability of released DTG following oral administration of prodrug 6 in LCT-based formulation (**Figure 4-15B**). Interestingly, *in vitro* lipolysis has been reported not to predict the oral bioavailability of drugs with high intestinal lymphatic transport. The model only simulates the intraluminal processing of drugs rather than the overall absorption and transport process, including intestinal lymphatic transport [260, 382-385]. The exact mechanism and reasons for the substantial precipitation of orally administered lipophilic esters of DTG during the *in vitro* lipolysis studies are unclear and warrant further investigation. However, these results indicate that despite previous reports of the non-predictability of *in vitro* lipolysis for systemic bioavailability of compounds prone to intestinal lymphatic transport, in some cases, *in vitro* lipolysis could be highly

predictive. It could be useful to include in vitro lipolysis studies in screening routine for drugs or prodrug candidates for intestinal lymphatic targeting.

4.4.7. Conclusion

Oral administration of unmodified DTG in rats resulted in good absolute oral bioavailability, but with levels in tissues, including MLNs, below the levels in serum. A lipophilic prodrug system was designed and assessed for selective targeting of DTG to MLNs through intestinal lymphatic transport. Although the selected prodrug candidate showed limited systemic exposure to DTG, the tissue/serum ratio of DTG levels in MLNs, and thus targeting selectivity, was improved by this approach. Two unexpected phenomena were found in this study. Firstly, poor oral bioavailability was observed with lipophilic prodrug in the presence of LCT. Secondly, in this work in vitro lipolysis model predicted quite well the in vivo systemic bioavailability of a compound with substantial intestinal lymphatic transport. Both phenomena warrant further investigation, but it could be useful to include in vitro lipolysis assessment in studies aimed to select lipophilic drugs and prodrugs for targeting the MLNs.

5. GENERAL DISCUSSION AND FUTURE WORK

The benefits from intestinal lymphatic transport of orally administered drugs include the improvement of systemic oral bioavailability and directly targeting drugs to the mesenteric and retroperitoneal lymphatic system. This PhD work focuses on delivering antiretroviral drugs (ARVs) to the HIV reservoirs in mesenteric lymph nodes (MLNs) utilising the drug-chylomicrons (CM) association-driven intestinal lymphatic transport. In the first part of this work, a lipophilic HIV protease inhibitor (PI), tipranavir (TPV), was investigated for intestinal lymphatic transport facilitated by a long-chain triglyceride (LCT)-based formulation approach. The second part of this study is to optimise the intestinal lymphatic targeting of dolutegravir (DTG), an HIV integrase strand inhibitor (INSTI), to the viral reservoir in MLNs by means of a combination approach of lipophilic ester prodrugs and LCT-based formulation.

5.1. General discussion

5.1.1. LCT-based formulation facilitated intestinal lymphatic transport of tipranavir (TPV)

5.1.1.1. Intestinal lymphatic transport potential of TPV

Based on the *in silico* prediction of all protease inhibitors, only lopinavir (LPV) and TPV have moderate (> 50%) association with chylomicrons (CM) (**Figure 3-4** and **Table 3-2**). Among the physicochemical properties applied to the *in silico* model, log $D_{7.4}$ seems to be the primary parameter that affects the affinity of protease inhibitors to chylomicrons (CM) and

subsequent intestinal lymphatic transport. The TPV has the highest log $D_{7.4}$ and have the highest affinity to CM and potential of intestinal lymphatic transport. Other physiochemical properties used in the *in silico* prediction of protease inhibitors did not have relevant for intestinal lymphatic transport. TPV is highly lipophilic with an experimental log P of 6.9 [386] but a low LCT solubility of 5.9 ± 0.3 mg/mL (section **3.3.2**, **Chapter 3**). It seems that TPV does not meet the requirements (log $D_{7.4}$ > 5 [238] and LCT solubility > 50 mg/mL [224]) for intestinal lymphatic transport due to insufficient LCT solubility. However, these two factors were challenged in many studies. Myers et al. reported that penclomedine (log $D_{7.4}$ 5.48 and LCT solubility at 175 mg/mL) only has 3% lymphatic bioavailability in rats after being administered in soybean oil and triolein emulsion [387]. Another study of a lipid modulator, CI-976 (log $D_{7.4}$ 5.83, LCT solubility >100 mg/mL), demonstrated that the recovered dose in the rat mesenteric lymph was less than 1% following administration in a lipidic emulsion [388]. Trevaskis et al. investigated the intestinal lymphatic transport of two cholesterol ester transfer protein inhibitors (CETPis), CP524,515 (Log $D_{7.4}$ 6.13, LCT solubility > 50 mg/mL) and CP532,623 (Log $D_{7.4}$ 5.68, LCT solubility < 50mg/mL), following oral administration in a lipid-based formulation to dogs [389]. Although the LCT solubility of CP532,623 does not exceed 50 mg/mL, it has substantial intestinal lymphatic transport. This indicates that, in some cases, these criteria are not predictive of intestinal lymphatic transport of drugs. Gershkovich and Hoffman demonstrated that the degree of association of lipophilic compounds with CM strongly correlates with their

intestinal lymphatic transport in rats [237]. TPV was predicted to have a moderate affinity to CM (57%) *in silico* [238] and actually had moderate to high experimental association with artificial (32 ± 5%) and natural CM (67 ± 6%) (**Figure 3-4B**, **Chapter 3**). In our previous study, cannabidiol (CBD) was found to have a high affinity to artificial (78.1%), rat (73.7%) and human (67.7%) CM [254]. The subsequent biodistribution study has consistently shown profoundly higher concentrations of CBD in mesenteric lymph compared to plasma (as much as 250-fold) following oral administration with LCT to rats, suggesting that CBD has intestinal lymphatic transport in the presence of lipids. A study of lopinavir (LPV) demonstrated that LPV has a negligible affinity to CM, which is consistent with the absence of intestinal lymphatic transport after administration in an LCT-based formulation to rats [229]. Therefore, the moderate to high affinity of TPV to CM indicates the potential for intestinal lymphatic transport when administered orally with lipids, especially LCT.

5.1.1.2. The mechanism of association of TPV with CM

In this study, the affinity of TPV to natural CM (66.2%) is significantly higher than artificial CM (31.7%). The artificial CM used for *in vitro* assessment of drug association with CM in this study is intralipid®. Intralipid is an emulsion of triglyceride-rich particles which comprises soybean oil, egg yolk phospholipids, glycerine and water. The components of soybean oil are TG comprised of long-chain fatty acid, including linoleic acid (C18:2, 44-62%), oleic acid (C18:1, 19-30%), palmitic acid (C16:0, 7-14%), linolenic acid (C18:3, 4-11%), and stearic

acid (C18:0, 1.4-5.5%) [390]. Similar to intralipid, the core of natural CM is mainly composed of TG (85-92%) and cholesterol esters, coated by phospholipids (6-12%), cholesterol (1-3%) and proteins (2%) [391]. Since intralipid and natural CM have similar components, intralipid has been commonly used as a surrogate of natural CM in many studies [229, 238, 239, 254, 256, 392]. Since the difference between intralipid and natural CM is the emulsion droplet surface material, we suspected that TPV might interact with the interfacial components of natural CM. A similar case was reported in a study of the lymphatic absorption of the two CETPis, CP524,515 and CP532,623 [228]. Firstly, the ratio of the maximum mass of CP532,623 to TG (mg/g) in the lymph was significantly higher than its LCT solubility following the duodenal administration to rats. This indicates that additional factors other than LCT solubility also drive the lymphatic absorption of CP532,623. Furthermore, CP524,515 and CP532,623 have shown a higher affinity to natural CM or colloidal spherical particles with TG-rich core and amphiphilic surface than a simple homogenous lipids mixture. This suggests that interfacial interaction sometimes impacts the association of drugs with CM. In current study, only approximately 35% of TPV was associated with CM and other lipoproteins in rat mesenteric lymph (**Figure 3-7**, **Chapter 3**). It is worth noting that the environment in the lymph fluid is more complex than the conditions we used in the *in vitro* and *ex vivo* models. Lymph fluid contains CM, very low-density lipoprotein (VLDL), proteins and cells. Since the association of compounds with CM happens within the enterocytes [251], the associated compounds may redistribute to VLDL,

proteins and cells once they are secreted into the lymph fluid. Gershkovich et al. [238] previously found that the apolipoproteins on the surface of lipoproteins play a certain role in the process of drug uptake and may lead to a weaker association than other compounds. Thus, TPV is likely to redistribute to VLDL, proteins and cells in the lymph fluid.

5.1.1.3. Intestinal lymphatic transport of TPV, but not targeting to MLNs

The plasma pharmacokinetic profiles of TPV did not show significant differences when TPV was administered to rats in either lipid-free or LCT-based formulations (**Figure 3-5** and **Table 3-3**, **Chapter 3**). Our result demonstrated a moderate oral bioavailability of TPV (36 ± 3%) after administering of lipid-free formulation to rats. Although the high-fat meal was reported to increase the systemic bioavailability of TPV in human volunteers [182], in this study, the LCT-based formulation did not significantly increase the oral bioavailability (44 ± 4%) of TPV in rats (**Table 3-3**, **Chapter 3**). It is believed that only oral administration of highly lipophilic drugs or prodrugs with LCT can achieve high drug levels in mesenteric lymph and MLNs by intestinal lymphatic transport. Zgair et al. have shown that the concentrations of CBD in MLNs were profoundly higher at plasma $t_{max\text{-}1}$ and t_{max} after oral administration in LCT-based formulation in comparison to lipid-free formulation [255]. However, despite TPV having moderate intestinal lymphatic transport, the levels of TPV in MLNs at plasma $t_{max\text{-}1}$ and t_{max} after oral administration in LCT-based formulation were comparable to lipid-free formulation (**Figure 3-6**,

Chapter 3). The extent of drug distribution into tissues is mainly determined by plasma protein binding and tissue binding. A drug circulating in the systemic blood can be either unbound (free fraction) or protein-bound. Only unbound drugs can distribute into tissues. The proteins responsible for binding to drugs in the plasma are albumin, alpha-1 acid glycoprotein, and lipoproteins. Acidic drugs are mainly bound to albumin, and basic drugs are usually bound to alpha-1 acid glycoprotein and lipoproteins [393]. TPV is an acidic molecule at physiological pH with a high affinity to plasma albumin (>99.9%). The required concentration of TPV to saturate the plasma albumin binding site is between 10 and 100 µM (6027 to 60266 ng/mL) [173]. Plasma concentration beyond this threshold will increase the fraction of unbound TPV. Since the albumin concentration in the interstitial fluid is 20 to 30% of that in plasma [394], the saturated concentration of TPV to the albumin in the lymph should be between 2 and 30 µM (1205 to 18080 ng/mL). Following oral administration in LCT-based formulation, the concentrations of TPV in rat mesenteric lymph at both t_{max} and t_{max-1} time points were 6140 and 5915 ng/mL, respectively (**Figure 3-6A-B**, **Chapter 3**), which did not exceed the threshold to saturate the albumin in the lymph. This suggests that insufficient targeting of TPV to MLNs might be due to low levels of free TPV in mesenteric lymphatics.

5.1.2. Lipophilic ester prodrugs combined with LCT-based formulation to optimise the intestinal lymphatic transport of DTG

5.1.2.1. Pharmacokinetics and tissue distribution of unmodified DTG

Current work has shown that DTG has similar oral bioavailability when administered in lipid-free (polyethylene glycol 400 (PEG 400)/non-pyrogenic water/ethanol (70:20:10, *v*/*v*/*v*)) (57 ± 17%) and LCT (69 ± 19%) formulations at a dose of 5 mg/kg to rats (**Table 4-4**, **Chapter 4**). This is close to a previous study showing an oral bioavailability (75.6%) of DTG in rats when given in a lipid-free solution formulation (dimethylsulfoxide (DMSO): Solutol®:50mM *N*-methylglucamine in 3% mannitol (1:1:8, v:w:v)) at the same dose to ours [369]. Following IV and oral administration of unmodified DTG, we observed the enterohepatic circulation of the drug, which may contribute to the oral bioavailability (**Figure 4-8A-B**, **Chapter 4**). It has been shown that the absorption of DTG was limited by dissolution rate and solubility in the intestine [369]. When orally administered a suspension of DTG at a high dose (50 mg/kg) to rats, over 90% of the administered dose of intact DTG was recovered in faeces, indicating that unabsorbed DTG was primarily eliminated through faeces. The primary metabolism pathway of DTG is the orthologous UDP glucuronosyltransferase 1A1 (UGT1A1)-mediated glucuronidation [395]. The ether glucuronide-conjugated DTG was found in the bile following the oral administration of DTG [369], suggesting that

absorbed DTG could recirculate into the intestine through biliary excretion. However, the ether glucuronide-conjugated DTG was not detected in the faeces, meaning it may convert to the DTG in the intestine and excreted through the faeces or be reabsorbed into the systemic circulation (enterohepatic circulation).

To our knowledge, the tissue distribution profile of DTG in rats after oral administration has not been well established. In the current work, we demonstrated the tissue distribution profiles of DTG in a number of HIV reservoirs at 2, 4, and 8 hours following a single oral gavage administration of DTG in lipid-free and LCT formulations to rats (**Figure 4-9**, **Chapter 4**). The levels of DTG in MLNs and other reservoirs were lower than in serum, but above the PA-IC_{90} at 64 ng/mL, in both lipid-free and LCT groups. Labarthe et al. have studied the tissue distribution of tenofovir disoproxil fumarate, emtricitabine, and DTG, at the steady state following a seven-day oral administration to mice [365]. Among the tested drugs, DTG showed the lowest penetration (below the PA-IC_{90} at steady-state) to the HIV reservoir tissues, including the digestive tract (small intestine, caecum, and colon), the lymphatic system (lymph nodes, spleen, and thymus), the brain, the metabolism and excretion tissues (liver and kidney), and other tissues (pancreas, adipose tissue, and lung). It is important to note that poor drug distribution to mesenteric lymphatics (mesenteric lymph fluid and MLNs) and other HIV reservoirs could limit the treatment efficacy of ARVs for controlling or removing latent viruses within the viral sanctuaries. Intestinal lymphatic transport is a potential pathway for targeting orally administered drugs to MLNs and other deep

reservoirs. However, comparable levels of DTG in MLNs were observed between lipid-free and LCT groups, suggesting negligible or no intestinal lymphatic transport of unmodified DTG after oral administration in the presence of lipids. This is in accordance with the fact that DTG has no association with artificial and natural CM (**Figure 4-4**, **Chapter 4**) and lipoproteins in rat mesenteric lymph *in vivo* (**Figure 4-13**, **Chapter 4**). We previously demonstrated that LPV has no affinity for CM, consistent with its negligible intestinal lymphatic transport following oral administration in LCT formulation to rats [229]. A lipophilic ester prodrug approach is then required to enhance the drug-CM association for intestinal lymphatic transport.

5.1.2.2. Assessments of Intestinal lymphatic transport potential of lipophilic ester prodrugs of DTG

The lipophilic ester prodrugs approach has been commonly used for two purposes: enhancing the oral bioavailability and targeted delivery of drugs to mesenteric lymphatics [228, 229, 256, 274, 276, 277, 370, 371, 396, 397]. Since DTG does not possess the required physicochemical properties to associate with CM, a chemical modification approach has been applied in this work to increase the lipophilicity of DTG and its affinity to CM. We designed and synthesised a series of simple alkyl ester prodrugs of DTG and orally administered with LCT-based formulation to optimise the targeted delivery of DTG to viral reservoirs in MLNs (**Table 4-2, Chapter 4**). A series of *in vitro* and *ex vivo* assessments (affinity to CM, stability in the intestine lumen and lymphatic environment, and LCT

solubility) were performed to screen the best candidate for *in vivo* experiments.

Firstly, we assessed the affinity of prodrugs for CM *in silico*, *in vitro*, and *ex vivo*. The *in silico* predicted affinity of prodrugs to CM increased with the extension of the carbon chain length of conjugated fatty acid and decreased when the number of double bonds applied (**Table 4-2, Chapter 4**). However, the experimental association of prodrugs with CM showed the opposite trend when the carbon chain length was elongated above C12 (**Figure 4-4, Chapter 4**). Similar observations were reported in our previous study, in which the affinity of prodrugs to CM did not follow the trend of *in silico* prediction [229, 256]. It has been reported that the lipophilicity and molecular weight of parent drug and prodrugs need to meet a specific requirement to achieve an optimal affinity to CM [229]. In this work, we did not assess prodrugs with carbon chain length less than 12. Therefore, we cannot assess the effect of the size of alkyl chains on affinity to CM. However, free rotatable bond (FRB), density and molar volume, seem to have a trend in the association of prodrugs with CM, whereas these physiochemical properties do not have a correlation with the association of protease inhibitors with CM. It is worth noting that the *in silico* model used in current studies was primarily developed based on structures of bicyclic and tricyclic cannabinoids or similar small molecule compounds [238]. Although *the in silico* model has been validated by external molecules, it is sometimes not fully predictive for some drugs, suggesting some additional physiochemical parameters may affect the affinity to CM.

The stability and biotransformation of prodrugs were evaluated in fasted stated simulated intestinal fluid (FaSSIF) and plasma. In this work, the prodrugs were designed to be stable in the intestinal lumen, but rapidly release (ideally, immediately release) the parent drug in plasma or lymph. However, directly assessing stability of prodrugs in lymph would be difficult to perform as lymph sample is limited in volume and large number of animals will have to be used. Therefore, plasma was used as a surrogate for the environment of intestinal lymph although plasma does not completely mimic the environment in lymph (although enzymatic composition is similar between these 2 biological fluids, with overall lower concentrations of enzymes in lymph). We found that increasing the carbon chain length of the conjugated fatty acid improved the stability of prodrugs in either FaSSIF or plasma, while introducing double bond(s) facilitated the biotransformation of prodrugs (**Figure 4-5, Chapter 4**). It has been reported that the increasing size of conjugated esters could lead to a greater effect of steric hindrance, resulting in a slower hydrolysis rate [398]. Our results suggest that unsaturated fatty acid moieties could overcome the barrier of steric hindrance, allowing the efficient release of the parent drug.

Unmodified DTG and saturated prodrugs 1-4 exhibited low solubility in LCT (sesame and olive oils), while unsaturated prodrugs 5 and 6 have much higher LCT solubility (**Table 4-3, Chapter 4**). Both sesame and olive oils contain a high proportion of oleic and linoleic acid. These are also the conjugated fatty acid of prodrugs 5 and 6, respectively, and could lead to high compatibility between oils and prodrugs.

5.1.2.3. Targeted delivery of DTG to mesenteric lymph and MLNs by means of simple alkyl esters

In our previous reports, simple alkyl ester prodrugs did not rapidly release active parent drugs in the lymphatic system, limiting the levels of active drugs in the target sites [229, 256]. An activated ester approach was shown to release parent drugs more efficiently than simple alkyl esters. However, in this work, all synthesised DTG prodrugs have shown efficient release profiles in plasma *in vitro* (**Figure 4-6**, **Chapter 4**). In the further pharmacokinetics and biodistribution studies, selected prodrugs 5 and 6 rapidly released DTG in the blood (**Figure 4-8D-E, Chapter 4**) and lymph (**Figure 4-10**, **Chapter 4**) following oral administration to rats. Thus, the activated ester approach does not seem to be necessary in the case of DTG.

Oral administration of prodrug 5 in LCT-based formulation increased the DTG concentration ratio in lymph-to-serum and MLNs-to-serum up to 9.4-fold and 4.8-fold, respectively, compared to oral administration of unmodified DTG (**Figure 4-12**, **Chapter 4**). The drug concentration ratio in tissues versus blood has been used to evaluate the efficiency of tissue penetration [365]. A high ratio of tissue/blood indicates an efficient tissue penetration of a drug. The increased lymph/serum and MLNs/serum ratio of DTG concentration following oral administration of prodrug 5 suggests an improved selectivity of mesenteric lymphatic targeting.

5.1.2.4. Intraluminal processing of DTG prodrugs in LCT-based formulation

Although the lipophilic ester prodrug approach improved the selectivity of DTG targeting to mesenteric lymphatic system, it significantly attenuates the systemic exposure to DTG. The oral bioavailability of DTG was only 5% following oral administration of prodrug 5 with LCT (**Table 4-4**, **Chapter 4**). Interestingly, we found very high concentrations of intact prodrug 5 in the small intestine and colon (**Figure 4-11**, **Chapter 4**), indicating that the low oral bioavailability of DTG might be associated with the intraluminal processing of the administered prodrug.

In vitro lipolysis is a useful model to shed light on the pre-systemic absorption events in the intestinal lumen for drugs formulated with lipids. It simulates the enzymatic digestion process of lipids in the GI tract. Based on the simulated compartment (multi- or mono-compartment) and enzymatic activity, many *in vitro* lipolysis models have been developed [378]. The most commonly used model in studying lipid-based drug delivery systems is the pH-stat lipolysis model, which mimics intestinal lipolysis and maintains the pH throughout the study. In the *in vitro* lipolysis model, lipidic formulations are digested and then separated into three phases by ultracentrifugation: lipid, micelle, and sediment fractions. Drugs distributed into the micelle phase represent a readily absorbed fraction. The lipid and sediment fractions are not readily absorbable. Quantifying the amount of the drug in each phase can assess the capability of the formulation to disperse the co-formulated drug in the intestine.

After *in vitro* lipolysis, we showed that around 5.8% and 12% of prodrugs 5 and 6 doses were recovered in the micellar phase (absorbable fraction) (**Figure 4-15**, **Chapter 4**). Similar degrees of the oral bioavailability of released DTG were observed following oral administration of prodrugs 5 (5.4%) and 6 (9.6%) in LCT-based formulation to rats (**Table 4-4**, **Chapter 4**). Although several studies have ranked the contributions of lipidic formulations to *in vivo* bioavailability through *in vitro* lipolysis [382, 383, 399, 400], most *in vitro* lipolysis performances of lipidic formulations did not reflect the actual *in vivo* bioavailability of these compounds, especially highly lipophilic molecules. Dahan and Hoffman proposed that the *in vitro* lipolysis models may not accurately predict the *in vivo* performance of highly lipophilic drugs with substantial intestinal lymphatic transport [383]. They studied the absorption of vitamin D3 in different lipid-based formulations (short-chain triglyceride (SCT), MCT and LCT) and investigated the correlation between *in vitro* lipolysis and *in vivo* pharmacokinetic performances. Although the MCT formulation dispersed the highest amount of vitamin D3 in the micellar phase across the three formulations *in vitro* (SCT: 66.1%, MCT: 96.6%, LCT: 70.7%), the LCT-formulated vitamin D3 showed superior *in vivo* absorption (40.7%) over the MCT (30.3%) and SCT (20%) formulations. The *in vitro* lipolysis results did not reflect the actual oral bioavailability *in vivo* and failed to rank the contribution of lipid-based formulations to *in vivo* performance. A similar observation was reported by Zgair and colleagues [254]. They assessed the systemic bioavailability of LCT-formulated cannabinoids, including CBD and Δ9-tetrahydrocannabinol (THC). *In vitro* lipolysis of

LCT-based formulation has shown 32.8% and 31.2% of CBD and THC doses recovered in the micellar phase, respectively. The *in vivo* oral bioavailability of CBD (22.3%) and THC (21.5%) are lower than those observed in the micellar phase *in vitro*. In a subsequent study, a number of MCT/LCT blended formulations of CBD were compared for the dispersibility in micelles to the pure LCT-containing oil [257]. Interestingly, *in vitro* lipolysis of pure LCT oil-formulated CBD resulted in the lowest concentration distributed into the micellar fraction but had the highest *in vivo* systemic bioavailability compared to LCT/MCT blended formulations. It is important to note that both vitamin D3 and CBD have substantial intestinal lymphatic transport when co-administered with lipids [255, 401]. Since the *in vitro* lipolysis model only simulates the pre-absorption events, the overall absorption (portal and lymphatic absorption) of highly lipophilic drugs could be under or overestimated.

However, in the current work we found a near-perfect *in vitro-in vivo* correlation (IVIVC) following oral administration of prodrugs in LCT formulation. Dahan and Hoffman have reported a good IVIVC of dexamethasone in SCT, MCT and LCT [382]. After *in vitro* lipolysis, 95.3%, 96.2%, and 92.1% of dexamethasone doses were recovered in the micellar phase of SCT, MCT, and LCT, respectively. Orally administered dexamethasone to rats in SCT, MCT, and LCT resulted in 83%, 86.5%, and 91.2% oral bioavailability, respectively. The *in vitro* lipolysis of LCT (92.1% of dexamethasone dose in the micellar phase) indicated the actual *in vivo* bioavailability (91.2%). However, dexamethasone has no intestinal lymphatic transport, differing from

prodrugs in our work, which are absorbed into the lymphatic system when administered orally with lipids. The detailed mechanism of the good IVIVC of highly lipophilic prodrugs in this study is unclear and will be subjected for further investigation.

On the other hand, more than 90% of the prodrug 5 dose was distributed into lipid and sediment fractions (non-absorbable fractions) in *in vitro* lipolysis (**Figure 4-15A**, **Chapter 4**), which is consistent with the high levels of prodrug 5 found in the intestinal contents *in vivo* (**Figure 4-11**, **Chapter 4**). The preliminary pharmacokinetic study of prodrug 6 showed slightly improved but still low oral bioavailability of released DTG (9.6%) following administration of prodrug 6 in LCT-based formulation in comparison to prodrug 5 (5%) (**Table 4-4, Chapter 4**). *In vitro* lipolysis of prodrug 6 resulted in around 90% of the drug dose in the non-readily absorbed phases (undigested lipid and sediment) (**Figure 4-15B**, **Chapter 4**). These findings suggest that the limited oral bioavailability of released DTG after oral administration of prodrugs is most likely associated with poor intestinal absorption. Notably, lipid-based formulations (including lipids and lipophilic excipients) were developed to improve the solubilisation and absorption of orally administered lipophilic compounds and have been widely investigated in clinical studies [249, 251, 402, 403]. In a previous study by Kaukonen et al., a number of poorly water-soluble compounds, including two highly lipophilic drugs, cinnarizine and halofantrine, have been investigated for their luminal solubilisation/precipitation behaviours in either MCT or LCT formulations *in vitro* [404]. Since MCT formulation is digested faster and more

completely than LCT vehicle, only two phases (aqueous and sediment) will be generated after the *in vitro* lipolysis. As *in vitro* lipolysis used in their study is a non-dynamic intestinal lipid digestion model, digested lipids are prone to accumulate in the *in vitro* lipolysis media, allowing a supersaturation of highly lipophilic drugs in the micellar phase. In contrast, supersaturation is unlikely in LCT formulation as the co-formulated drugs will be concentrated in the undigested lipid fraction due to the slow digestion. A complete *in vitro* digestion of the LCT vehicle might lead to drug precipitation [404]. In this work, we demonstrated substantial precipitation of LCT-formulated highly lipophilic prodrugs (53% of prodrug 5 dose and 33% of prodrug 6 dose, respectively) before the complete digestion of LCT formulation in *in vitro* lipolysis. This is the first time in our group that the lipid-based formulation, especially LCT, did not facilitate the absorption of highly lipophilic molecules and resulted in substantial precipitation. In our previous studies, oral administration of highly lipophilic drugs or prodrugs, such as CBD [254, 255], bexarotene prodrugs [256], and LPV prodrugs [229], with LCT had favourable effects on intestinal absorption and mesenteric lymphatic targeting.

Most lipid-based formulations result in distribution of lipophilic drugs in the hydrophobic core of mixed micelles formed during lipid digestion, eventually resulting in higher bioavailability [405]. However, LCT-based formulation did not improve the systemic absorption of oleic and linoleic fatty acid-conjugated prodrugs (prodrugs 5 and 6, respectively) of DTG in this study. An ideal lipid-based formulation has to fully solubilise the administered dose of drugs and maintain the drug in solution during and

after digestion. Since the dispersion of drugs from the formulation solution to the micellar phase involves several intermediate steps, there is a considerable risk of drug precipitation during processing [406]. Therefore, prodrugs 5 and 6 may precipitate during drug dispersion from the oil solution to micelles. Rapid precipitation of halofantrine during *in vitro* lipolysis digestion was found when it was formulated as a supersaturated self-nanoemulsifying drug delivery system (super-SNEDDS) [379]. However, since the precipitation of halofantrine was in an amorphous form, the precipitated pellets had a high dissolution rate in the lipolysis medium. The nature of the precipitated form (amorphous or crystalline) of the compounds depends on their physicochemical properties [378, 381]. In this study, prodrugs 5 and 6 potentially precipitated as crystalline pellets (hard to redissolve) rather than in amorphous forms (easy to redissolve). Alskär et al. proposed that compounds with low molecular weight (< 350 g/mol) and high melting point (> 200 ºC) are likely to precipitate in the crystalline form [381]. However, the prodrugs in this study do not meet these factors as both prodrugs 5 and 6 have a high molecular weight (684 g/mol and 682 g/mol, respectively) and a melting point lower than 200 ºC (prodrug 5: 98 ºC, prodrug 6 is a colourless oil). This indicates that there are other factors affecting the drug precipitation form. Further studies are needed to investigate the precipitation of highly lipophilic drugs or prodrugs following administration of LCT-based formulations.

5.2. Future work

5.2.1. Updating the *in silico* computational model for the prediction of drug-CM association

The *in silico* model predicting the association of drugs with CM was established in 2009 [238] and has been used in several studies [229, 239, 256]. However, the predicted drug-CM association values did not always indicate the experimental results (*in vitro* and *ex vivo*) [229]. For example, LPV was predicted to have a 50% association with CM. However, negligible affinities of LPV to artificial and natural CM were found *in vitro* and *ex vivo* [229]. In this PhD work, the opposite trend of the predicted association of prodrugs with CM and the experimental degree of association with CM was observed. Since the computational model is a tool for screening candidates for intestinal lymphatic transport, limited predictive power may mislead the selection of candidates. Therefore, updating the current *in silico* model can provide a more powerful screening tool for future intestinal lymphatic transport studies.

5.2.2. The association mechanisms of drugs with CM

CM are spherical structures with a TG-rich core embedded in a shell of phospholipids, cholesterol, cholesterol ester and apolipoproteins (mainly apoB-48) [407]. Lipophilic drugs are believed to be incorporated into the TG-rich core of CM during or after CM assembly for intestinal lymphatic transport to take place [237]. In addition, interfacial interactions between drugs and CM were reported to affect the extent of drug-CM association [228, 239]. In this work, we observed that TPV has a higher affinity to

natural CM than artificial CM, indicating that the surface materials of CM, especially apolipoproteins, may play essential roles in the drug-CM association. This interfacial interaction between TPV and CM might be weaker than the TG core association, resulting in the redistribution of TPV to other cells and proteins once entering mesenteric lymph. This is a rare case in lipophilic compounds associated with CM by interfacial interaction rather than TG-rich core incorporation. The underlying mechanism is unclear and requires further investigation. Since drug-lipoproteins association can have other applications, such as the distribution of drugs to peripheral tissues or adipocytes, investigation of the mechanisms of interfacial interactions between drugs and surface molecules on lipoproteins can provide new aspects in drug delivery and have important implications for drug disposition.

5.2.3. Investigating the good IVIVC of highly lipophilic drugs and prodrugs

The IVIVC was used to develop extended-release dosage forms of oral drugs based on the correlation between *in vitro* assessments and *in vivo* pharmacokinetics profiles [408]. Since *in vitro* lipolysis model can mimic the lipid digestion process in the small intestine, it is widely used to assess the intraluminal digestion and absorption of lipophilic drugs formulated in lipid-based formulations [254, 257, 260, 378-380, 383, 385, 399]. However, *in vitro* lipolysis model cannot simulate the entire systemic absorption, including intestinal lymphatic transport, as it only simulates the conditions in the intestinal lumen. Therefore, *in vitro*

lipolysis might not predict the actual *in vivo* pharmacokinetic profile of highly lipophilic compounds with substantial intestinal lymphatic transport [260, 382, 383]. In this work, the poor oral bioavailability of DTG was attributed to poor absorption and substantial precipitation in the intestinal lumen following oral administration of prodrugs with LCT. The lipophilic ester prodrugs approach combined with lipid-based formulation has been well documented to enhance intestinal lymphatic transport and improve systemic exposure to parent drugs [229, 256, 274-277, 371]. This study demonstrated an unexpected phenomenon that lipid-based formulation did not facilitate the absorption of lipophilic ester prodrugs and led to low systemic bioavailability of the parent drug. Investigating the precipitation of lipophilic ester prodrugs and good *in vitro* lipolysis model predictability to *in vivo* bioavailability can provide ideas to optimise the current drug delivery approach for ARVs and other lipophilic drugs or prodrugs.

5.2.4. Applying MLNs targeting for HIV cure strategies

Latent HIV reservoirs are the major obstacle to the cure of HIV infection. Several strategies are proposed to overcome these barriers. These strategies are classified into three categories: eradication cure (complete removal of viral reservoirs), functional cure (immune control without eliminating viral reservoirs) and hybrid cure (enhanced immune control with reduction of viral reservoirs) [409]. Eradication cure was reported occasionally in stem-cell transplant patients whose donor had CCR5 co-receptor mutation [410, 411]. The first functional cure was in an infant born to an HIV-1-positive mother and initiated ART 30 hours after birth

[412]. These successful cases have encouraged tremendous scientific efforts to explore potential approaches to cure HIV, including stem cell transplant, ‘kick and kill’, ‘block and lock’, gene therapy, early initiation of ART, and immune-based therapies.

Latent HIV in resting $CD4^+$ T cells can escape from the host immune response and provide resources for persistent viral replication. The ‘kick and kill’ strategy uses latency-reversing agents (LRAs) to awaken latent HIV reservoirs (kick) under ART for cytopathic killing and innate immune response targeting (kill) [413]. Although ‘kick and kill’ is considered an attractive and practical strategy for HIV cure, some challenges remain to be resolved. Firstly, LRAs might not fully induce latent HIV [414, 415]. Furthermore, individual variation of reactivation degree of resting $CD4^+$ T cells indicates this approach might not be feasible for some patients [415]. The most critical challenge is that the poor penetration of ART in viral reservoirs may lead to high levels of reactivated viruses and endanger the patients [132, 416-418]. Although numerous studies have revealed that LRAs can largely reactivate the latent HIV reservoirs, the impact on the size of latent reservoirs was minimum [414]. This means that the immune system is insufficient to eliminate the awakened reservoirs. It has been suggested to add-on agents to assist the ‘kill’ strategy. However, adding drugs is likely to increase the risk of side effects. Since the ‘kick’ strategy is under ART, selectively targeting ARVs to difficult-to-reach viral reservoirs could prevent the reproduction of reactivated reservoirs. MLNs are one of the most critical HIV reservoirs and an ideal fortress for the virus to hide from ARVs. Delivering ARVs to

MLNs and combining the ‘kick and kill’ strategy to reactivate latent HIV could eliminate this viral reservoir and move towards eradication cure.

Intestinal lymphatic transport is the ideal pathway for mesenteric lymphatic targeting of ARVs. We previously developed an activated ester of LPV, which efficiently targeted LPV to mesenteric lymphatics following co-administration with LCT-containing oil (sesame oil). However, LPV concomitants with RTV (LPV/r) are currently a second-line ART for children and neonates [209]. On the other hand, DTG is involved in the first-line ART regimens for HIV-infected adults, adolescents, and children. Targeted delivery of DTG to MLNs may have more contributions to clinical treatment. DTG does not have intestinal lymphatic transport without chemical modifications. Although lipophilic esters of DTG improved the lymphatic absorption and selectivity of mesenteric lymphatic targeting of DTG, poor intestinal absorption limited the drug levels in systemic circulation and MLNs. This suggests current lipophilic ester prodrug approach might not be feasible for some compounds. Therefore, optimisation of the lipophilic ester prodrug approach for enhancing mesenteric lymphatic targeting will be the first step towards eradicating HIV reservoirs.

APPENDICES

Appendix 1. Characterization of tipranavir extracted from Aptivus® soft capsules

Extraction of TPV was performed using dichloromethane and ethyl acetate. The purity of product was more than 99% by HPLC-UV. TPV was appeared as white solid (50% yield), melting point 58.0-61.0°C. H^1 NMR (400 MHz, Methanol-d4): δ 8.95 (s, 1H), 8.21 (d, 1H, J = 8.24 Hz), 8.02 (d, 1H, J = 8.20 Hz), 7.24 (s, 1H), 7.21 (t, 2H, J = 7.36 Hz), 7.13 (t, 1H, J = 7.32 Hz), 7.06 (t, 2H, J = 2.82 Hz), 7.01 (d, 2H, J = 7.14 Hz), 6.96 (m, 1H), 3.92 (q, 1H, J = 5.41 Hz), 2.68-2.52 (m, 4H), 2.20-2.07 (m, 1H), 1.98-1.57 (m, 6H), 0.89 (t, 4H, J = 7.22 Hz), 0.83 (t, 3H, J = 7.34 Hz). ^{13}C NMR (100 MHz, Methanol-d4): 169.88, 166.93, 161.57, 148.06, 147.61, 142.83, 137.71, 137.02, 130.22, 129.89, 129.50, 129.24, 126.95, 126.08, 124.13, 122.55, 120.26, 106.16, 81.80, 43.61, 40.84, 40.49, 37.38, 30.86, 25.75, 17.88, 14.67, 13.29. HR-MS (ESI+): m/z $[M+ H]^+$ calculated for C31H34F3N2O5S, 603.2135, found 603.2124.

Appendix 2. Characterisation of ester prodrugs of dolutegravir

1 (dolutegravir lauryl ester), (4R,12aS)-9-((2,4-difluorobenzyl)carbamoyl)-4-methyl-6,8-dioxo-3,4,6,8,12,12a-hexahydro-2H-pyrido[1',2':4,5]pyrazino[2,1-b][1,3]oxazin-7-yl dodecanoate was synthesised using DTG sodium as starting material and lauroyl chloride as reagent. The purity of the final compound was more than 95% by HPLC-UV, white solid (47% yield), melting point 143.0-145.0°C. ^{1}H NMR spectrum specifics:(400 MHz, $(CD_3)_2SO$): δ 10.17 (t, *J* = 5.66 Hz, 1H), 8.68 (s, 1H), 7.34-7.44 (m, 1H), 7.17-7.27 (m, 1H), 6.99-7.09 (m, 1H), 5.39 (dd, *J* = 3.95, 1.58 Hz, 1H), 4.65-4.78 (m, 1H), 4.61 (dd, *J* = 13.9, 3.7 Hz, 1H), 4.53 (d, *J* = 5.81 Hz, 2H), 4.41 (dd, *J* = 13.8, 5.7 Hz, 1H), 3.98 (t, *J* = 11.29 Hz, 1H), 3.80-3.90 (m, 1H), 2.56 (t, *J* = 7.39 Hz, 2H), 1.93 (br. s, 1H), 1.63 (p, *J* = 7.4 Hz, 2H), 1.43-1.55 (m, 1H), 1.33-1.43 (m, 2H), 1.12-1.33 (m, 18H), 0.77-0.91 (t, *J* = 6.58 Hz, 3H). ^{13}C NMR spectrum specifics: (100 MHz, $(CD_3)_2SO$): δ 171.33, 170.67, 163.25, 155.27, 144.58, 131.31, 130.16, 122.57, 118.57, 111.97, 111.74, 104.44, 104.07, 76.35, 52.44, 35.84, 33.14, 31.26, 29.21, 28.99, 28.72, 28.32, 24.14, 22.10, 15.57, 13.99. HR-MS (ESI^+): *m/z* $[M+H]^+$ calculated for $C_{32}H_{42}F_2N_3O_6$, 602.3036, found 602.3060.

2 (dolutegravir myristyl ester), (4R,12aS)-9-((2,4-difluorobenzyl)carbamoyl)-4-methyl-6,8-dioxo-3,4,6,8,12,12a-hexahydro-2H-pyrido[1',2':4,5]pyrazino[2,1-b][1,3]oxazin-7-yl

tetradecanoate was synthesised using DTG sodium as starting material and myristyl chloride as reagent. The purity of the final compound was more than 95% by HPLC-UV, white solid (60% yield), melting point 129.0-131.0°C. H^1 NMR spectrum specifics:(400 MHz, $(CD_3)_2SO$): δ 10.18 (t, *J* = 5.91 Hz, 1H), 8.68 (s, 1H), 7.35-7.44 (m, 1H), 7.18-7.27 (m, 1H), 7.01-7.09 (m, Hz, 1H), 5.39 (dd, *J* = 5.7, 3.8 Hz, 1H), 4.68-4.74 (m, 1H), 4.61 (dd, *J* = 13.56, 2.9 Hz, 1H), 4.53 (d, *J* = 5.80 Hz, 2H), 4.42 (dd, *J* = 13.74, 5.72 Hz, 1H), 3.98 (t, *J* = 11.55, Hz, 1H), 3.81-3.90 (m, 1H), 2.56 (t, *J* = 7.35 Hz, 2H), 1.93 (br. s, 1H), 1.63 (p, *J* = 7.3 Hz, 2H), 1.5 (dd, *J* = 14.14, 1.79 Hz, 1H), 1.34-1.43 (m, 2H), 1.19-1.33 (m, 22H), 0.79-0.90 (t, *J* = 6.30 Hz, 3H). ^{13}C NMR spectrum specifics: (100 MHz, $(CD_3)_2SO$): δ 170.82, 170.17, 162.81, 154.88, 144.10, 130.92, 130.87, 130.82 129.69, 122.21, 122.06, 118.06, 111.49, 111.45, 111.28, 111.24, 104.07, 103.80, 103.55, 75.85, 51.88, 35.81, 33.16, 31.29, 29.16, 29.00, 28.96, 28.90, 28.72, 28.67, 28.28, 24.15, 22.05, 15.50, 13.95. HR-MS (ESI^+): *m/z* $[M+ H]^+$ calculated for $C_{34}H_{46}F_2N_3O_6$, 630.3349, found 630.3348.

3 (dolutegravir palmitoyl ester), (4R,12aS)-9-((2,4-difluorobenzyl)carbamoyl)-4-methyl-6,8-dioxo-3,4,6,8,12,12a-hexahydro-2H-pyrido[1',2':4,5]pyrazino[2,1-b][1,3]oxazin-7-yl palmitate was synthesised using DTG sodium as starting material and palmitoyl chloride as reagent. The purity of the final compound was more than 95% by HPLC-UV, white solid (22% yield), melting point 82.0-84.0°C. ^1H NMR spectrum specifics:(400 MHz, $(CD_3)_2SO$): δ 10.17 (t, *J* = 5.93 Hz, 1H),

8.68 (s, 1H), 7.34-7.44 (m, 1H), 7.18-7.28 (m, 2H), 7.00-7.10 (m, 1H), 5.4 (dd, *J* = 5.87, 3.87 Hz, 1H), 4.66-4.76 (m, 1H), 4.61 (dd, *J* = 13.89, 3.17,1H), 4.53 (d, *J* = 5.81 Hz, 2H), 4.42 (dd, *J* = 13.84, 5.81 Hz, 1H), 3.98 (t, *J* = 11.50 Hz, 1H), 3.81-3.91 (m, 1H), 2.56 (t, *J* = 7.21 Hz, 2H), 1.93 (br. s, 1H), 1.63 (p, *J* = 7.3 Hz, 2H), 1.5 (d, *J* = 13.75 Hz, 1H), 1.33-1.44 (m, 2H), 1.10-1.33 (m, 24H), 0.84 (t, *J* = 6.58, 3H). ^{13}C NMR spectrum specifics: (100 MHz, $(CD_3)_2SO$): δ 170.81, 170.18, 162.80, 154.88, 144.07, 143.58, 130.94, 130.87, 130.77, 129.68, 122.18, 122.05, 118.07, 111.49, 111.25, 104.06, 103.84, 103.55, 75.87, 51.87, 35.82, 33.17, 31.29, 29.18, 29.05, 28.99, 28.95, 28.89, 28.68, 28.27, 24.14, 22.08, 15.51, 13.93. HR-MS (ESI^+): *m/z* $[M+ Na]^+$ calculated for $C_{36}H_{49}F_2N_3NaO_6$, 680.3482, found 680.3497.

4 (dolutegravir stearyl ester), (4R,12aS)-9-((2,4-difluorobenzyl)carbamoyl)-4-methyl-6,8-dioxo-3,4,6,8,12,12a-hexahydro-2H-pyrido[1',2':4,5]pyrazino[2,1-b][1,3]oxazin-7-yl stearate was synthesised using DTG sodium as starting material and stearoyl chloride as reagent. The purity of the final compound was more than 95% by HPLC-UV, white solid (25% yield), melting point 82.0-84.0°C. ^{1}H NMR (400 MHz, $(CD_3)_2SO$): δ 10.18 (t, *J* = 5.8 Hz, 1H), 8.68 (s, 1H), 7.33-7.45 (m, 1H), 7.18-7.27 (m, 1H), 7.11 – 7.01 (m, 1H), 5.40 (dd, *J* = 5.98, 3.99 Hz, 1H), 4.66 – 4.76 (m, 1H), 4.62 (dd, *J* = 13.8, 2.99 Hz, 1H), 4.54 (d, *J* = 5.9 Hz, 2H), 4.42 (dd, *J* = 13.7, 5.8 Hz, 1H), 3.98 (t, *J* = 11.7 Hz, 1H), 3.81-3.91 (m, 1H), 2.57 (t, *J* = 7.3 Hz, 2H), 1.94 (s, 1H), 1.63 (p, *J* = 7.4, 2H), 1.50 (d, *J* = 14.0 Hz, 1H), 1.33-1.43 (m, 2H), 1.18-1.32 (m, 30H),

0.85 (t, *J* = 6.96 Hz, 3H). ^{13}C NMR (101 MHz, DMSO): δ 174.46, 170.83, 170.17, 162.81, 154.89, 144.11, 130.92, 130.86, 130.82, 130.76, 129.68, 111.48, 111.24, 104.06, 103.81, 103.54, 75.87, 51.87, 35.83, 35.79, 33.65, 33.16, 31.29, 29.16, 29.03, 29.00, 28.97, 28.91, 28.75, 28.70, 28.55, 28.30, 24.49, 24.15, 22.09, 15.51, 13.93. HR-MS (ESI$^+$): *m/z* [M+ H]$^+$ calculated for $C_{38}H_{54}F_2N_3O_6$, 686.3975, found 686.3977

5 (dolutegravir oleyl ester), (4R,12aS)-9-((2,4-difluorobenzyl)carbamoyl)-4-methyl-6,8-dioxo-3,4,6,8,12,12a-hexahydro-2H-pyrido[1',2':4,5]pyrazino[2,1-b][1,3]oxazin-7-yl oleate was synthesised using DTG sodium as starting material and oleoyl chloride as reagent. The purity of the final compound was more than 95% by HPLC-UV, white solid (75% yield), melting point 97.0-99.0°C. ^{1}H NMR (400 MHz, $(CD_3)_2SO$): δ 10.18 (t, *J* = 5.9 Hz, 1H), 8.68 (s, 1H), 7.34-7.44 (m, 1H), 7.17-7.27 (m, 1H), 7.11 – 7.01 (m, 1H), 5.40 (dd, *J* = 5.7, 3.8 Hz, 1H), 5.26-5.37 (m, 2H), 4.75 – 4.67 (m, 1H), 4.61 (dd, *J* = 13.8, 3.7 Hz, 1H), 4.53 (d, *J* = 5.9 Hz, 2H), 4.42 (dd, *J* = 13.8, 5.7 Hz, 1H), 3.98 (t, *J* = 11.8 Hz, 1H), 3.81-3.90 (m, 1H), 2.56 (t, *J* = 7.3 Hz, 2H), 1.93-2.02 (m, 5H), 1.63 (p, *J* = 7.3 Hz, 2H), 1.46-1.50 (m, 1H), 1.09-1.43 (m, 23H), 0.89 – 0.80 (m, 3H). ^{13}C NMR spectrum specifics: (100 MHz, $(CD_3)_2SO$): δ 170.8, 170.17, 162.78, 154.86, 144.12, 130.87, 129.64, 122.12, 118.06, 111.46, 111.26, 103.80, 75.87, 51.85, 35.85, 33.16, 31.28, 29.16, 29.09, 29.04, 28.97, 28.80, 28.67, 28.58, 28.53, 28.47, 28.28, 26.60, 26.54, 24.13, 22.07, 15.50, 13.92. HR-MS (ESI$^+$): *m/z* [M+ H]$^+$ calculated for $C_{38}H_{52}F_2N_3O_6$, 684.3819, found 684.3814.

6 (dolutegravir linoleyl ester), (4R,12aS)-9-((2,4-difluorobenzyl)carbamoyl)-4-methyl-6,8-dioxo-3,4,6,8,12,12a-hexahydro-2H-pyrido[1',2':4,5]pyrazino[2,1-b][1,3]oxazin-7-yl (9Z,12Z)-octadeca-9,12-dienoate was synthesised using DTG sodium as starting material and linoleoyl chloride as reagent. The purity of the final compound was more than 95% by HPLC-UV, colorless oil (24% yield). ^{1}H NMR (400 MHz, $(CD_3)_2SO$): δ 10.18 (t, *J* = 6.03 Hz, 1H), 8.68 (s, 1H), 7.36-7.44 (m, 1H), 7.18-7.28 (m, 1H), 7.01-7.10 (m, 1H), 5.38-5.43 (m, 1H), 5.25-5.36 (m, 3H), 4.66-4.76 (m, 1H), 4.61 (dd, *J* = 13.64, 3.26 Hz, 1H), 4.53 (d, *J* = 5.84 Hz, 2H), 4.42 (dd, *J* = 13.87, 5.84 Hz, 1H), 3.97 (t, *J* = 11.58 Hz, 1H), 3.81-3.90 (m, 1H), 2.73 (t, *J* = 6.31 Hz, 2H), 2.56 (t, *J* = 7.26 Hz, 2H), 1.96-2.07 (m, 4H), 1.90 (br. s, 1H), 1.63 (p, *J* = 7.4 Hz, 2H), 1.45-1.54 (m, 1H), 1.10-1.44 (m, 18H), 0.84 (t, *J* = 6.68 Hz, 3H). ^{13}C NMR (100 MHz, $(CD_3)_2SO$): δ 170.85, 170.16, 162.80, 154.86, 144.14, 130.84, 129.66, 127.76, 118.05, 111.54, 111.26, 104.10, 103.84, 103.56, 75.91, 51.89, 35.83, 33.67, 31.32, 30.87, 28.64, 26.56, 25.23, 24.52, 24.22, 22.10, 21.95, 15.50, 13.90. HR-MS (ESI^+): *m/z* $[M+H]^+$ calculated for $C_{38}H_{50}F_2N_3O_6$, 682.3662, found 682.3648.

Appendix 3. Half-life of hydrolysis of prodrugs in FaSSIF and plasma.

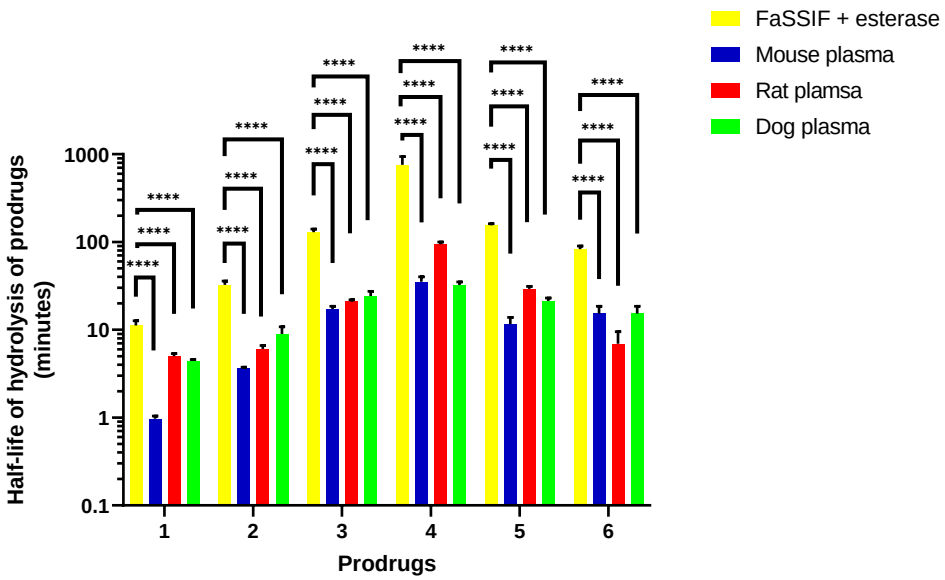

Figure A3-1. Estimated half-lives of hydrolysis of prodrugs. One-way ANOVA followed by Dunnett's multiple comparison test was used for statistical analysis. ****, $p < 0.0001$.

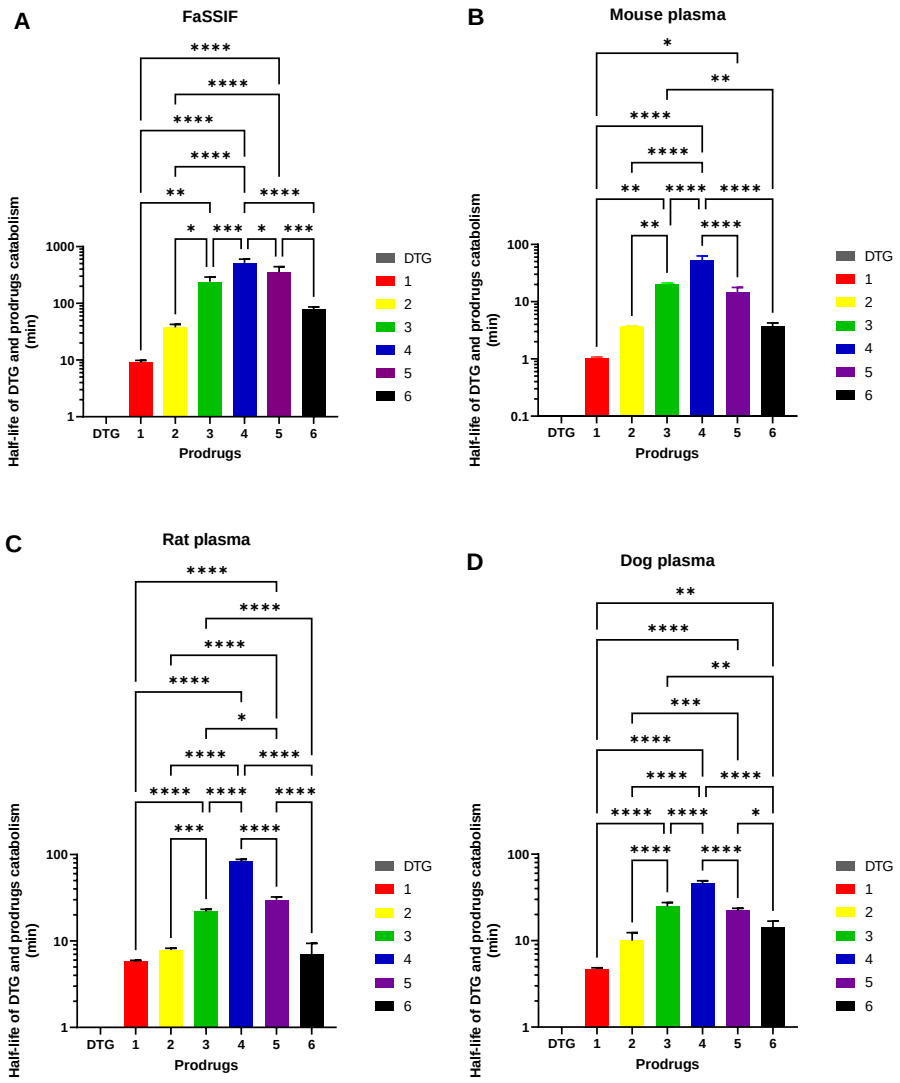

Figure A3-2. The hydrolysis half-lives of prodrugs in (A) FaSSIF; (B) mouse plasma; (C) rat plasma; (D) dog plasma. One-way ANOVA followed by Dunnett's multiple comparison test was used for statistical analysis of differences between prodrugs. *, $p < 0.05$; **, $p < 0.01$; ***, $p < 0.001$; ****, $p < 0.0001$.

REFERENCE

[1] P.A. Luciw, Human immunodeficiency viruses and their replication, in: B.N. Fields (Ed.) Virology, 1996, pp. 1881-1952.

[2] P.M. Sharp, B.H. Hahn, Origins of HIV and the AIDS pandemic, Cold Spring Harb Perspect Med, 1 (2011) a006841, https://doi.org/10.1101/cshperspect.a006841.

[3] N.R. Faria, A. Rambaut, M.A. Suchard, G. Baele, T. Bedford, M.J. Ward, A.J. Tatem, J.D. Sousa, N. Arinaminpathy, J. Pepin, D. Posada, M. Peeters, O.G. Pybus, P. Lemey, HIV epidemiology. The early spread and epidemic ignition of HIV-1 in human populations, Science, 346 (2014) 56-61, https://doi.org/10.1126/science.1256739.

[4] M.S. Gottlieb, R. Schroff, H.M. Schanker, J.D. Weisman, P.T. Fan, R.A. Wolf, A. Saxon, Pneumocystis carinii pneumonia and mucosal candidiasis in previously healthy homosexual men: evidence of a new acquired cellular immunodeficiency, The New England Journal of Medicine, 305 (1981) 1425-1431, https://doi.org/10.1056/nejm198112103052401.

[5] F. Barré-Sinoussi, J.C. Chermann, F. Rey, M.T. Nugeyre, S. Chamaret, J. Gruest, C. Dauguet, C. Axler-Blin, F. Vézinet-Brun, C. Rouzioux, W. Rozenbaum, L. Montagnier, Isolation of a T-Lymphotropic Retrovirus from a Patient at Risk for Acquired Immune Deficiency Syndrome (AIDS), Science, 220 (1983) 868-871, https://doi.org/10.1126/science.6189183.

[6] S. Nyamweya, A. Hegedus, A. Jaye, S. Rowland-Jones, K.L. Flanagan, D.C. Macallan, Comparing HIV-1 and HIV-2 infection: Lessons for viral immunopathogenesis, Rev Med Virol, 23 (2013) 221-240, https://doi.org/10.1002/rmv.1739.

[7] R.N. Shepard, J. Schock, K. Robertson, D.C. Shugars, J. Dyer, P.H. Vernazza, C., M.S. Cohen, S.A. Fiscus, Quantitation of Human Immunodeficiency Virus Type 1 RNA in Different Biological Compartments, Journal of Clinical Microbiology, 38 (2000) 1414-1418, https://doi.org/10.1128/JCM.38.4.1414-1418.2000.

[8] C.D. Pilcher, D.C. Shugars, S.A. Fiscus, W.C. Miller, P. Menezes, J. Giner, B. Dean, K. Robertson, C.E. Hart, J.L. Lennox, J.J.J. Eron, C.B. Hicks, HIV in body fluids during primary HIV infection: implications for pathogenesis, treatment and public health, AIDS, 15 (2001) 837-845, https://doi.org/10.1097/00002030-200105040-00004.

[9] G. John-Stewart, D. Mbori-Ngacha, R. Ekpini, E.N. Janoff, J. Nkengasong, J.S. Read, P. Van de Perre, M.L. Newell, Ghent IAS Working Group on HIV in Women Children, Breast-

feeding and Transmission of HIV-1, Journal of Acquired Immune Deficiency Syndromes, 35 (2004) 196-202, https://doi.org/10.1097/00126334-200402010-00015.
[10] N.a. listed, Epidemiologic Aspects of the Current Outbreak of Kaposi's Sarcoma and Opportunistic Infections, The New England Journal of Medicine, 306 (1982) 248-252, https://doi.org/10.1056/NEJM198201283060431.
[11] M. Marmor, A.E. Friedman-Kien, L. Laubenstein, R.D. Byrum, D.C. William, S. D'Onofrio, N. Dubin, Risk factors for Kaposi's sarcoma in homosexual men, The Lancet, 1 (1982) 1083-1087, https://doi.org/10.1016/s0140-6736(82)92275-9.
[12] Centers for Disease Control (CDC), Possible transfusion-associated acquired immune deficiency syndrome (AIDS), Morbidity and Mortality Weekly Report, 31 (1982) 652-654.
[13] D. Sherman, N. Sherman, HIV/AIDS and pregnancy, 2001.
[14] A. Katz, The evolving art of caring for pregnant women with HIV infection, Journal of Obstetric Gynecologic and Neonatal Nursing, 32 (2003) 102-108, https://doi.org/10.1177/0884217502239807.
[15] Y.J. Bryson, Perinatal HIV-1 transmission: recent advances and therapeutic interventions, AIDS, 10 (supplement) (1996) S33-S42.
[16] UNAIDS/World Health Organization, Summary of global HIV epidemic, 2021, (2022).
[17] S.G. Deeks, J. Overbaugh, A. Phillips, S. Buchbinder, HIV infection, Nat Rev Dis Primers, 1 (2015) 15035, https://doi.org/10.1038/nrdp.2015.35.
[18] A.G. Dalgleish, P.C. Beverley, P.R. Clapham, D.H. Crawford, M.F. Greaves, R.A. Weiss, The CD4 (T4) antigen is an essential component of the receptor for the AIDS retrovirus, Nature, 312 (1984) 763-767, https://doi.org/10.1038/312763a0.
[19] P.J. Maddon, A.G. Dalgleish, J.S.C. McDougal, P. R., R.A.A. Weiss, R., The T4 gene encodes the AIDS virus receptor and is expressed in the immune system and the brain, Cell, 47 (1986) 333-348, https://doi.org/10.1016/0092-8674(86)90590-8.
[20] J.S. McDougal, M.S.S. Kennedy, J. M., S.P. Cort, A. Mawle, J.K. Nicholson, Binding of HTLV-III-LAV to T4+ T Cells by a Complex of the 110K Viral Protein and the T4 Molecule, Science, 231 (1986) 382-385, https://doi.org/10.1126/science.3001934.
[21] F. Cocchi, A.L.G.-D. DeVico, A. Arya, S. K., R.C.L. Gallo, P., Identification of RANTES, MIP-1 alpha, and MIP-1 beta as the major HIV-suppressive factors produced by CD8+ T

cells, Science, 270 (1995) 1811-1815, https://doi.org/10.1126/science.270.5243.1811.
[22] B.J. Doranz, J.Y. Rucker, Y. Smyth, R. J., M. Samson, S.C. Peiper, M.C. Parmentier, R. G., R.W. Doms, A Dual-Tropic Primary HIV-1 Isolate That Uses Fusin and the β-Chemokine Receptors CKR-5, CKR-3, and CKR-2b as Fusion Cofactors, Cell, 85 (1996) 1149-1158, https://doi.org/10.1016/s0092-8674(00)81314-8.
[23] Y. Feng, C.C. Broder, P.E. Kennedy, E.A. Berger, HIV-1 Entry Cofactor: Functional cDNA Cloning of a Seven-Transmembrane, G Protein-Coupled Receptor, Science, 272 (1996) 872-877, https://doi.org/10.1126/science.272.5263.872.
[24] G. Alkhatib, C. Combadiere, C.C. Broder, Y. Feng, P.E. Kennedy, P.M. Murphy, E.A. Berger, CC CKR5: A RANTES, MIP-1α, MIP-1β Receptor as a Fusion Cofactor for Macrophage-Tropic HIV-1, Science, 272 (1996) 1955-1958, https://doi.org/10.1126/science.272.5270.1955.
[25] M.J. Endres, P.R. Clapham, M. Marsh, M. Ahuja, J.D. Turner, A. McKnight, J.F. Thomas, B. Stoebenau-Haggarty, S.V. Choe, P. J., T.N. Wells, C.A. Power, S.S. Sutterwala, R.W. Doms, N.R.H. Landau, J. A., CD4-Independent Infection by HIV-2 Is Mediated by Fusin-CXCR4, Cell, 87 (1996) 745-756, https://doi.org/10.1016/s0092-8674(00)81393-8.
[26] T. Dragic, V. Litwin, G.P. Allaway, S.R.H. Martin, Y. Nagashima, K. A. Cayanan, C., P.J.K. Maddon, R. A., J.P. Moore, W.A. Paxton, HIV-1 entry into CD4+ cells is mediated by the chemokine receptor CC-CKR-5, Nature, 381 (1996) 667-673, https://doi.org/10.1038/381667a0.
[27] H. Deng, R.E. Liu, W. Choe, S. Unutmaz, D. Burkhart, M. Di Marzio, P. Marmon, S., R.E. Sutton, C.M. Hill, C.B. Davis, S.C. Peiper, T.J. Schall, D.R. Littman, N.R. Landau, Identification of a major co-receptor for primary isolates of HIV-1, Nature, 381 (1996) 661-666, https://doi.org/10.1038/381661a0.
[28] M. Samson, O. Labbe, C. Mollereau, G. Vassart, M. Parmentier, Molecular cloning and functional expression of a new human CC-chemokine receptor gene, Biochemistry, 35 (1996) 3362-3367, https://doi.org/10.1021/bi952950g.
[29] H. Choe, M.S. Farzan, Y., N. Sullivan, B. Rollins, P.D.W. Ponath, L. Mackay, C. R., G.N. LaRosa, W., N. Gerard, C.S. Gerard, J., The β-Chemokine Receptors CCR3 and CCR5 Facilitate Infection by Primary HIV-1 Isolates, Cell, 85 (1996) 1135-1148, https://doi.org/10.1016/s0092-8674(00)81313-6.
[30] D.C. Chan, D.B. Fass, J. M. Kim, P. S., Core Structure of gp41 from the HIV Envelope Glycoprotein, Cell, 89 (1997)

263-273, https://doi.org/10.1016/s0092-8674(00)80205-6.
[31] W. Weissenhorn, A. Dessen, S.C. Harrison, J.J. Skehel, D.C. Wiley, Atomic structure of the ectodomain from HIV-1 gp41, Nature, 387 (1997) 426-430, https://doi.org/10.1038/387426a0.
[32] V. Buzon, G. Natrajan, D. Schibli, F. Campelo, M.M. Kozlov, W. Weissenhorn, Crystal structure of HIV-1 gp41 including both fusion peptide and membrane proximal external regions, PLoS Pathog, 6 (2010) e1000880, https://doi.org/10.1371/journal.ppat.1000880.
[33] J.A. Briggs, K. Grunewald, B. Glass, F. Forster, H.G. Krausslich, S.D. Fuller, The mechanism of HIV-1 core assembly: insights from three-dimensional reconstructions of authentic virions, Structure, 14 (2006) 15-20, https://doi.org/10.1016/j.str.2005.09.010.
[34] M.P. D'Souza, V.A. Harden, Chemokines and HIV-1 second receptors. Confluence of two fields generates optimism in AIDS research, Nature Medicine, 2 (1997), https://doi.org/10.1038/nm1296-1293.
[35] W.S. Hu, S.H. Hughes, HIV-1 reverse transcription, Cold Spring Harb Perspect Med, 2 (2012), https://doi.org/10.1101/cshperspect.a006882.
[36] J.D. Dvorin, M.H. Malim, Intracellular trafficking of HIV-1 cores: journey to the center of the cell, Current Topics in Microbiology and Immunology, 281 (2003) 179-208, https://doi.org/10.1007/978-3-642-19012-4_5.
[37] S.P. Goff, Intracellular trafficking of retroviral genomes during the early phase of infection-- viral exploitation of cellular pathways, The Journal of Gene Medicine, 3 (2001) 517-528, https://doi.org/10.1002/jgm.234.
[38] R. Craigie, F.D. Bushman, HIV DNA integration, Cold Spring Harb Perspect Med, 2 (2012) a006890, https://doi.org/10.1101/cshperspect.a006890.
[39] Y.H. Zheng, N. Lovsin, B.M. Peterlin, Newly identified host factors modulate HIV replication, Immunol Lett, 97 (2005) 225-234, https://doi.org/10.1016/j.imlet.2004.11.026.
[40] R.D. Liu, J. Wu, R. Shao, Y.H. Xue, Mechanism and factors that control HIV-1 transcription and latency activation, J Zhejiang Univ Sci B, 15 (2014) 455-465, https://doi.org/10.1631/jzus.B1400059.
[41] G.M. Schiralli Lester, A.J. Henderson, Mechanisms of HIV Transcriptional Regulation and Their Contribution to Latency, Molecular Biology International, 2012 (2012) 614120, https://doi.org/10.1155/2012/614120.
[42] W.I. Sundquist, H.G. Krausslich, HIV-1 assembly, budding, and maturation, Cold Spring Harbor Perspectives Medicine,

2 (2012) a006924, https://doi.org/10.1101/cshperspect.a006924.
[43] M.S. Cohen, G.M. Shaw, A.J. McMichael, B.F. Haynes, Acute HIV-1 Infection, N Engl J Med, 364 (2011) 1943-1954, https://doi.org/10.1056/NEJMra1011874.
[44] A.J. McMichael, P. Borrow, G.D. Tomaras, N. Goonetilleke, B.F. Haynes, The immune response during acute HIV-1 infection: clues for vaccine development, Nat Rev Immunol, 10 (2010) 11-23, https://doi.org/10.1038/nri2674.
[45] Centers for Disease Control and Prevention and Association of Public Health Laboratories, Laboratory Testing for the Diagnosis of HIV Infection: updated recommendations, (2014).
[46] T. Schacker, S. Little, E. Connick, K. Gebhard, Z.Q. Zhang, J. Krieger, J. Pryor, D. Havlir, J.K. Wong, R.T. Schooley, D. Richman, L. Corey, A.T. Haase, Productive infection of T cells in lymphoid tissues during primary and early human immunodeficiency virus infection, J Infect Dis, 183 (2001) 555-562, https://doi.org/10.1086/318524.
[47] J.J. Mattapallil, D.C. Douek, B. Hill, Y. Nishimura, M. Martin, M. Roederer, Massive infection and loss of memory CD4+ T cells in multiple tissues during acute SIV infection, Nature, 434 (2005) 1093-1097, https://doi.org/10.1038/nature03501.
[48] D.D. Ho, A.U. Neumann, A.S. Perelson, W. Chen, J.M. Leonard, M. Markowitz, Rapid turnover of plasma virions and CD4 lymphocytes in HIV-1 infection, Nature, 373 (1995) 123-126, https://doi.org/10.1038/373123a0.
[49] T.W. Schacker, J.P. Hughes, T. Shea, R.W. Coombs, L. Corey, Biological and Virologic Characteristics of Primary HIV Infection, Ann Intern Med, 128 (1998) 613-620, https://doi.org/10.7326/0003-4819-128-8-199804150-00001.
[50] B. Rodríguez, A.K. Sethi, V.K. Cheruvu, W. Mackay, R.J. Bosch, M. Kitahata, S.L. Boswell, W.C. Mathews, D.R. Bangsberg, J. Martin, C.C. Whalen, S. Sieg, S. Yadavalli, S.G. Deeks, M.M. Lederman, Predictive Value of Plasma HIV RNA Level on Rate of CD4 T-Cell Decline in Untreated HIV Infection, JAMA, 296 (2006) 1498-1506, https://doi.org/10.1001/jama.296.12.1498.
[51] J.M. Coffin, S.H. Hughes, H.E. Varmus, Retroviruses, 1997.
[52] E. Schneider, S. Whitmore, M.K. Glynn, K. Dominguez, A. Mitsch, M.T. McKenna, N.C.f.H.A. Division of HIV/AIDS Prevention, Viral Hepatitis, STD, and TB Prevention., Revised Surveillance Case Definitions for HIV Infection Among Adults, Adolescents, and Children Aged <18 Months and for HIV Infection and AIDS Among Children Aged 18

Months to <13 Years --- United States, 2008, MMWR, 57 (2008) 1-12.
[53] J. Poorolajal, E. Hooshmand, H. Mahjub, N. Esmailnasab, E. Jenabi, Survival rate of AIDS disease and mortality in HIV-infected patients: a meta-analysis, Public Health, 139 (2016) 3-12, https://doi.org/10.1016/j.puhe.2016.05.004.
[54] J.K. Wong, M.G. Hezareh, H. F., D.V. Havlir, C.C. Ignacio, C.A. Spina, D.D. Richman, Recovery of Replication-Competent HIV Despite Prolonged Suppression of Plasma Viremia, Science, 278 (1997) 1291-1295, https://doi.org/10.1126/science.278.5341.1291.
[55] D. Finzi, M.P. Hermankova, T. Carruth, L. M., C. Buck, R.E. Chaisson, T.C. Quinn, K. Chadwick, J. Margolick, R. Brookmeyer, J. Gallant, M. Markowitz, D.D. Ho, D.D.S. Richman, R. F., Identification of a Reservoir for HIV-1 in Patients on Highly Active Antiretroviral Therapy, Science, 278 (1997) 1295-1300, https://doi.org/10.1126/science.278.5341.1295.
[56] T.W. Chun, L. Stuyver, S.B.E. Mizell, L. A., J.A. Mican, M. Baseler, A.L. Lloyd, M.A. Nowak, A.S. Fauci, Presence of an inducible HIV-1 latent reservoir during highly active antiretroviral therapy, Proceedings of the National Academy of Sciences of the United States of America, 94 (1997) 13193-13197, https://doi.org/10.1073/pnas.94.24.13193.
[57] G. Nabel, D. Baltimore, An inducible transcription factor activates expression of human immunodeficiency virus in T cells, Nature, 326 (1987) 711-713, https://doi.org/10.1038/326711a0.
[58] T. Folks, J. Kelly, S. Benn, A. Kinter, J. Justement, J. Gold, R. Redfield, K.W. Sell, A.S. Fauci, Susceptibility of normal human lymphocytes to infection with HTLV-III/LAV, J Immunol, 136 (1986) 4049-4053.
[59] T.W. Chun, D. Engel, M.M. Berrey, T. Shea, L.F. Corey, A. S., Early establishment of a pool of latently infected, resting CD4+ T cells during primary HIV-1 infection, Proceedings of the National Academy of Sciences of the United States of America, 95 (1998) 8869-8873, https://doi.org/10.1073/pnas.95.15.8869.
[60] M.A. Ostrowski, T.W. Chun, S.J. Justement, I. Motola, M.A. Spinelli, J. Adelsberger, L.A. Ehler, S.B. Mizell, C.W. Hallahan, A.S. Fauci, Both Memory and CD45RA+/CD62L+ Naive CD4+ T Cells Are Infected in Human Immunodeficiency Virus Type 1-Infected Individuals, Journal of Virology, 73 (1999) 6430-6435, https://doi.org/10.1128/jvi.73.8.6430-6435.1999.
[61] T.W. Chun, L. Carruth, D. Finzi, X. Shen, J.A. DiGiuseppe, H. Taylor, M. Hermankova, K. Chadwick, J. Margolick, T.C.

Quinn, Y.H. Kuo, R. Brookmeyer, M.A.B.-C. Zeiger, P., R.F. Siliciano, Quantification of latent tissue reservoirs and total body viral load in HIV-1 infection, Nature, 387 (1997) 183-188, https://doi.org/10.1038/387183a0.
[62] A. Alexaki, Y. Liu, B. Wigdahl, Cellular Reservoirs of HIV-1 and their Role in Viral Persistence, Current HIV Research, 6 (2008) 388-400, https://doi.org/10.2174/157016208785861195.
[63] D. Finzi, J. Blankson, J.D. Siliciano, J.B. Margolick, K. Chadwick, T. Pierson, K. Smith, J. Lisziewicz, F. Lori, C. Flexner, T.C. Quinn, R.E. Chaisson, E. Rosenberg, B. Walker, S. Gange, J. Gallant, R.F. Siliciano, Latent infection of CD4+ T cells provides a mechanism for lifelong persistence of HIV-1, even in patients on effective combination therapy, Nature Medicine, 5 (1999) 512-517, https://doi.org/10.1038/8394.
[64] J. Chen, T. Zhou, Y. Zhang, S. Luo, H. Chen, D. Chen, C. Li, W. Li, The reservoir of latent HIV, Front Cell Infect Microbiol, 12 (2022) 945-956, https://doi.org/10.3389/fcimb.2022.945956.
[65] B. Lee, M.M. Sharron, L. J., D. Weissman, R.W. Doms, Quantification of CD4, CCR5, and CXCR4 levels on lymphocyte subsets, dendritic cells, and differentially conditioned monocyte-derived macrophages, Proc Natl Acad Sci U S A, 96 (1999) 5215-5220, https://doi.org/10.1073/pnas.96.9.5215.
[66] A. Kumar, W. Abbas, G. Herbein, HIV-1 latency in monocytes/macrophages, Viruses, 6 (2014) 1837-1860, https://doi.org/10.3390/v6041837.
[67] Z. Kruize, N.A. Kootstra, The Role of Macrophages in HIV-1 Persistence and Pathogenesis, Front Microbiol, 10 (2019) 2828, https://doi.org/10.3389/fmicb.2019.02828.
[68] V. Le Douce, G. Herbein, O. Rohr, C. Schwartz, Molecular mechanisms of HIV-1 persistence in the monocyte-macrophage lineage, Retrovirology, 7 (2010), https://doi.org/10.1186/1742-4690-7-32.
[69] M. Pope, S. Gezelter, N. Gallo, L. Hoffman, R.M. Steinman, Low levels of HIV-1 infection in cutaneous dendritic cells promote extensive viral replication upon binding to memory CD4+ T cells, J Exp Med, 182 (1995) 2045-2056, https://doi.org/10.1084/jem.182.6.2045.
[70] K. Lore, A. Smed-Sorensen, J. Vasudevan, J.R. Mascola, R.A. Koup, Myeloid and plasmacytoid dendritic cells transfer HIV-1 preferentially to antigen-specific CD4+ T cells, J Exp Med, 201 (2005) 2023-2033, https://doi.org/10.1084/jem.20042413.
[71] M.J. Churchill, P.R. Gorry, D. Cowley, L. Lal, S. Sonza, D.F. Purcell, K.A. Thompson, D. Gabuzda, J.C. McArthur, C.A.

Pardo, S.L. Wesselingh, Use of laser capture microdissection to detect integrated HIV-1 DNA in macrophages and astrocytes from autopsy brain tissues, J Neurovirol, 12 (2006) 146-152, https://doi.org/10.1080/13550280600748946.
[72] S. Valdebenito, P. Castellano, D. Ajasin, E.A. Eugenin, Astrocytes are HIV reservoirs in the brain: A cell type with poor HIV infectivity and replication but efficient cell-to-cell viral transfer, J Neurochem, 158 (2021) 429-443, https://doi.org/10.1111/jnc.15336.
[73] V. Lutgen, S.D. Narasipura, H.J. Barbian, M. Richards, J. Wallace, R. Razmpour, T. Buzhdygan, S.H. Ramirez, L. Prevedel, E.A. Eugenin, L. Al-Harthi, HIV infects astrocytes in vivo and egresses from the brain to the periphery, PLoS Pathog, 16 (2020) e1008381, https://doi.org/10.1371/journal.ppat.1008381.
[74] K.A. Thompson, C.L. Cherry, J.E. Bell, C.A. McLean, Brain cell reservoirs of latent virus in presymptomatic HIV-infected individuals, Am J Pathol, 179 (2011) 1623-1629, https://doi.org/10.1016/j.ajpath.2011.06.039.
[75] R. Lorenzo-Redondo, H.R. Fryer, T. Bedford, E.Y. Kim, J. Archer, S.L.K. Pond, Y.S. Chung, S. Penugonda, J. Chipman, C.V. Fletcher, T.W. Schacker, M.H. Malim, A. Rambaut, A.T. Haase, A.R. McLean, S.M. Wolinsky, Persistent HIV-1 replication maintains the tissue reservoir during therapy, Nature, 530 (2016) 51-56, https://doi.org/10.1038/nature16933.
[76] J.K. Wong, S.A. Yukl, Tissue reservoirs of HIV, Curr Opin HIV AIDS, 11 (2016) 362-370, https://doi.org/10.1097/COH.0000000000000293.
[77] M.C. Zink, J.E. Clements, The two faces of HIV infection of cerebrospinal fluid Response, COMMENT, 8 (2000) 390-391, https://doi.org/10.1016/S0966-842X(00)01822-9.
[78] V. Valcour, T. Chalermchai, N. Sailasuta, M. Marovich, S.S. Lerdlum, D., N.C. Suwanwela, L. Jagodzinski, N. Michael, S. Spudich, F. van Griensven, M. de Souza, J. Kim, J. Ananworanich, Rv Search Study Group, Central nervous system viral invasion and inflammation during acute HIV infection, J Infect Dis, 206 (2012) 275-282, https://doi.org/10.1093/infdis/jis326.
[79] E.S. Roberts, E.M. Burudi, C. Flynn, L.J. Madden, K.L. Roinick, D.D. Watry, M.A. Zandonatti, M.A. Taffe, H.S. Fox, Acute SIV infection of the brain leads to upregulation of IL6 and interferon-regulated genes: expression patterns throughout disease progression and impact on neuroAIDS, J Neuroimmunol, 157 (2004) 81-92, https://doi.org/10.1016/j.jneuroim.2004.08.030.

[80] M.K. Ash, L. Al-Harthi, J.R. Schneider, HIV in the Brain: Identifying Viral Reservoirs and Addressing the Challenges of an HIV Cure, Vaccines (Basel), 9 (2021), https://doi.org/10.3390/vaccines9080867.
[81] C.A. Jordan, B.A.K. Watkins, C. Dubois-Dalcq, M., Infection of brain microglial cells by human immunodeficiency virus type 1 is CD4 dependent, J Virol, 65 (1991) 736-742, https://doi.org/10.1128/jvi.65.2.736-742.1991.
[82] A. Chauhan, R. Mehla, T.S. Vijayakumar, I. Handy, Endocytosis-mediated HIV-1 entry and its significance in the elusive behavior of the virus in astrocytes, Virology, 456-457 (2014) 1-19, https://doi.org/10.1016/j.virol.2014.03.002.
[83] S.L. Lamers, R.R. Gray, M. Salemi, L.C.M. Huysentruyt, M. S., HIV-1 phylogenetic analysis shows HIV-1 transits through the meninges to brain and peripheral tissues, Infect Genet Evol, 11 (2011) 31-37, https://doi.org/10.1016/j.meegid.2010.10.016.
[84] S.L. Lamers, R. Rose, L.C. Ndhlovu, D.J. Nolan, M. Salemi, E. Maidji, C.A. Stoddart, M.S. McGrath, The meningeal lymphatic system: a route for HIV brain migration?, J Neurovirol, 22 (2016) 275-281, https://doi.org/10.1007/s13365-015-0399-y.
[85] Y. Koyanagi, S. Miles, R.T. Mitsuyasu, J.E. Merrill, H.V. Vinters, I.S. Chen, Dual infection of the central nervous system by AIDS viruses with distinct cellular tropisms, Science, 236 (1987) 819-822, https://doi.org/10.1126/science.3646751.
[86] C. Cheng-Mayer, J.A. Levy, Distinct biological and serological properties of human immunodeficiency viruses from the brain, Ann Neurol, 23 Suppl (1988) S58-61, https://doi.org/10.1002/ana.410230716.
[87] F. Chiodi, A.K. Valentin, B. Schwartz, S. Asjö, B., S. Gartner, M. Popovic, J. Albert, V.A.F. Sundqvist, E. M., Biological characterization of paired human immunodeficiency virus type 1 isolates from blood and cerebrospinal fluid, Virology, 173 (1989) 178-187, https://doi.org/10.1016/0042-6822(89)90233-x.
[88] B.T. Korber, K.J. Kunstman, B.K.F. Patterson, M., M.M. McEvilly, R. Levy, S.M. Wolinsky, Genetic differences between blood- and brain-derived viral sequences from human immunodeficiency virus type 1-infected patients: evidence of conserved elements in the V3 region of the envelope protein of brain-derived sequences, J Virol, 68 (1994) 7467-7481, https://doi.org/10.1128/JVI.68.11.7467-7481.

[89] J.K. Wong, C.C. Ignacio, F. Torriani, D. Havlir, N.J. Fitch, D.D. Richman, In vivo compartmentalization of human immunodeficiency virus: evidence from the examination of pol sequences from autopsy tissues, J Virol, 71 (1997) 2059-2071, https://doi.org/10.1128/JVI.71.3.2059-2071.
[90] M.C. Strain, S.l. Letendre, S.K. Pillai, T. Russell, C.C.G. Ignacio, H. F., B. Good, D.M. Smith, S.M. Wolinsky, M. Furtado, J. Marquie-Beck, J. Durelle, I. Grant, D.D. Richman, T. Marcotte, J.A. McCutchan, R.J. Ellis, J.K. Wong, Genetic composition of human immunodeficiency virus type 1 in cerebrospinal fluid and blood without treatment and during failing antiretroviral therapy, J Virol, 79 (2005) 1772-1788, https://doi.org/10.1128/JVI.79.3.1772-1788.2005.
[91] P.R. Harrington, G. Schnell, S.L. Letendre, K. Ritola, K. Robertson, C. Hall, C.L. Burch, C.B. Jabara, D.T. Moore, R.J. Ellis, R.W. Price, R. Swanstrom, Cross-sectional characterization of HIV-1 env compartmentalization in cerebrospinal fluid over the full disease course, AIDS, 23 (2009) 907-915, https://doi.org/10.1097/QAD.0b013e3283299129.
[92] G. Schnell, S. Spudich, P. Harrington, R.W. Price, R. Swanstrom, Compartmentalized human immunodeficiency virus type 1 originates from long-lived cells in some subjects with HIV-1-associated dementia, PLoS Pathog, 5 (2009) e1000395, https://doi.org/10.1371/journal.ppat.1000395.
[93] J.T. Blackard, HIV compartmentalization-- a review on a clinically important phenomenon, Curr HIV Res, 10 (2012) 133-142, https://doi.org/10.2174/157016212799937245.
[94] P. Chan, S. Spudich, HIV Compartmentalization in the CNS and Its Impact in Treatment Outcomes and Cure Strategies, Curr HIV/AIDS Rep, 19 (2022) 207-216, https://doi.org/10.1007/s11904-022-00605-1.
[95] M. Airoldi, A. Bandera, D. Trabattoni, B. Tagliabue, B. Arosio, A. Soria, V. Rainone, G. Lapadula, G. Annoni, M. Clerici, A. Gori, Neurocognitive impairment in HIV-infected naive patients with advanced disease: the role of virus and intrathecal immune activation, Clin Dev Immunol, 2012 (2012) 467154, https://doi.org/10.1155/2012/467154.
[96] S. Hong, W.A. Banks, Role of the immune system in HIV-associated neuroinflammation and neurocognitive implications, Brain Behav Immun, 45 (2015) 1-12, https://doi.org/10.1016/j.bbi.2014.10.008.
[97] N. Sacktor, R.H. Lyles, R. Skolasky, C. Kleeberger, O.A. Selnes, E.N. Miller, J.T. Becker, B. Cohen, J.C. McArthur, Multicenter AIDS Cohort Study, HIV-associated neurologic disease incidence changes-- Multicenter AIDS Cohort Study,

1990-1998, Neurology, 56 (2001) 257-260, https://doi.org/10.1212/wnl.56.2.257.
[98] S.B. Joseph, L.P. Kincer, N.M. Bowman, C. Evans, M.J. Vinikoor, C.K. Lippincott, M. Gisslen, S. Spudich, P. Menezes, K. Robertson, N. Archin, A. Kashuba, J.J. Eron, R.W. Price, R. Swanstrom, Human Immunodeficiency Virus Type 1 RNA Detected in the Central Nervous System (CNS) After Years of Suppressive Antiretroviral Therapy Can Originate from a Replicating CNS Reservoir or Clonally Expanded Cells, Clin Infect Dis, 69 (2019) 1345-1352, https://doi.org/10.1093/cid/ciy1066.
[99] I. Perez-Valero, R. Ellis, R. Heaton, R. Deutsch, D. Franklin, D.B. Clifford, A. Collier, B. Gelman, C. Marra, J.A. McCutchan, A. Navis, N. Sacktor, D. Simpson, I. Grant, S. Letendre, Cerebrospinal fluid viral escape in aviremic HIV-infected patients receiving antiretroviral therapy: prevalence, risk factors and neurocognitive effects, AIDS, 33 (2019) 475-481, https://doi.org/10.1097/QAD.0000000000002074.
[100] A.F. Fois, B.J. Brew, The Potential of the CNS as a Reservoir for HIV-1 Infection: Implications for HIV Eradication, Curr HIV/AIDS Rep, 12 (2015) 299-303, https://doi.org/10.1007/s11904-015-0257-9.
[101] M.J. Peluso, F. Ferretti, J. Peterson, E. Lee, D. Fuchs, A. Boschini, M. Gisslen, N. Angoff, R.W. Price, P. Cinque, S. Spudich, Cerebrospinal fluid HIV escape associated with progressive neurologic dysfunction in patients on antiretroviral therapy with well controlled plasma viral load, AIDS, 26 (2012) 1765-1774, https://doi.org/10.1097/QAD.0b013e328355e6b2.
[102] R. Bingham, N. Ahmed, P. Rangi, M. Johnson, M. Tyrer, J. Green, HIV encephalitis despite suppressed viraemia: a case of compartmentalized viral escape, International Journal of STD & AIDS, 22 (2011) 608-609, https://doi.org/10.1258/ijsa.2011.010507.
[103] J.D. Estes, C. Kityo, F. Ssali, L. Swainson, K.N. Makamdop, G.Q. Del Prete, S.G. Deeks, P.A. Luciw, J.G. Chipman, G.J. Beilman, T. Hoskuldsson, A. Khoruts, J. Anderson, C. Deleage, J. Jasurda, T.E. Schmidt, M. Hafertepe, S.P. Callisto, H. Pearson, T. Reimann, J. Schuster, J. Schoephoerster, P. Southern, K. Perkey, L. Shang, S.W. Wietgrefe, C.V. Fletcher, J.D. Lifson, D.C. Douek, J.M. McCune, A.T. Haase, T.W. Schacker, Defining total-body AIDS-virus burden with implications for curative strategies, Nat Med, 23 (2017) 1271-1276, https://doi.org/10.1038/nm.4411.
[104] R.S. Veazey, M. DeMaria, L.V. Chalifoux, D.E. Shvetz, D.R. Pauley, H.L. Knight, M. Rosenzweig, R.P. Johnson, R.C.

Desrosiers, A.A. Lackner, Gastrointestinal Tract as a Major Site of CD4+ T Cell Depletion and Viral Replication in SIV Infection, Science, 280 (1998) 427-431, https://doi.org/10.1126/science.280.5362.427.
[105] T.W. Chun, D.C. Nickle, J.S. Justement, J.H. Meyers, G. Roby, C.W. Hallahan, S. Kottilil, S. Moir, J.M. Mican, J.I. Mullins, D.J. Ward, J.A. Kovacs, P.J. Mannon, A.S. Fauci, Persistence of HIV in gut-associated lymphoid tissue despite long-term antiretroviral therapy, J Infect Dis, 197 (2008) 714-720, https://doi.org/10.1086/527324.
[106] A. Zgair, Wong, J. C. M., Gershkovich, P., Targeting immunomodulatory agents to the gut-associated lymphoid tissue, in: Neuro-Immuno-Gastroenterology, Springer International Publishing, Switzerland, 2016, pp. 237–261.
[107] A.M. Mowat, J.L. Viney, The anatomical basis of intestinal immunity, Immunological Reviews, 156 (1997) 145-166, https://doi.org/10.1111/j.1600-065x.1997.tb00966.x.
[108] H. Nakajima-Adachi, A. Kikuchi, Y. Fujimura, K. Shibahara, T. Makino, M. Goseki-Sone, M. Kihara-Fujioka, T. Nochi, Y. Kurashima, O. Igarashi, M. Yamamoto, J. Kunisawa, M. Toda, S. Kaminogawa, R. Sato, H. Kiyono, S. Hachimura, Peyer's patches and mesenteric lymph nodes cooperatively promote enteropathy in a mouse model of food allergy, PLoS One, 9 (2014) e107492, https://doi.org/10.1371/journal.pone.0107492.
[109] A.M. Mowat, Anatomical basis of tolerance and immunity to intestinal antigens, Nat Rev Immunol, 3 (2003) 331-341, https://doi.org/10.1038/nri1057.
[110] M.L. Forchielli, W.A. Walker, The role of gut-associated lymphoid tissues and mucosal defence, Br J Nutr, 93 Suppl 1 (2005) S41-48, https://doi.org/10.1079/bjn20041356.
[111] A.J. Macpherson, K. Smith, Mesenteric lymph nodes at the center of immune anatomy, J Exp Med, 203 (2006) 497-500, https://doi.org/10.1084/jem.20060227.
[112] F.P. Huang, N. Platt, M. Wykes, J.R. Major, T.J. Powell, C.D. Jenkins, G.G. MacPherson, A discrete subpopulation of dendritic cells transports apoptotic intestinal epithelial cells to T cell areas of mesenteric lymph nodes, J Exp Med, 191 (2000) 435-444, https://doi.org/10.1084/jem.191.3.435.
[113] C.G. Thompson, C.L. Gay, A.D.M. Kashuba, HIV Persistence in Gut-Associated Lymphoid Tissues: Pharmacological Challenges and Opportunities, AIDS Research and Human Retroviruses, 33 (2017) 513-523, https://doi.org/10.1089/AID.2016.0253.
[114] G. Pantaleo, C. Graziosi, L. Butini, P.A.S. Pizzo, S. M. Kotler, D. P., A.S. Fauci, Lymphoid organs function as major reservoirs for human immunodeficiency virus, Proceedings

of the National Academy of Sciences of the United States of America, 88 (1991) 9838-9842, https://doi.org/10.1073/pnas.88.21.9838.
[115] J. Musumali, P. Julius, S.N. Siyumbwa, D. Yalcin, G. Kang, S. Munsaka, J.T. West, C. Wood, Systematic post-mortem analysis of brain tissue from an HIV-1 subtype C viremic decedent revealed a paucity of infection and pathology, J Neurovirol, 28 (2022) 527-536, https://doi.org/10.1007/s13365-022-01099-8.
[116] S. Siddiqui, S. Perez, Y. Gao, L. Doyle-Meyers, B.T. Foley, Q. Li, B. Ling, Persistent Viral Reservoirs in Lymphoid Tissues in SIV-Infected Rhesus Macaques of Chines-Origin on Suppressive Antiretroviral Therapy, Viruses, 11 (2019) 105, https://doi.org/10.3390/v11020105.
[117] P.K. Riggs, A. Chaillon, G. Jiang, S.L. Letendre, Y. Tang, J. Taylor, A. Kaytes, D.M. Smith, K. Dube, S. Gianella, Lessons for Understanding Central Nervous System HIV Reservoirs from the Last Gift Program, Curr HIV/AIDS Rep, 19 (2022) 566-579, https://doi.org/10.1007/s11904-022-00628-8.
[118] A. Chaillon, S. Gianella, S. Dellicour, S.A. Rawlings, T.E. Schlub, M.F. De Oliveira, C. Ignacio, M. Porrachia, B. Vrancken, D.M. Smith, HIV persists throughout deep tissues with repopulation from multiple anatomical sources, J Clin Invest, 130 (2020) 1699-1712, https://doi.org/10.1172/JCI134815.
[119] A. Cheret, C. Bacchus-Souffan, V. Avettand-Fenoel, A. Melard, G. Nembot, C. Blanc, A. Samri, A. Saez-Cirion, L. Hocqueloux, C. Lascoux-Combe, C. Allavena, C. Goujard, M.A. Valantin, A. Leplatois, L. Meyer, C. Rouzioux, B. Autran, O.A.-S. Group., Combined ART started during acute HIV infection protects central memory CD4+ T cells and can induce remission, J Antimicrob Chemother, 70 (2015) 2108-2120, https://doi.org/10.1093/jac/dkv084.
[120] J. Ananworanich, N. Chomont, L.A. Eller, E. Kroon, S. Tovanabutra, M. Bose, M. Nau, J.L.K. Fletcher, S. Tipsuk, C. Vandergeeten, R.J. O'Connell, S. Pinyakorn, N. Michael, N. Phanuphak, M.L. Robb, R.a.R.S.s. groups., HIV DNA Set Point is Rapidly Established in Acute HIV Infection and Dramatically Reduced by Early ART, EBioMedicine, 11 (2016) 68-72, https://doi.org/10.1016/j.ebiom.2016.07.024.
[121] L. Hocqueloux, V. Avettand-Fenoel, S. Jacquot, T. Prazuck, E. Legac, A.N. Melard, M., C. Mille, G. Le Moal, J.P. Viard, C. Rouzioux, A.C.o.t.A.N.d.R.s.l.S.e.l.H. Virales., Long-term antiretroviral therapy initiated during primary HIV-1 infection is key to achieving both low HIV reservoirs

and normal T cell counts, J Antimicrob Chemother, 68 (2013) 1169-1178, https://doi.org/10.1093/jac/dks533.
[122] M. Laanani, J. Ghosn, A. Essat, A. Melard, R. Seng, M. Gousset, H. Panjo, E. Mortier, P.M. Girard, C. Goujard, L. Meyer, C. Rouzioux, P.C.S.G. Agence Nationale de Recherche sur le Sida, Impact of the Timing of Initiation of Antiretroviral Therapy During Primary HIV-1 Infection on the Decay of Cell-Associated HIV-DNA, Clin Infect Dis, 60 (2015) 1715-1721, https://doi.org/10.1093/cid/civ171.
[123] W.J. Hey-Cunningham, J.M. Murray, V. Natarajan, J. Amin, C.L. Moore, S. Emery, D.A. Cooper, J. Zaunders, A.D. Kelleher, K.K. Koelsch, P.s. team., Early antiretroviral therapy with raltegravir generates sustained reductions in HIV reservoirs but not lower T-cell activation levels, AIDS, 29 (2015) 911-919, https://doi.org/10.1097/QAD.0000000000000625.
[124] J. Ananworanich, A. Schuetz, C. Vandergeeten, I. Sereti, M. de Souza, R. Rerknimitr, R. Dewar, M. Marovich, F. van Griensven, R. Sekaly, S. Pinyakorn, N. Phanuphak, R. Trichavaroj, W. Rutvisuttinunt, N. Chomchey, R. Paris, S. Peel, V. Valcour, F. Maldarelli, N. Chomont, N. Michael, P. Phanuphak, J.H. Kim, R.S.S. Group., Impact of multi-targeted antiretroviral treatment on gut T cell depletion and HIV reservoir seeding during acute HIV infection, PLoS One, 7 (2012) e33948, https://doi.org/10.1371/journal.pone.0033948.
[125] K.K. Koelsch, C. Boesecke, K. McBride, L. Gelgor, P. Fahey, V. Natarajan, D. Baker, M. Bloch, J.M. Murray, J. Zaunders, S. Emery, D.A. Cooper, A.D. Kelleher, P.s. team., Impact of treatment with raltegravir during primary or chronic HIV infection on RNA decay characteristics and the HIV viral reservoir, AIDS, 25 (2011) 2069-2078, https://doi.org/10.1097/QAD.0b013e32834b9658.
[126] L. Leyre, E. Kroon, C. Vandergeeten, C. Sacdalan, D.J. Colby, S. Buranapraditkun, A. Schuetz, N. Chomchey, M. de Souza, W. Bakeman, R. Fromentin, S. Pinyakorn, S. Akapirat, R. Trichavaroj, S. Chottanapund, S. Manasnayakorn, R. Rerknimitr, P. Wattanaboonyoungcharoen, J.H. Kim, S. Tovanabutra, T.W. Schacker, R. O'Connell, V.G. Valcour, P. Phanuphak, M.L. Robb, N. Michael, L. Trautmann, N. Phanuphak, J. Ananworanich, N. Chomont, R.V.S.S.s.g. Rv254/Search, Abundant HIV-infected cells in blood and tissues are rapidly cleared upon ART initiation during acute HIV infection, Sci Transl Med, 12 (2020), https://doi.org/10.1126/scitranslmed.aav3491.

[127] T.A. Crowell, N. Phanuphak, S. Pinyakorn, E. Kroon, J.L. Fletcher, D. Colby, S. Tipsuk, P. Karnsomlap, N. Laopraynak, R.J. O'Connell, M.L. Robb, J. Ananworanich, R.S.S. Group., Virologic failure is uncommon after treatment initiation during acute HIV infection, AIDS, 30 (2016) 1943-1950, https://doi.org/10.1097/QAD.0000000000001148.
[128] M. Massanella, R.A. Bender Ignacio, J.R. Lama, A. Pagliuzza, S. Dasgupta, R. Alfaro, J. Rios, C. Ganoza, D. Pinto-Santini, T. Gilada, A. Duerr, N. Chomont, Long-term effects of early antiretroviral initiation on HIV reservoir markers: a longitudinal analysis of the MERLIN clinical study, The Lancet Microbe, 2 (2021) e198-e209, https://doi.org/10.1016/s2666-5247(21)00010-0.
[129] C.M. Rueda, P.A. Velilla, C.A. Chougnet, C.J.R. Montoya, M. T., HIV-induced T-cell activation/exhaustion in rectal mucosa is controlled only partially by antiretroviral treatment, PLoS One, 7 (2012) e30307, https://doi.org/10.1371/journal.pone.0030307.
[130] N.B. Kiviat, C.W.H. Critchlow, S. E., J.S. Kuypers, C., G. Goldbaum, J.A. van Burik, T. Lampinen, K.K. Holmes, Determinants of human immunodeficiency virus DNA and RNA shedding in the anal-rectal canal of homosexual men, The Journal of Infectious Diseases, 177 (1998) 571-578, https://doi.org/10.1086/514239.
[131] O. Bourry, A. Mannioui, P. Sellier, C. Roucairol, L. Durand-Gasselin, N. Dereuddre-Bosquet, H. Benech, P. Roques, R. Le Grand, Effect of a short-term HAART on SIV load in macaque tissues is dependent on time of initiation and antiviral diffusion, Retrovirology, 7 (2010) 78, https://doi.org/10.1186/1742-4690-7-78.
[132] C.V. Fletcher, K. Staskus, S.W. Wietgrefe, M. Rothenberger, C. Reilly, J.G. Chipman, G.J. Beilman, A. Khoruts, A. Thorkelson, T.E. Schmidt, J. Anderson, K. Perkey, M. Stevenson, A.S. Perelson, D.C. Douek, A.T. Haase, T.W. Schacker, Persistent HIV-1 replication is associated with lower antiretroviral drug concentrations in lymphatic tissues, Proc Natl Acad Sci U S A, 111 (2014) 2307-2312, https://doi.org/10.1073/pnas.1318249111.
[133] H. Mitsuya, K.J. Weinhold, P.A. Furman, M.H. St Clair, S.N. Lehrman, R.C. Gallo, D. Bolognesi, D.W. Barry, S. Broder, 3'-Azido-3'-deoxythymidine (BW A509U) an antiviral agent that inhibits the infectivity and cytopathic effect of human T-lymphotropic virus type III llymphadenopathy-associated virus in vitro, Proceedings of the National Academy of Sciences of the United States of America, 82 (1985) 7096-7100, https://doi.org/10.1073/pnas.82.20.7096.

[134] M.A. Fischl, D.D. Richman, M.H. Grieco, M.S.V. Gottlieb, P. A., O.L.L. Laskin, J. M., J.E. Groopman, D. Mildvan, R.T. Schooley, The Efficacy of Azidothymidine (AZT) in the Treatment of Patients with AIDS and AIDS-Related Complex, The New England Journal of Medicine, 317 (1987) 185-191, https://doi.org/10.1056/NEJM198707233170401.
[135] B.A. Larder, G. Darby, D.D. Richman, HIV with Reduced Sensitivity to Zidovudine (AZT) Isolated During Prolonged Therapy, Science, 243 (1989) 1731-1734, https://doi.org/10.1126/science.2467383.
[136] R. Rooke, M. Tremblay, H. Soudeyns, L.Y. DeStephano, X. J., M. Fanning, J.S. Montaner, M. O'Shaughnessy, K. Gelmon, C.G. Tsoukas, J., J. Ruedy, M.A. Wainberg, Isolation of drug-resistant variants of HIV-1 from patients on long-term zidovudine therapy. Canadian Zidovudine Multi-Centre Study Group, AIDS, 3 (1989) 411-415, https://doi.org/10.1097/00002030-198907000-00001.
[137] S. Land, G. Terloar, D. McPhee, C. Birch, R.C. Doherty, D., I. Gust, Decreased In Vitro Susceptibility to Zidovudine of HIV Isolates Obtained from Patients with AIDS, The Journal of Infectious Diseases, 161 (1990) 326-329, https://doi.org/10.1093/infdis/161.2.326.
[138] M.A.R. Wainberg, R., M. Tremblay, X.P. Li, M. A. Gao, Q. Yao, X. J., C. Tsoukas, J. Montaner, M. Fanning, J. Ruedy, Clinical significance and characterization of AZT-resistant strains of HIV-1, Canadian Journal of Infectious Diseases and Medical Microbiology, 2 (1991) 5-11, https://doi.org/10.1155/1991/124860.
[139] S.M. Hammer, D.A. Katzenstein, M.D. Hughes, H. Gundacker, R.T. Schooley, R.H.H. Haubrich, W. K., M.M. Lederman, J.P. Phair, M. Niu, M.S. Hirsch, T.C. Merigan, A Trial Comparing Nucleoside Monotherapy with Combination Therapy in HIV-Infected Adults with CD4 Cell Counts from 200 to 500 per Cubic Millimeter, N Engl J Med, 335 (1996) 1081-1090, https://doi.org/10.1056/NEJM199610103351501.
[140] J.H. Darbyshire, Delta: a randomised double-blind controlled trial comparing combinations of zidovudine plus didanosine or zalcitabine with zidovudine alone in HIV-infected individuals, The Lancet, 348 (1996) 283-291, https://doi.org/10.1016/s0140-6736(96)05387-1.
[141] S. Vella, B. Schwartlander, S.P. Sow, S.P. Eholie, R.L. Murphy, The history of antiretroviral therapy and of its implementation in resource-limited areas of the world, AIDS, 26 (2012) 1231-1241, https://doi.org/10.1097/QAD.0b013e32835521a3.

[142] R.W. Shafer, D.A. Vuitton, Highly active antiretroviral therapy (Haart) for the treatment of infection with human immunodeficiency virus type 1, Biomedicine & Pharmacotherapy, 53 (1999) 73-86, https://doi.org/10.1016/s0753-3322(99)80063-8.
[143] R.M. Gulick, J.W. Mellors, D. Havlir, J.J. Eron, C.M. Gonzalez, D. Richman, D. D., F.T. Valentine, L. Jonas, A. Meibohm, E.A. Emini, J.A. Chodakewitz, Treatment with indinavir, zidovudine, and lamivudine in adults with human immunodeficiency virus infection and prior antiretroviral therapy, The New England Journal of Medicine, 337 (1997) 734-739, https://doi.org/10.1056/NEJM199709113371102.
[144] S.M. Hammer, K.E.H. Squires, M. D., J.M.D. Grimes, L. M., J.S.E. Currier, J. J. Jr. Feinberg, J. E., H.H.J.D. Balfour, L. R., J.A. Chodakewitz, M.A. Fischl, A controlled trial of two nucleoside analogues plus indinavir in persons with human immunodeficiency virus infection and CD4 cell counts of 200 per cubic millimeter or less. AIDS Clinical Trials Group 320 Study Team, The New England Journal of Medicine, 337 (1997) 725-733, https://doi.org/10.1056/NEJM199709113371101.
[145] R.D. Moore, R.E. Chaisson, Natural history of HIV infection in the era of combination antiretroviral therapy, AIDS, 13 (1999) 1933-1942, https://doi.org/10.1097/00002030-199910010-00017.
[146] J.S.R. Montaner, P., D.V. Cooper, S., M.C. Harris, B. Wainberg, M. A., D. Smith, P. Robinson, D. Hall, M. Myers, J.M. Lange, A Randomized, Double-blind Trial Comparing Combinations of Nevirapine, Didanosine, and Zidovudine for HIV-Infected Patients: The INCAS Trial, JAMA, 279 (1998) 930-937, https://doi.org/10.1001/jama.279.12.930.
[147] HIVinfo.NIH.gov, FDA Approval of HIV Medicines, in.
[148] N.E. Kohl, E.A. Emini, W.A. Schleif, L.J. Davis, J.C. Heimbach, R.A. Dixon, E.M. Scolnick, I.S. Sigal, Active human immunodeficiency virus protease is required for viral infectivity, Proceedings of the National Academy of Sciences of the United States of America, 85 (1988) 4686-4690, https://doi.org/10.1073/pnas.85.13.4686.
[149] R.A. Kramer, M.D. Schaber, A.M. Skalka, K. Ganguly, F. Wong-Staal, E.P. Reddy, HTLV-III gag Protein Is Processed in Yeast Cells by the Virus pol-Protease, Science, 231 (1986) 1580-1584, https://doi.org/10.1126/science.2420008.
[150] J.R. Huff, HIV protease-- a novel chemotherapeutic target for AIDS, Journal of Medicinal Chemistry, 34 (1991) 2305-2314, https://doi.org/10.1021/jm00112a001.

[151] A. Brik, C.H. Wong, HIV-1 protease: mechanism and drug discovery, Org Biomol Chem, 1 (2003) 5-14, https://doi.org/10.1039/b208248a.
[152] A. Wlodawer, M. Miller, M.S. Jaskólski, B. K. Baldwin, E. Weber, I. T. Selk, L. M. Clawson, L., J. Schneider, S.B. Kent, Conserved folding in retroviral proteases: crystal structure of a synthetic HIV-1 protease, Science, 245 (1989) 616-621, https://doi.org/10.1126/science.2548279.
[153] M.A. Navia, P.M. Fitzgerald, B.M. McKeever, C.T. Leu, J.C. Heimbach, W.K. Herber, I.S. Sigal, P.L. Darke, J.P. Springer, Three-dimensional structure of aspartyl protease from human immunodeficiency virus HIV-1, Nature, 337 (1989) 615-620, https://doi.org/10.1038/337615a0.
[154] A.M.J. Wensing, A. Fun, M. Nijhuis, HIV Protease Inhibitor Resistance, in: Handbook of Antimicrobial Resistance, 2017, pp. 567-602.
[155] Y. Hamada, Y. Kiso, New directions for protease inhibitors directed drug discovery, Biopolymers, 106 (2016) 563-579, https://doi.org/10.1002/bip.22780.
[156] N.A. Roberts, J.A.K. Martin, D. Broadhurst, A. V., J.C. Craig, I.B. Duncan, S.A. Galpin, B.K.K. Handa, J., A. Kröhn, R.W. Lambert, J.H. Merrett, J.S.P. Mills, K. E. B., S. Redshaw, A.J.T. Ritchie, D. L. Thomas, G. J., P.J. Machin, Rational Design of Peptide-Based HIV Proteinase Inhibitors, Science, 248 (1990) 358-361, https://doi.org/10.1126/science.2183354.
[157] E. De Clercq, The history of antiretrovirals: key discoveries over the past 25 years, Rev Med Virol, 19 (2009) 287-299, https://doi.org/10.1002/rmv.624.
[158] A.M. Wensing, N.M. van Maarseveen, M. Nijhuis, Fifteen years of HIV Protease Inhibitors: raising the barrier to resistance, Antiviral Res, 85 (2010) 59-74, https://doi.org/10.1016/j.antiviral.2009.10.003.
[159] S.G. Deeks, M. Smith, M. Holodniy, J.O. Kahn, HIV-1 Protease Inhibitors a review for clinicians, JAMA, 277 (1997) 145-153, https://doi.org/10.1001/jama.1997.03540260059037.
[160] F.J.J. Palella, K.M. Delaney, A.C. Moorman, M.O. Loveless, J. Fuhrer, G.A.A. Satten, D. J., S.D. Holmberg, Declining morbidity and mortality among patients with advanced human immunodeficiency virus infection. HIV Outpatient Study Investigators, The New England Journal of Medicine, 338 (1998) 853-860, https://doi.org/10.1056/NEJM199803263381301.
[161] K.A. Sepkowitz, Effect of HAART on natural history of AIDS-related opportunistic disorders, The Lancet, 351 (1998)

228-230, https://doi.org/10.1016/s0140-6736(05)78279-9.
[162] H.R. Brodt, B.S. Kamps, P. Gute, B. Knupp, S. Staszewski, E.B. Helm, Changing incidence of AIDS-defining illnesses in the era of antiretroviral combination therapy, AIDS, 11 (1997) 1731-1738, https://doi.org/10.1097/00002030-199714000-00010.
[163] J.H.S. Condra, W. A., O.M.G. Blahy, L. J. Graham, D. J., J.C.R. Quintero, A., H.L.R. Robbins, E. Shivaprakash, M. Titus, D. Yang, T., H. Teppler, K.E. Squires, P.J. Deutsch, E.A. Emini, In vivo emergence of HIV-1 variants resistant to multiple protease inhibitors, Nature, 374 (1995) 569-571, https://doi.org/10.1038/374569a0.
[164] N. van Maarseveen, C. Boucher, Resistance to protease inhibitors, in: A.M. Geretti (Ed.) Antiretroviral Resistance in Clinical Practice, London, 2006, pp. Chapter 3.
[165] B. Luna, M.U. Townsend, Tipranavir: The First Nonpeptidic Protease Inhibitor for the treatment of protease resistant, Clinical therapeutics, 29 (2007) 2309-2318, https://doi.org/10.1016/j.clinthera.2007.11.007.
[166] Y. Kashman, K.R.F. Gustafson, R. W., J.H.n. Cardellina, J.B.C. McMahon, M. J., R.W.J. Buckheit, S.H.C. Hughes, G. M., M.R. Boyd, The calanolides, a novel HIV-inhibitory class of coumarin derivatives from the tropical rainforest tree, Calophyllum lanigerum, Journal of Medicinal Chemistry, 353 (1992) 2735-2743, https://doi.org/10.1021/jm00093a004.
[167] S.R. Turner, J.W. Strohbach, R.A.A. Tommasi, P. A., P.D.S. Johnson, H. I., L.A. Dolak, E.P. Seest, P.K. Tomich, M.J. Bohanon, M.M. Horng, J.C. Lynn, K.T. Chong, R.R. Hinshaw, K.D. Watenpaugh, M.N. Janakiraman, S. Thaisrivongs, Tipranavir (PNU-140690): A Potent, Orally Bioavailable Nonpeptidic HIV Protease Inhibitor of the 5,6-Dihydro-4-hydroxy-2-pyrone Sulfonamide class, Journal of Medicinal Chemistry, 41 (1998) 3467-3476, https://doi.org/10.1021/jm9802158.
[168] B.A. Larder, K. Hertogs, S. Bloor, C.H.D. van den Eynde, W., Y. Wang, W.W. Freimuth, G. Tarpley, Tipranavir inhibits broadly protease inhibitor-resistant HIV-1 clinical samples, AIDS, 14 (2000) 1943-1948, https://doi.org/10.1097/00002030-200009080-00009.
[169] S. Muzammil, A.A.K. Armstrong, L. W., A. Jakalian, P.R. Bonneau, V. Schmelmer, L.M. Amzel, E. Freire, Unique thermodynamic response of tipranavir to human immunodeficiency virus type 1 protease drug resistance mutations, J Virol, 81 (2007) 5144-5154, https://doi.org/10.1128/JVI.02706-06.

[170] Z. Temesgen, J. Feinberg, Tipranavir: a new option for the treatment of drug-resistant HIV infection, Clin Infect Dis, 45 (2007) 761-769, https://doi.org/10.1086/520847.
[171] S. Dieter, How flexible is tipranavir in complex with the HIV-1 protease active site?, AIDS, 18 (2004) 579-580, https://doi.org/10.1097/01.aids.0000111467.61782.bf.
[172] S. Thaisrivongs, H.I. Skulnick, S.R. Turner, J.W.T. Strohbach, R. A., P.D. Johnson, P.A. Aristoff, T.M. Judge, R.B. Gammill, J.K. Morris, K.R. Romines, R.A. Chrusciel, R.R. Hinshaw, K.T. Chong, W.G. Tarpley, S.M. Poppe, D.E. Slade, J.C. Lynn, M.M. Horng, P.K. Tomich, E.P. Seest, L.A. Dolak, W.J. Howe, G.M. Howard, K.D. Watenpaugh, e. al., Structure-based design of HIV protease inhibitors: sulfonamide-containing 5,6-dihydro-4-hydroxy-2-pyrones as non-peptidic inhibitors, J Med Chem, 39 (1996) 4349-4353, https://doi.org/10.1021/jm960541s.
[173] European Medicines Agency, Aptivus-epar-scientific-discussion_en, in, 2005.
[174] J.R. King, H. Wynn, R. Brundage, E.P. Acosta, Pharmacokinetic enhancement of protease inhibitor therapy, Clin Pharmacokinet, 43 (2004) 291-310, https://doi.org/10.2165/00003088-200443050-00003.
[175] N.H.C. Loos, J.H. Beijnen, A.H. Schinkel, The Mechanism-Based Inactivation of CYP3A4 by Ritonavir: What Mechanism?, Int J Mol Sci, 23 (2022), https://doi.org/10.3390/ijms23179866.
[176] S. McCallister, J.P. Sabo, D. Mayers, L. Galitz, An Open-Label, Steady-State Investigation of the Pharmacokinetics (PK) of Tipranavir (TPV) and Ritonavir (RTV) and Their Effects on Cytochrome P-450 (3A4) Activity in Normal, Healthy Volunteers (BI 1182.5), in: the 9th Conference on Retroviruses and Opportunistic Infections, Seattle, WA, U.S.A.,, 2002.
[177] D. Neubacher, M. Markowitz, L. Slater, R. Curry, V. Kohlbrenner, S. McCallister, Tipranavir: phase II study, 80 week follow-up, in: 9th European AIDS Conference (EACS), Waesaw, Poland, 2003.
[178] Aptivus®(tipranavir) capsules, 250mg: prescribing information, in, Boehringer Ingelheim, Ridgefield (CT), 2005.
[179] The European Agency for the Evaluation of Medical Products, POLYOXYL CASTOR OIL POLYOXYL HYDROGENATED CASTOR OIL SUMMARY REPORT, in: V.M.E. Unit (Ed.), 1999.
[180] G. Cornaire, J. Woodley, S. Saivin, J.Y. Legendre, S. Decourt, A. Cloarec, G. Houin, Effect of Polyoxyl 35 Castor Oil and Polysorbate 80 on the Intestinal Absorption of

Digoxin in vitro, Arzneimittelforschung, 50 (2000) 576-579, https://doi.org/10.1055/s-0031-1300252.
[181] K. Katneni, S.A.P. Charman, C. J., Impact of cremophor-EL and polysorbate-80 on digoxin permeability across rat jejunum: delineation of thermodynamic and transporter related events using the reciprocal permeability approach, J Pharm Sci, 96 (2007) 280-293, https://doi.org/10.1002/jps.20779.
[182] J.R. Baldwin, M.T. Borin, Y. Wang, Effects of food and antacid on bioavailability of the protease inhibitor PNU-140690 in healthyvolunteers, Presented at: 5th Conference on Retroviruses and Opportunistic Infections, (1998).
[183] K.M. Chan-Tack, K.A.B. Struble, D. B., Intracranial hemorrhage and liver-associated deaths associated with tipranavir/ritonavir: review of cases from the FDA's Adverse Event Reporting System, AIDS Patient Care STDS, 22 (2008) 843-850, https://doi.org/10.1089/apc.2008.0043.
[184] D.O. Passos, M. Li, I.K. Jozwik, X.Z. Zhao, D. Santos-Martins, R. Yang, S.J. Smith, Y. Jeon, S. Forli, S.H. Hughes, T.R.J. Burke, R. Craigie, D. Lyumkis, Structural basis for strand-transfer inhibitor binding to HIV intasomes, Science, 367 (2020) 810-814, https://doi.org/10.1126/science.aay8015.
[185] M.G. Nowotny, S. A., R.J. Crouch, W. Yang, Crystal structures of RNase H bound to an RNA/DNA hybrid: substrate specificity and metal-dependent catalysis, Cell, 121 (2005) 1005-1016, https://doi.org/10.1016/j.cell.2005.04.024.
[186] F. Maldarelli, The role of HIV integration in viral persistence: no more whistling past the proviral graveyard, The Journal of Clinical Investigation, 126 (2016) 438-447, https://doi.org/10.1172/JCI80564.
[187] D.J. Hazuda, P. Felock, M. Witmer, A. Wolfe, K. Stillmock, J.A. Grobler, A. Espeseth, L. Gabryelski, W. Schleif, C. Blau, M.D. Miller, Inhibitors of strand transfer that prevent integration and inhibit HIV-1 replication in cells, Science, 287 (2000) 646-650, https://doi.org/10.1126/science.287.5453.646.
[188] S. Hare, S.S. Gupta, E. Valkov, A. Engelman, P. Cherepanov, Retroviral intasome assembly and inhibition of DNA strand transfer, Nature, 464 (2010) 232-236, https://doi.org/10.1038/nature08784.
[189] S. Hare, A.M. Vos, R.F. Clayton, J.W. Thuring, M.D. Cummings, P. Cherepanov, Molecular mechanisms of retroviral integrase inhibition and the evolution of viral resistance, Proc Natl Acad Sci U S A, 107 (2010) 20057-20062, https://doi.org/10.1073/pnas.1010246107.

[190] G.N. Maertens, S. Hare, P. Cherepanov, The mechanism of retroviral integration from X-ray structures of its key intermediates, Nature, 468 (2010) 326-329, https://doi.org/10.1038/nature09517.
[191] I.K. Jozwik, D.O. Passos, D. Lyumkis, Structural Biology of HIV Integrase Strand Transfer Inhibitors, Trends Pharmacol Sci, 41 (2020) 611-626, https://doi.org/10.1016/j.tips.2020.06.003.
[192] M.R. Fesen, K.W.L. Kohn, F., Y. Pommier, Inhibitors of human immunodeficiency virus integrase, Proceedings of the National Academy of Sciences of the United States of America, 90 (1993) 2399-2403, https://doi.org/10.1073/pnas.90.6.2399.
[193] D.J. Hazuda, M.D. Miller, B.Y. Nguyen, J. Zhao, Resistance to the HIV-Integrase Inhibitor Raltegravir: Analysis of Protocol 005, a Phase 2 Study in Patients with Triple-Class Resistant HIV-1 Infection, in: 16th Intl HIV Drug Resistance Workshop, Barbados, 2007.
[194] E. DeJesus, C. Cohen, R. Elion, e. al., First report of raltegravir (RAL, MK-0518) use after virologic rebound on elvitegravir (EVT, GS 9137). in: Program and abstracts of the 4th International AIDS Society Conference on HIV Pathogenesis, Treatment and Prevention, Sydney, Australia, 2007
[195] D.J. McColl, S. Fransen, S. Gupta, N. Parkin, N. Margot, R. Ledford, J. Ledford, S. Chuck, A.K.M. Cheng, M. D. , Resistance and Cross-Resistance to First Generation Integrase Inhibitors: Insights from a Phase 2 Study of Elvitegravir (GS-9137), in: 16th Intl HIV Drug resistance Workshop, Barbados, 2007.
[196] C. Garrido, J. Villacian, N. Zahonero, T. Pattery, F. Garcia, F. Gutierrez, E. Caballero, M. Van Houtte, V. Soriano, C. de Mendoza, S. Group., Broad phenotypic cross-resistance to elvitegravir in HIV-infected patients failing on raltegravir-containing regimens, Antimicrob Agents Chemother, 56 (2012) 2873-2878, https://doi.org/10.1128/AAC.06170-11.
[197] P.K. Quashie, T. Mesplede, M.A. Wainberg, Evolution of HIV integrase resistance mutations, Curr Opin Infect Dis, 26 (2013) 43-49, https://doi.org/10.1097/QCO.0b013e32835ba81c.
[198] K. Anstett, B. Brenner, T. Mesplede, M.A. Wainberg, HIV drug resistance against strand transfer integrase inhibitors, Retrovirology, 14 (2017) 36, https://doi.org/10.1186/s12977-017-0360-7.
[199] S. Min, I. Song, J. Borland, S. Chen, Y. Lou, T. Fujiwara, S.C. Piscitelli, Pharmacokinetics and safety of S/GSK1349572, a next-generation HIV integrase inhibitor,

in healthy volunteers, Antimicrob Agents Chemother, 54 (2010) 254-258, https://doi.org/10.1128/AAC.00842-09.
[200] M. Tsiang, G.S. Jones, J. Goldsmith, A. Mulato, D. Hansen, E. Kan, L. Tsai, R.A. Bam, G. Stepan, K.M. Stray, A. Niedziela-Majka, S.R. Yant, H. Yu, G. Kukolj, T. Cihlar, S.E. Lazerwith, K.L. White, H. Jin, Antiviral Activity of Bictegravir (GS-9883), a Novel Potent HIV-1 Integrase Strand Transfer Inhibitor with an Improved Resistance Profile, Antimicrob Agents Chemother, 60 (2016) 7086-7097, https://doi.org/10.1128/AAC.01474-16.
[201] D. Cattaneo, C. Gervasoni, Pharmacokinetics and Pharmacodynamics of Cabotegravir, a Long-Acting HIV Integrase Strand Transfer Inhibitor, Eur J Drug Metab Pharmacokinet, 44 (2019) 319-327, https://doi.org/10.1007/s13318-018-0526-2.
[202] T. Kawasuji, B.A. Johns, H. Yoshida, J.G. Weatherhead, T. Akiyama, T. Taishi, Y. Taoda, M. Mikamiyama-Iwata, H. Murai, R. Kiyama, M. Fuji, N. Tanimoto, T. Yoshinaga, T. Seki, M. Kobayashi, A. Sato, E.P. Garvey, T. Fujiwara, Carbamoyl pyridone HIV-1 integrase inhibitors. 2. Bi- and tricyclic derivatives result in superior antiviral and pharmacokinetic profiles, J Med Chem, 56 (2013) 1124-1135, https://doi.org/10.1021/jm301550c.
[203] M.L. Cottrell, T. Hadzic, A.D. Kashuba, Clinical pharmacokinetic, pharmacodynamic and drug-interaction profile of the integrase inhibitor dolutegravir, Clin Pharmacokinet, 52 (2013) 981-994, https://doi.org/10.1007/s40262-013-0093-2.
[204] S. Hare, S.J. Smith, M. Metifiot, A. Jaxa-Chamiec, Y. Pommier, S.H. Hughes, P. Cherepanov, Structural and functional analyses of the second-generation integrase strand transfer inhibitor dolutegravir (S/GSK1349572), Mol Pharmacol, 80 (2011) 565-572, https://doi.org/10.1124/mol.111.073189.
[205] S. Munir, E. Thierry, I. Malet, F. Subra, V. Calvez, A.G. Marcelin, E. Deprez, O. Delelis, G118R and F121Y mutations identified in patients failing raltegravir treatment confer dolutegravir resistance, J Antimicrob Chemother, 70 (2015) 739-749, https://doi.org/10.1093/jac/dku474.
[206] J.M. Llibre, F. Pulido, F. García, M. García Deltoro, J.L. Blanco, R. Delgado, Genetic barrier to resistance for dolutegravir, AIDS Rev, 17 (2015) 56-64.
[207] K.E. Hightower, R. Wang, F. Deanda, B.A. Johns, K. Weaver, Y. Shen, G.H. Tomberlin, H.L. Carter, B. 3rd, T., S. Sigethy, T. Seki, M. Kobayashi, M.R. Underwood, Dolutegravir (S/GSK1349572) exhibits significantly slower dissociation than raltegravir and elvitegravir from wild-type

and integrase inhibitor-resistant HIV-1 integrase-DNA complexes, Antimicrob Agents Chemother, 55 (2011) 4552-4559, https://doi.org/10.1128/AAC.00157-11.
[208] R.C. Rathbun, S.M. Lockhart, M.M. Miller, M.D. Liedtke, Dolutegravir, a second-generation integrase inhibitor for the treatment of HIV-1 infection, Ann Pharmacother, 48 (2014) 395-403, https://doi.org/10.1177/1060028013513558.
[209] World Health Organization, CONSOLIDATED GUIDELINES ON HIV PREVENTION, TESTING, TREATMENT, SERVICE DELIVERY AND MONITORING: RECOMMENDATIONS FOR A PUBLIC HEALTH APPROACH, (2021).
[210] F. Maggiolo, R. Gulminetti, L. Pagnucco, M. Digaetano, S. Benatti, D. Valenti, A. Callegaro, D. Ripamonti, C. Mussini, Lamivudine/dolutegravir dual therapy in HIV-infected, virologically suppressed patients, BMC Infect Dis, 17 (2017) 215, https://doi.org/10.1186/s12879-017-2311-2.
[211] P. Cahn, J.S. Madero, J.R. Arribas, A. Antinori, R. Ortiz, A.E. Clarke, C.C. Hung, J.K. Rockstroh, P.M. Girard, J. Sievers, C.Y. Man, R. Urbaityte, D.J. Brandon, M. Underwood, A.R. Tenorio, K.A. Pappa, B. Wynne, M. Gartland, M. Aboud, J. van Wyk, K.Y. Smith, Durable Efficacy of Dolutegravir Plus Lamivudine in Antiretroviral Treatment–Naive Adults With HIV-1 Infection-- 96-Week Results From the GEMINI-1 and GEMINI-2 Randomized Clinical Trials, J Acquir Immune Defic Syndr, 83 (2020) 310-318, https://doi.org/10.1097/QAI.0000000000002275.
[212] O. Osiyemi, S. De Wit, F. Ajana, F. Bisshop, J. Portilla, J.P. Routy, C. Wyen, M. Ait-Khaled, P. Leone, K.A. Pappa, R. Wang, J. Wright, N. George, B. Wynne, M. Aboud, J. van Wyk, K.Y. Smith, Efficacy and Safety of Switching to Dolutegravir/Lamivudine Versus Continuing a Tenofovir Alafenamide-Based 3- or 4-Drug Regimen for Maintenance of Virologic Suppression in Adults Living With Human Immunodeficiency Virus Type 1: Results Through Week 144 From the Phase 3, Noninferiority TANGO Randomized Trial, Clin Infect Dis, 75 (2022) 975-986, https://doi.org/10.1093/cid/ciac036.
[213] F. Maggiolo, R. Gulminetti, L. Pagnucco, M. Digaetano, A. Cervo, D. Valenti, A. Callegaro, C. Mussini, Long-term outcome of lamivudine/dolutegravir dual therapy in HIV-infected, virologically suppressed patients, BMC Infect Dis, 22 (2022) 782, https://doi.org/10.1186/s12879-022-07769-6.
[214] J. Fokam, D. Takou, E.N.J. Semengue, G. Teto, G. Beloumou, B. Dambaya, M.M. Santoro, L. Mossiang, S.C. Billong, F. Cham, S.M. Sosso, E.S. Temgoua, A.J. Nanfack, S. Moudourou, N. Kamgaing, R. Kamgaing, J.N. Ngako

Pamen, M.M.N. Etame, A.Z. Bissek, J.N. Elat, E.E. Moussi, V. Colizzi, C.F. Perno, A. Ndjolo, Viroforum, First case of Dolutegravir and Darunavir/r multi drug-resistant HIV-1 in Cameroon following exposure to Raltegravir: lessons and implications in the era of transition to Dolutegravir-based regimens, Antimicrob Resist Infect Control, 9 (2020) 143, https://doi.org/10.1186/s13756-020-00799-2.

[215] D.L. Braun, T. Scheier, U. Ledermann, M. Flepp, K.J. Metzner, J. Boni, H.F. Gunthard, Emergence of Resistance to Integrase Strand Transfer Inhibitors during Dolutegravir Containing Triple-Therapy in a Treatment-Experienced Patient with Pre-Existing M184V/I Mutation, Viruses, 12 (2020), https://doi.org/10.3390/v12111330.

[216] K. Huik, S. Hill, J. George, A. Pau, S. Kuriakose, C.M. Lange, N. Dee, P. Stoll, M. Khan, T. Rehman, C.A. Rehm, R. Dewar, Z. Grossman, F. Maldarelli, High-level dolutegravir resistance can emerge rapidly from few variants and spread by recombination: implications for integrase strand transfer inhibitor salvage therapy, AIDS, 36 (2022) 1835-1840, https://doi.org/10.1097/QAD.0000000000003288.

[217] M. Cevik, C. Orkin, P.E. Sax, Emergent Resistance to Dolutegravir Among INSTI-Naive Patients on First-line or Second-line Antiretroviral Therapy: A Review of Published Cases, Open Forum Infect Dis, 7 (2020) ofaa202, https://doi.org/10.1093/ofid/ofaa202.

[218] B. Sillman, A.N. Bade, P.K. Dash, B. Bhargavan, T. Kocher, S. Mathews, H. Su, G.D. Kanmogne, L.Y. Poluektova, S. Gorantla, J. McMillan, N. Gautam, Y. Alnouti, B. Edagwa, H.E. Gendelman, Creation of a long-acting nanoformulated dolutegravir, Nat Commun, 9 (2018) 443, https://doi.org/10.1038/s41467-018-02885-x.

[219] J. McMillan, A. Szlachetka, L. Slack, B. Sillman, B. Lamberty, B. Morsey, S. Callen, N. Gautam, Y. Alnouti, B. Edagwa, H.E. Gendelman, H.S. Fox, Pharmacokinetics of a Long-Acting Nanoformulated Dolutegravir Prodrug in Rhesus Macaques, Antimicrob Agents Chemother, 62 (2017) e01316-01317, https://doi.org/10.1128/AAC.01316-17.

[220] S. Deodhar, B. Sillman, A.N. Bade, S.N. Avedissian, A.T. Podany, J.M. McMillan, N. Gautam, B. Hanson, B.L. Dyavar Shetty, A. Szlachetka, M. Johnston, M. Thurman, D.J. Munt, A.K. Dash, M. Markovic, A. Dahan, Y. Alnouti, A. Yazdi, B.D. Kevadiya, S.N. Byrareddy, S.M. Cohen, B. Edagwa, H.E. Gendelman, Transformation of dolutegravir into an ultra-long-acting parenteral prodrug formulation, Nat Commun, 13 (2022) 3226, https://doi.org/10.1038/s41467-022-30902-7.

[221] J. Shao, J.C. Kraft, B. Li, J. Yu, J. Freeling, J. Koehn, R.J. Ho, Nanodrug formulations to enhance HIV drug exposure in lymphoid tissues and cells: clinical significance and potential impact on treatment and eradication of HIV/AIDS, Nanomedicine (Lond), 11 (2016) 545-564, https://doi.org/10.2217/nnm.16.1.
[222] L.A. McConnachie, L.M. Kinman, J. Koehn, J.C. Kraft, S. Lane, W. Lee, A.C. Collier, R.J.Y. Ho, Long-Acting Profile of 4 Drugs in 1 Anti-HIV Nanosuspension in Nonhuman Primates for 5 Weeks After a Single Subcutaneous Injection, J Pharm Sci, 107 (2018) 1787-1790, https://doi.org/10.1016/j.xphs.2018.03.005.
[223] S. Perazzolo, D.D. Shen, R.J.Y. Ho, Physiologically Based Pharmacokinetic Modeling of 3 HIV Drugs in Combination and the Role of Lymphatic System after Subcutaneous Dosing. Part 2: Model for the Drug-combination Nanoparticles, J Pharm Sci, 111 (2022) 825-837, https://doi.org/10.1016/j.xphs.2021.10.009.
[224] W.N. Charman, V.J. Stella, Estimating the maximal potential for intestinal lymphatic transport of lipophilic drug molecules, International Journal of Pharmaceutics, 34 (1986) 175-178, https://doi.org/10.1016/0378-5173(86)90027-X.
[225] T. Noguchi, W.N.A. Charman, V.J. Stella, The effect of drug lipophilicity and lipid vehicles on the lymphatic absorption of various testosterone esters, int J Pharm, 24 (1985) 173-184, https://doi.org/10.1016/0378-5173(85)90018-3.
[226] C.M. O'Driscoll, Lipid-based formulations for intestinal lymphatic delivery, Eur J Pharm Sci, 15 (2002) 405-415, https://doi.org/10.1016/s0928-0987(02)00051-9.
[227] C.J. Porter, S.A.C. Charman, W. N., Lymphatic transport of halofantrine in the triple-cannulated anesthetized rat model: effect of lipid vehicle dispersion, J Pharm Sci, 85 (1996) 351-356, https://doi.org/10.1021/js950221g.
[228] N.L. Trevaskis, R.M. Shanker, W.N. Charman, C.J. Porter, The mechanism of lymphatic access of two cholesteryl ester transfer protein inhibitors (CP524,515 and CP532,623) and evaluation of their impact on lymph lipoprotein profiles, Pharmaceutical Research, 27 (2010) 1949-1964, https://doi.org/10.1007/s11095-010-0199-2.
[229] C. Qin, Y. Chu, W. Feng, C. Fromont, S. He, J. Ali, J.B.Z. Lee, A., M. Berton, S. Bettonte, R. Liu, L. Yang, T. Monmaturapoj, C. Medrano-Padial, A.A.R. Ugalde, D. Vetrugno, S.Y. Ee, C. Sheriston, Y. Wu, M.J. Stocks, P.M. Fischer, P. Gershkovich, Targeted delivery of lopinavir to HIV reservoirs in the mesenteric lymphatic system by lipophilic ester prodrug approach, J Control Release, 329

(2021) 1077-1089, https://doi.org/10.1016/j.jconrel.2020.10.036.
[230] J.A. Yanez, S.W. Wang, I.W. Knemeyer, M.A. Wirth, K.B. Alton, Intestinal lymphatic transport for drug delivery, Adv Drug Deliv Rev, 63 (2011) 923-942, https://doi.org/10.1016/j.addr.2011.05.019.
[231] H. Mu, C.E. Hoy, The digestion of dietary triacylglycerols, Progress in Lipid Research, 43 (2004) 105-133, https://doi.org/10.1016/s0163-7827(03)00050-x.
[232] A.C. Ross, B. Caballero, R.J. Cousins, K.L. Tucker, T.R. Ziegler, Modern nutrition in health and disease, 2012.
[233] B. Borgström, C. Erlanson, Pancreatic Lipase and Co-Lipase, European Journal of Biochemistry, 37 (1973) 60-68, https://doi.org/10.1111/j.1432-1033.1973.tb02957.x.
[234] J.M. Johnston, B. Borgstroem, THE INTESTINAL ABSORPTION AND METABOLISM OF MICELLAR SOLUTIONS OF LIPIDS, Biochimica et Biophysica Acta, 5 (1964) 412-423.
[235] H.M. Cunningham, W.M. Leat, Lipid synthesis by the monoglyceride and alpha-glycerophosphate pathways in sheep intestine, Canadian Journal of Biochemistry, 47 (1969) 1013-1020, https://doi.org/10.1139/o69-163.
[236] Y.F. Shiau, Mechanisms of intestinal fat absorption, American Journal of Physiology-Gastrointestinal and Liver Physiology, 240 (1981) G1-G9, https://doi.org/10.1152/ajpgi.1981.240.1.G1.
[237] P. Gershkovich, A. Hoffman, Uptake of lipophilic drugs by plasma derived isolated chylomicrons: linear correlation with intestinal lymphatic bioavailability, European Journal of Pharmaceutical Sciences, 26 (2005) 394-404, https://doi.org/10.1016/j.ejps.2005.07.011.
[238] P. Gershkovich, J. Fanous, B. Qadri, A.A. Yacovan, S., A. Hoffman, The role of molecular physicochemical properties and apolipoproteins in association of drugs with triglyceride-rich lipoproteins: in-silico prediction of uptake by chylomicrons, Journal of Pharmacy and Pharmacology, 61 (2009) 31-39, https://doi.org/10.1211/jpp/61.01.0005.
[239] Y. Chu, C. Qin, W. Feng, C. Sheriston, Y. Jane Khor, C. Medrano-Padial, B.E. Watson, T. Chan, B. Ling, M.J. Stocks, P.M. Fischer, P. Gershkovich, Oral administration of tipranavir with long-chain triglyceride results in moderate intestinal lymph targeting but no efficient delivery to HIV-1 reservoir in mesenteric lymph nodes, International Journal of Pharmaceutics, 602 (2021) 120621, https://doi.org/10.1016/j.ijpharm.2021.120621.
[240] Z. Zhang, Y. Lu, J. Qi, W. Wu, An update on oral drug delivery via intestinal lymphatic transport, Acta Pharm Sin

B, 11 (2021) 2449-2468, https://doi.org/10.1016/j.apsb.2020.12.022.
[241] H. Frey, A. Aakvaag, D. Saanum, J. Falch, Bioavailability of oral testosterone in males, Eur J Clin Pharmacol, 16 (1979) 345-349, https://doi.org/10.1007/BF00605634.
[242] W.M. Bagchus, R. Hust, F. Maris, P.G. Schnabel, N.S. Houwing, Important effect of food on the bioavailability of oral testosterone undecanoate, Pharmacotherapy, 23 (2003) 319-325, https://doi.org/10.1592/phco.23.3.319.32104.
[243] S.M. Caliph, W.N. Charman, C.J. Porter, Effect of Short-, Medium-, and Long-Chain Fatty Acid-Based Vehicles on the Absolute Oral Bioavailability and Intestinal Lymphatic Transport of Halofantrine and Assessment of Mass B, Journal of pharmaceutical sciences, 89 (2000) 1073-1084, https://doi.org/10.1002/1520-6017(200008)89:8<1073::aid-jps12>3.0.co;2-v.
[244] A. Dahan, A. Hoffman, Rationalizing the selection of oral lipid based drug delivery systems by an in vitro dynamic lipolysis model for improved oral bioavailability of poorly water soluble drugs, J Control Release, 129 (2008) 1-10, https://doi.org/10.1016/j.jconrel.2008.03.021.
[245] D. Gentilcore, R. Chaikomin, K.L. Jones, A. Russo, C. Feinle-Bisset, J.M. Wishart, C.K. Rayner, M. Horowitz, Effects of fat on gastric emptying of and the glycemic, insulin, and incretin responses to a carbohydrate meal in type 2 diabetes, J Clin Endocrinol Metab, 91 (2006) 2062-2067, https://doi.org/10.1210/jc.2005-2644.
[246] W.N. Charman, C.J.M. Porter, S. Dressman, J. B., Physicochemical and Physiological Mechanisms for the Effects of Food on Drug Absorption-- The Role of Lipids and pH, J Pharm Sci, 86 (1997) 269-282, https://doi.org/10.1021/js960085v.
[247] G.A. Kossena, W.N. Charman, C.G.O.M. Wilson, B., B. Lindsay, J.M. Hempenstall, C.L. Davison, P.J. Crowley, C.J. Porter, Low dose lipid formulations: effects on gastric emptying and biliary secretion, Pharm Res, 24 (2007) 2084-2096, https://doi.org/10.1007/s11095-007-9363-8.
[248] P. Gershkovich, A. Hoffman, Effect of a high-fat meal on absorption and disposition of lipophilic compounds: the importance of degree of association with triglyceride-rich lipoproteins, Eur J Pharm Sci, 32 (2007) 24-32, https://doi.org/10.1016/j.ejps.2007.05.109.
[249] C.J. Porter, H.D. Williams, N.L. Trevaskis, Recent advances in lipid-based formulation technology, Pharm Res, 30 (2013) 2971-2975, https://doi.org/10.1007/s11095-013-1229-7.

[250] C.W. Pouton, C.J. Porter, Formulation of lipid-based delivery systems for oral administration: materials, methods and strategies, Adv Drug Deliv Rev, 60 (2008) 625-637, https://doi.org/10.1016/j.addr.2007.10.010.
[251] C.J. Porter, N.L. Trevaskis, W.N. Charman, Lipids and lipid-based formulations: optimizing the oral delivery of lipophilic drugs, Nature Reviews Drug Discovery, 6 (2007) 231-248, https://doi.org/10.1038/nrd2197.
[252] P. Gershkovich, B. Qadri, A. Yacovan, S. Amselem, A. Hoffman, Different impacts of intestinal lymphatic transport on the oral bioavailability of structurally similar synthetic lipophilic cannabinoids: dexanabinol and PRS-211,220, Eur J Pharm Sci, 31 (2007) 298-305, https://doi.org/10.1016/j.ejps.2007.04.006.
[253] A. Dahan, R. Duvdevani, I. Shapiro, A. Elmann, E. Finkelstein, A. Hoffman, The oral absorption of phospholipid prodrugs: in vivo and in vitro mechanistic investigation of trafficking of a lecithin-valproic acid conjugate following oral administration, J Control Release, 126 (2008) 1-9, https://doi.org/10.1016/j.jconrel.2007.10.025.
[254] A. Zgair, J.C. Wong, J.B. Lee, J. Mistry, O. Sivak, K.M. Wasan, I.M. Hennig, D.A. Barrett, C.S. Constantinescu, P.M. Fischer, P. Gershkovich, Dietary fats and pharmaceutical lipid excipients increase systemic exposure to orally administered cannabis and cannabis-based medicines, American journal of translational research, 8 (2016) 3448-3459.
[255] A. Zgair, J.B. Lee, J.C.M. Wong, D.A. Taha, J. Aram, D. Di Virgilio, J.W. McArthur, Y.K. Cheng, I.M. Hennig, D.A. Barrett, P.M. Fischer, C.S. Constantinescu, P. Gershkovich, Oral administration of cannabis with lipids leads to high levels of cannabinoids in the intestinal lymphatic system and prominent immunomodulation, Sci Rep, 7 (2017) 14542, https://doi.org/10.1038/s41598-017-15026-z.
[256] J.B. Lee, A. Zgair, J. Malec, T.H. Kim, M.G. Kim, J. Ali, C. Qin, W. Feng, M. Chiang, X. Gao, G. Voronin, A.E. Garces, C.L. Lau, T.H. Chan, A. Hume, T.M. McIntosh, F. Soukarieh, M. Al-Hayali, E. Cipolla, H.M. Collins, D.M. Heery, B.S. Shin, S.D. Yoo, L. Kagan, M.J. Stocks, T.D. Bradshaw, P.M. Fischer, P. Gershkovich, Lipophilic activated ester prodrug approach for drug delivery to the intestinal lymphatic system, J Control Release, 286 (2018) 10-19, https://doi.org/10.1016/j.jconrel.2018.07.022.
[257] W. Feng, C. Qin, E. Cipolla, J.B. Lee, A. Zgair, Y. Chu, C.A. Ortori, M.J. Stocks, C.S. Constantinescu, D.A. Barrett, P.M. Fischer, P. Gershkovich, Inclusion of Medium-Chain Triglyceride in Lipid-Based Formulation of Cannabidiol

Facilitates Micellar Solubilization In Vitro, but In Vivo Performance Remains Superior with Pure Sesame Oil Vehicle, Pharmaceutics, 13 (2021), https://doi.org/10.3390/pharmaceutics13091349.
[258] W. Feng, Qin, C., Chu, Y., Berton, M., Lee, J. B., Zgair, A., Bettonte, S., Stocks, M. J., Constantinescu, C. S., Barrett, D. A., Fischer, P. M., Gershkovich, P., Natural sesame oil is superior to pre-digested lipid formulations and purified triglycerides in promoting the intestinal lymphatic transport and systemic bioavailability of cannabidiol, Eur J Pharm Biopharm, 162 (2021) 43-49, 10.1016/j.ejpb.2021.02.013.
[259] C.T. Tian, J.J. Guo, Y.F. Miao, H.L. Wang, Q. Ye, C.L. Guo, M.Y. Zhang, Z.G. He, J. Sun, Long chain triglyceride-lipid formulation promotes the oral absorption of the lipidic prodrugs through coincident intestinal behaviors, Eur J Pharm Biopharm, 176 (2022) 122-132, https://doi.org/10.1016/j.ejpb.2022.05.015.
[260] W. Feng, C. Qin, S. Abdelrazig, Z. Bai, M. Raji, R. Darwish, Y. Chu, L. Ji, D.A. Gray, M.J. Stocks, C.S. Constantinescu, D.A. Barrett, P.M. Fischer, P. Gershkovich, Vegetable oils composition affects the intestinal lymphatic transport and systemic bioavailability of co-administered lipophilic drug cannabidiol, Int J Pharm, 624 (2022) 121947, https://doi.org/10.1016/j.ijpharm.2022.121947.
[261] A. Jewell, A. Brookes, W. Feng, M. Ashford, P. Gellert, J. Butler, P.M. Fischer, D.J. Scurr, M.J. Stocks, P. Gershkovich, Distribution of a highly lipophilic drug cannabidiol into different lymph nodes following oral administration in lipidic vehicle, Eur J Pharm Biopharm, 174 (2022) 29-34, https://doi.org/10.1016/j.ejpb.2022.03.014.
[262] N.L. Trevaskis, L.M. Kaminskas, C.J. Porter, From sewer to saviour - targeting the lymphatic system to promote drug exposure and activity, Nat Rev Drug Discov, 14 (2015) 781-803, https://doi.org/10.1038/nrd4608.
[263] C.J. Porter, W.N. Charman, Uptake of drugs into the intestinal lymphatics after oral administration, Adv Drug Deliv Rev, 25 (1997) 71-89, https://doi.org/10.1016/S0169-409X(96)00492-9.
[264] W.N. Charman, C.J.H. Porter, Lipophilic prodrugs designed for intestinal lymphatic transport, Advanced Drug Delivery Reviews, 19 (1996) 149-169, https://doi.org/10.1016/0169-409X(95)00105-G.
[265] M.S. Khan, M. Akhter, Synthesis, pharmacological activity and hydrolytic behavior of glyceride prodrugs of ibuprofen, Eur J Med Chem, 40 (2005) 371-376, https://doi.org/10.1016/j.ejmech.2004.11.009.

[266] M.S. Khan, M. Akhter, Glyceride derivatives as potential prodrugs: synthesis, biological activity and kinetic studies of glyceride derivatives of mefenamic acid, Pharmazie, 60 (2005) 110-114.
[267] M.S. Khan, M. Akhter, Synthesis, biological evaluation and kinetic studies of prodrugs of diclofenac, Indian J Exp Biol, 42 (2004) 1066-1072.
[268] A. Dahan, R. Duvdevani, E. Dvir, A.H. Elmann, A., A novel mechanism for oral controlled release of drugs by continuous degradation of a phospholipid prodrug along the intestine: in-vivo and in-vitro evaluation of an indomethacin-lecithin conjugate, J Control Release, 119 (2007) 86-93, https://doi.org/10.1016/j.jconrel.2006.12.032.
[269] A. Sakai, N. Mori, S. Shuto, T. Suzuki, Deacylation-Reacylation Cycle: A Possible Absorption Mechanism for the Novel Lymphotropic Antitumor Agent Dipalmitoylphosphatidylfluorouridine in Rats, J Pharm Sci, 82 (1993) 575-578, https://doi.org/10.1002/jps.2600820606.
[270] J. Sugihara, S. Furuuchi, K. Nakano, S. Harigaya, Studies on intestinal lymphatic absorption of drugs. I. Lymphatic absorption of alkyl ester derivatives and alpha-monoglyceride derivatives of drugs, J Pharmacobiodyn, 11 (1988) 369-376, https://doi.org/10.1248/bpb1978.11.369.
[271] J. Sugihara, S.A. Furuuchi, H., K. Takashima, S. Harigaya, Studies on intestinal lymphatic absorption of drugs. II. Glyceride prodrugs for improving lymphatic absorption of naproxen and nicotinic acid, J Pharmacobiodyn, 11 (1988) 555-562, https://doi.org/10.1248/bpb1978.11.555.
[272] D.M. Shackleford, W.A. Faassen, N. Houwing, H. Lass, G.A. Edwards, C.J. Porter, W.N. Charman, Contribution of lymphatically transported testosterone undecanoate to the systemic exposure of testosterone after oral administration of two andriol formulations in conscious lymph duct-cannulated dogs, J Pharmacol Exp Ther, 306 (2003) 925-933, https://doi.org/10.1124/jpet.103.052522.
[273] J.K. Amory, G.K. Scriba, D.W. Amory, W.J. Bremner, Oral testosterone-triglyceride conjugate in rabbits: single-dose pharmacokinetics and comparison with oral testosterone undecanoate, J Androl, 24 (2003) 716-720, https://doi.org/10.1002/j.1939-4640.2003.tb02732.x.
[274] R. Kochappan, E. Cao, S. Han, L. Hu, T. Quach, D. Senyschyn, V.I. Ferreira, G. Lee, N. Leong, G. Sharma, S.F. Lim, C.J. Nowell, Z. Chen, U.H. von Andrian, D. Bonner, J.D. Mintern, J.S. Simpson, N.L. Trevaskis, C.J.H. Porter, Targeted delivery of mycophenolic acid to the mesenteric

lymph node using a triglyceride mimetic prodrug approach enhances gut-specific immunomodulation in mice, J Control Release, 332 (2021) 636-651, https://doi.org/10.1016/j.jconrel.2021.02.008.
[275] A.S. Elz, N.L. Trevaskis, C.J.H. Porter, J.M. Bowen, C.A. Prestidge, Smart design approaches for orally administered lipophilic prodrugs to promote lymphatic transport, J Control Release, 341 (2022) 676-701, https://doi.org/10.1016/j.jconrel.2021.12.003.
[276] L. Hu, T. Quach, S. Han, S.F. Lim, P. Yadav, D. Senyschyn, N.L. Trevaskis, J.S. Simpson, C.J. Porter, Glyceride-Mimetic Prodrugs Incorporating Self-Immolative Spacers Promote Lymphatic Transport, Avoid First-Pass Metabolism, and Enhance Oral Bioavailability, Angew Chem Int Ed Engl, 55 (2016) 13700-13705, https://doi.org/10.1002/anie.201604207.
[277] S. Han, T. Quach, L. Hu, A. Wahab, W.N. Charman, V.J. Stella, N.L. Trevaskis, J.S. Simpson, C.J. Porter, Targeted delivery of a model immunomodulator to the lymphatic system: comparison of alkyl ester versus triglyceride mimetic lipid prodrug strategies, Journal of Controlled Release, 177 (2014) 1-10, https://doi.org/10.1016/j.jconrel.2013.12.031.
[278] N. Borkar, B. Li, R. Holm, A.E. Hakansson, A. Mullertz, M. Yang, H. Mu, Lipophilic prodrugs of apomorphine I: preparation, characterisation, and in vitro enzymatic hydrolysis in biorelevant media, European Journal of Pharmaceutics and Biopharmaceutics, 89 (2015) 216-223, https://doi.org/10.1016/j.ejpb.2014.12.014.
[279] D.M. Lambert, Rationale and applications of lipids as prodrug carriers, Eur J Pharm Sci, 11 (2000) S15-S27, https://doi.org/10.1016/s0928-0987(00)00161-5.
[280] T.L. Huang, T. Shiotsuki, T. Uematsu, B. Borhan, Q.X.H. Li, B. D., Structure-activity relationships for substrates and inhibitors of mammalian liver microsomal carboxylesterases, Pharm Res, 13 (1996) 1495-1500, https://doi.org/10.1023/a:1016071311190.
[281] P. Gershkovich, J. Fanous, B. Qadri, A. Yacovan, S. Amselem, A. Hoffman, The role of molecular physicochemical properties and apolipoproteins in association of drugs with triglyceride-rich lipoproteins: in-silico prediction of uptake by chylomicrons, J Pharm Pharmacol, 61 (2009) 31-39, https://10.1211/jpp/61.01.0005.
[282] H.E. Gottlieb, V.N. Kotlyar, A., NMR Chemical Shifts of Common Laboratory Solvents as Trace Impurities, The

Journal of Organic Chemistry, 62 (1997) 7512-7515, https://doi.org/10.1021/jo971176v.
[283] P. Gershkovich, A. Hoffman, Uptake of lipophilic drugs by plasma derived isolated chylomicrons: linear correlation with intestinal lymphatic bioavailability, Eur J Pharm Sci, 26 (2005) 394-404, https://doi.org/10.1016/j.ejps.2005.07.011.
[284] E.L. McConnell, A.W. Basit, S. Murdan, Measurements of rat and mouse gastrointestinal pH, fluid and lymphoid tissue, and implications for in-vivo experiments, Journal of Pharmacy and Pharmacology, 60 (2008) 63-70, https://doi.org/10.1211/jpp.60.1.0008.
[285] M. Vertzoni, J. Dressman, J. Butler, J. Hempenstall, C. Reppas, Simulation of fasting gastric conditions and its importance for the in vivo dissolution of lipophilic compounds, Eur J Pharm Biopharm, 60 (2005) 413-417, https://doi.org/10.1016/j.ejpb.2005.03.002.
[286] M. Margareth, Dissolution Media Simulating Fasted and Fed States, Dissolution Technologies, 11 (2004) 16-16, https://doi.org/10.14227/dt110204p16.
[287] A. Zgair, J.C. Wong, J.B. Lee, J. Mistry, O. Sivak, K.M. Wasan, I.M. Hennig, D.A. Barrett, C.S. Constantinescu, P.M. Fischer, P. Gershkovich, Dietary fats and pharmaceutical lipid excipients increase systemic exposure to orally administered cannabis and cannabis-based medicines, Am J Transl Res, 8 (2016) 3448-3459.
[288] P. Benito-Gallo, A. Franceschetto, J.C. Wong, M. Marlow, V. Zann, P. Scholes, P. Gershkovich, Chain length affects pancreatic lipase activity and the extent and pH-time profile of triglyceride lipolysis, European Journal of Pharmaceutics and Biopharmaceutics, 93 (2015) 353-362, https://doi.org/10.1016/j.ejpb.2015.04.027.
[289] W. Kromdijk, H. Rosing, M.P. van den Broek, J.H. Beijnen, A.D. Huitema, Quantitative determination of oseltamivir and oseltamivir carboxylate in human fluoride EDTA plasma including the ex vivo stability using high-performance liquid chromatography coupled with electrospray ionization tandem mass spectrometry, J Chromatogr B Analyt Technol Biomed Life Sci, 891-892 (2012) 57-63, https://doi.org/10.1016/j.jchromb.2012.02.026.
[290] M.S. Kim, J.S. Song, H. Roh, J.S. Park, J.H. Ahn, S.H.B. Ahn, M. A., Determination of a peroxisome proliferator-activated receptor gamma agonist, 1-(trans-methylimino-N-oxy)-6-(2-morpholinoethoxy-3-phenyl-1H-indene-2-carboxylic acid ethyl ester (KR-62980) in rat plasma by liquid chromatography-tandem mass spectrometry, J Pharm

Biomed Anal, 54 (2011) 121-126, https://doi.org/10.1016/j.jpba.2010.07.033.
[291] C.M. Parkinson, A. O'Brien, T.M. Albers, M.A.C. Simon, C. B., K.R. Pritchett-Corning, Diagnostic necropsy and selected tissue and sample collection in rats and mice, J Vis Exp, (2011), https://doi.org/10.3791/2966.
[292] Food and Drug Administration, Bioanalytical Method Validation Guidance for Industry, in, 2018.
[293] S.M. Hammer, K.E. Squires, M.D. Hughes, J.M. Grimes, L.M. Demeter, J.S. Currier, J.J.J. Eron, J.E. Feinberg, H.H.J. Balfour, L.R. Deyton, J.A. Chodakewitz, M.A. Fischl, A Controlled Trial of Two Nucleoside Analogues plus Indinavir in Persons with Human Immunodeficiency Virus Infection and CD4 Cell Counts of 200 per Cubic Millimeter or Less, The New England Journal of Medicine, 337 (1997) 725-733, https://doi.org/10.1056/nejm199709113371101.
[294] L.K. Schrager, M.P. D'Souza, Cellular and Anatomical Reservoirs of HIV-1 in Patients Receiving Potent Antiretroviral Combination Therapy, JAMA, 280 (1998) 67-71, https://doi.org/10.1001/jama.280.1.67.
[295] J.K. Wong, S.A. Yukl, Tissue reservoirs of HIV, Current Opinion in HIV and AIDS, 11 (2016) 362-370, https://dx.doi.org/10.1097/COH.0000000000000293.
[296] J. Estaquier, B. Hurtrel, Mesenteric lymph nodes, a sanctuary for the persistance of HIV. Escape mechanisms, Medecine Sciences: M/S, 24 (2008) 1055-1060, https://doi.org/10.1051/medsci/200824121055.
[297] J.D. Deere, R.C. Kauffman, E. Cannavo, J. Higgins, A. Villalobos, L. Adamson, R.F. Schinazi, P.A. Luciw, T.W. North, Analysis of multiply spliced transcripts in lymphoid tissue reservoirs of rhesus macaques infected with RT-SHIV during HAART, PLoS One, 9 (2014) e87914, https://doi.org/10.1371/journal.pone.0087914.
[298] S. Siddiqui, S. Perez, Y. Gao, L. Doyle-Meyers, B.T. Foley, Q. Li, B. Ling, Persistent Viral Reservoirs in Lymphoid Tissues in SIV-Infected Rhesus Macaques of Chinese-Origin on Suppressive Antiretroviral Therapy, Viruses, 11 (2019) 105, https://doi.org/10.3390/v11020105.
[299] H. Rabezanahary, F. Moukambi, D. Palesch, J. Clain, G. Racine, G. Andreani, G. Benmadid-Laktout, O. Zghidi-Abouzid, C. Soundaramourty, C. Tremblay, G. Silvestri, J. Estaquier, Despite early antiretroviral therapy effector memory and follicular helper CD4 T cells are major reservoirs in visceral lymphoid tissues of SIV-infected macaques, Mucosal Immunol, 13 (2020) 149-160, https://doi.org/10.1038/s41385-019-0221-x.

[300] S.M. Sieber, V.H. Cohn, W.T. Wynn, The entry of foreign compounds into the thoracic duct lymph of the rat, Xenobiotica, 4 (1974) 265-284, https://doi.org/10.3109/00498257409052055.
[301] C.J. Porter, W.N. Charman, Uptake of drugs into the intestinal lymphatics after oral administration, Advanced Drug Delivery Reviews, 25 (1997) 71-89, https://doi.org/10.1016/S0169-409X(96)00492-9.
[302] H. Ahn, J.H. Park, Liposomal delivery systems for intestinal lymphatic drug transport, Biomaterial Research, 20 (2016) 36, https://dx.doi.org/10.1186%2Fs40824-016-0083-1.
[303] C.M. Mansbach, S.A. Siddiqi, The biogenesis of chylomicrons, Annual Review of Physiology, 72 (2010) 315-333, https://doi.org/10.1146/annurev-physiol-021909-135801.
[304] A. Zgair, J.B. Lee, J.C.M. Wong, D.A. Taha, J. Aram, D. Di Virgilio, J.W. McArthur, Y.K. Cheng, I.M. Hennig, D.A. Barrett, P.M. Fischer, C.S. Constantinescu, P. Gershkovich, Oral administration of cannabis with lipids leads to high levels of cannabinoids in the intestinal lymphatic system and prominent immunomodulation, Scientific Reports, 7 (2017) 14542, https://doi.org/10.1038/s41598-017-15026-z.
[305] N.L. Trevaskis, W.N. Charman, C.J.H. Porter, Lipid-based delivery systems and intestinal lymphatic drug transport: A mechanistic update, Advanced Drug Delivery Reviews, 60 (2008) 702-716, https://doi.org/10.1016/j.addr.2007.09.007.
[306] J.B. Lee, A. Zgair, J. Malec, T.H. Kim, M.G. Kim, J. Ali, C. Qin, W. Feng, M. Chiang, X. Gao, G. Voronin, A.E. Garces, C.L. Lau, T.H. Chan, A. Hume, T.M. McIntosh, F. Soukarieh, M. Al-Hayali, E. Cipolla, H.M. Collins, D.M. Heery, B.S. Shin, S.D. Yoo, L. Kagan, M.J. Stocks, T.D. Bradshaw, P.M. Fischer, P. Gershkovich, Lipophilic activated ester prodrug approach for drug delivery to the intestinal lymphatic system, Journal of Controlled Release, 286 (2018) 10-19, https://doi.org/10.1016/j.jconrel.2018.07.022.
[307] C. Qin, Y. Chu, W. Feng, C. Fromont, S. He, J. Ali, J.B. Lee, A. Zgair, M. Berton, S. Bettonte, R. Liu, L. Yang, T. Monmaturapoj, C. Medrano-Padial, A.R. Ugalde, D. Vetrugno, S.Y. Ee, C. Sheriston, Y. Wu, M.J. Stocks, P.M. Fischer, P. Gershkovich, Targeted delivery of lopinavir to HIV reservoirs in the mesenteric lymphatic system by lipophilic ester prodrug approach, Journal of Controlled Release, (2020), https://doi.org/10.1016/j.jconrel.2020.10.036.

[308] A. Mocroft, S. Vella, T.L. Benfield, A. Chiesi, V. Miller, P. Gargalianos, A.d.A. Monforte, I. Yust, J.N. Bruun, A.N. Phillips, J.D. Lundgren, Changing patterns of mortality across Europe in patients infected with HIV-1, The Lancet, 352 (1998) 1725-1730, https://doi.org/10.1016/s0140-6736(98)03201-2.
[309] D.W. Cameron, M. Heath-Chiozzi, S. Danner, C. Cohen, S. Kravcik, C. Maurath, E. Sun, D. Henry, R. Rode, A. Potthoff, J. Leonard, Randomised placebo-controlled trial of ritonavir in advanced HIV-1 disease, The Lancet, 351 (1998) 543-549, https://doi.org/10.1016/S0140-6736(97)04161-5.
[310] I. Perez-Valero, J.R. Arribas, Protease inhibitor monotherapy, Current Opinion in Infectious Diseases, 24 (2011) 7-11, https://doi.org/10.1097/qco.0b013e3283422cdf.
[311] S.R. Turner, J.W. Strohbach, R.A. Tommasi, P.A. Aristoff, P.D. Johnson, H.I. Skulnick, L.A. Dolak, E.P. Seest, P.K. Tomich, M.J. Bohanon, M.M. Horng, J.C. Lynn, K.T. Chong, R.R. Hinshaw, K.D. Watenpaugh, M.N. Janakiraman, S. Thaisrivongs, Tipranavir (PNU-140690) A Potent, Orally Bioavailable Nonpeptidic HIV Protease Inhibitor of the 5,6-Dihydro-4-hydroxy-2-pyrone Sulfonamide class, Journal of Medicinal Chemistry, 41 (1998) 3467-3476, https://doi.org/10.1021/jm9802158.
[312] R.M. Lascar, P. Benn, Role of darunavir in the management of HIV infection, HIV/AIDS – Research and Palliative Care, 1 (2009) 31-39, https://dx.doi.org/10.2147/hiv.s5397.
[313] R. Winzer, P. Langmann, Tipranavir A Review of its Use in Therapy of HIV Infection, Clinical Medicine: Therapeutics, 1 (2009), https://doi.org/10.4137/CMT.S2668.
[314] K.M. Chan-Tack, K.A. Struble, D.B. Birnkrant, Intracranial hemorrhage and liver-associated deaths associated with tipranavir/ritonavir: review of cases from the FDA's Adverse Event Reporting System, AIDS Patient Care STDS, 22 (2008) 843-850, https://doi.org/10.1089/apc.2008.0043.
[315] ACD/ChemSketch, version 2020.1.1, Advanced Chemistry Development, Inc., Toronto, ON, Canada, www.acdlabs.com, 2020., in.
[316] N.K. Saksena, B. Wang, L. Zhou, M. Soedjono, Y.S. Ho, V. Conceicao, HIV reservoirs in vivo and new strategies for possible eradication of HIV from the reservoir sites, HIV/AIDS – Research and Palliative Care, 2 (2010) 103-122, https://doi.org/10.2147/hiv.s6882.
[317] C.V. Fletcher, K. Staskus, S.W. Wietgrefe, M. Rothenberger, C. Reilly, J.G. Chipman, G.J. Beilman, A.

Khoruts, A. Thorkelson, T.E. Schmidt, J. Anderson, K. Perkey, M. Stevenson, A.S. Perelson, D.C. Douek, A.T. Haase, T.W. Schacker, Persistent HIV-1 replication is associated with lower antiretroviral drug concentrations in lymphatic tissues, Proceedings of the National Academy of Sciences of the United States of America, 111 (2014) 2307-2312, https://dx.doi.org/10.1073/pnas.1318249111.
[318] A.A. Lackner, M. Mohan, R.S. Veazey, The Gastrointestinal Tract and AIDS Pathogenesis, Gastroenterology, 136 (2009) 1965-1978, https://doi.org/10.1053/j.gastro.2008.12.071.
[319] Z. Lv, Y. Chu, Y. Wang, HIV protease inhibitors: a review of molecular selectivity and toxicity, HIV/AIDS – Research and Palliative Care, 7 (2015) 95-104, https://dx.doi.org/10.2147/HIV.S79956.
[320] European Medicine Agency Press officer, European Medicines Agency Announces Recall of Viracept, in, 2007, pp. 1.
[321] D.C. Boettiger, C.A. Sabin, A. Grulich, L. Ryom, F. Bonnet, P. Reiss, A. Monforte, O. Kirk, A. Phillips, M. Bower, G. Fatkenheuer, J.D. Lundgren, M. Law, Is nelfinavir exposure associated with cancer incidence in HIV-positive individuals?, AIDS, 30 (2016) 1629-1637, https://dx.doi.org/10.1097%2FQAD.0000000000001053.
[322] European Medicines Agency, Viracept (nelfinavir) Non-renewal of the marketing authorisation in the European Union, in, 2013, pp. 1.
[323] T. D'Aquila, Y.H. Hung, A. Carreiro, K.K. Buhman, Recent discoveries on absorption of dietary fat: Presence, synthesis, and metabolism of cytoplasmic lipid droplets within enterocytes, Biochimica et Biophysica Acta, 1861 (2016) 730-747, https://doi.org/10.1016/j.bbalip.2016.04.012.
[324] I.L. Chaikoff, B. Bloom, B.P. Stevens, W.O. Reinhardt, W.G. Dauben, Pentadecanoic acid-5-C14; its absorption and lymphatic transport, Journal of Biological Chemistry, 190 (1951) 431-435.
[325] B. Bloom, I.L. Chaikoff, W.O. Reinhardt, Intestinal Lymph as Pathway for Transport of Absorbed Fatty Acids of Different Chain Lengths, The American Journal of Physiology, 166 (1951) 451-455, https://doi.org/10.1152/ajplegacy.1951.166.2.451.
[326] W. Feng, C. Qin, Y. Chu, M. Berton, J. Bong Lee, A. Zgair, S. Bettonte, M.J. Stocks, C.S. Constantinescu, D.A. Barrett, P.M. Fischer, P. Gershkovich, Natural sesame oil is superior to pre-digested lipid formulations and purified triglycerides in promoting the intestinal lymphatic transport and systemic

bioavailability of cannabidiol, Eur J Pharm Biopharm, (2021), https://doi.org/10.1016/j.ejpb.2021.02.013.
[327] J.R. Baldwin, M.T. Boron, Y. Wang, D.W. Schneck, N.K. Hopkins, Effects of food and antacid on bioavailability of the protease inhibitor PNU-140690 in healthy volunteers [abstract 649], in: 5th Conference on Retroviruses Opportunistic Infections, Chicago, 1998.
[328] Food Drug Administration department of health and human services, Aptivus (tipranavir) [package insert], in: Ridgefield (CT): Boehringer Ingelheim, 2005, pp. 1-48.
[329] S. Thaisrivongs, H.I. Skulnick, S.R. Turner, J.W. Strohbach, R.A. Tommasi, P.D. Johnson, P.A. Aristoff, T.M. Judge, R.B. Gammill, J.K. Morris, K.R. Romines, R.A. Chrusciel, R.R. Hinshaw, K.T. Chong, W.G. Tarpley, S.M. Poppe, D.E. Slade, J.C. Lynn, M.M. Horng, P.K. Tomich, E.P. Seest, L.A. Dolak, W.J. Howe, G.M. Howard, F.J. Schwende, L.N. Toth, G.E. Padbury, G.J. Wilson, L. Shiou, G.L. Zipp, K.F. Wilkinson, B.D. Rush, M.J. Ruwart, K.A. Koeplinger, Z. Zhao, S. Cole, R.M. Zaya, T.J. Kakuk, M.N. Janakiraman, K.D. Watenpaugh, Structure-based design of HIV protease inhibitors: sulfonamide-containing 5,6-dihydro-4-hydroxy-2-pyrones as non-peptidic inhibitors, Journal of Medicinal Chemistry, 39 (1996) 4349-4353, https://doi.org/10.1021/jm960541s.
[330] N.L. Trevaskis, L.M. Kaminskas, C.J. Porter, From sewer to saviour - targeting the lymphatic system to promote drug exposure and activity, Nature Reviews. Drug Discovery, 14 (2015) 781-803, https://doi.org/10.1038/nrd4608.
[331] R.M. Gulick, J.W. Mellors, D. Havlir, J.J. Eron, C. Gonzalez, D. McMahon, D.D. Richman, F.T. Valentine, L. Jonas, A. Meibohm, E.A. Emini, J.A. Chodakewitz, Treatment with indinavir, zidovudine, and lamivudine in adults with human immunodeficiency virus infection and prior antiretroviral therapy, N Engl J Med, 337 (1997) 734-739, https://doi.org/10.1056/NEJM199709113371102.
[332] S.M. Hammer, K.E. Squires, M.D. Hughes, J.M. Grimes, L.M. Demeter, J.S. Currier, J.J.J. Eron, J.E. Feinberg, H.H.J. Balfour, L.R. Deyton, J.A. Chodakewitz, M.A. Fischl, A controlled trial of two nucleoside analogues plus indinavir in persons with human immunodeficiency virus infection and CD4 cell counts of 200 per cubic millimeter or less. AIDS Clinical Trials Group 320 Study Team, N Engl J Med, 337 (1997) 725-733, https://doi.org/10.1056/NEJM199709113371101.
[333] R.W. Shafer, D.A. Vuitton, Highly active antiretroviral therapy (Haart) for the treatment of infection with human immunodeficiency virus type 1, Biomed Pharmacother, 53

(1999) 73-86, https://doi.org/10.1016/s0753-3322(99)80063-8.
[334] J. Gallant, A. Lazzarin, A. Mills, C. Orkin, D. Podzamczer, P. Tebas, P.M. Girard, I. Brar, E.S. Daar, D. Wohl, J. Rockstroh, X. Wei, J. Custodio, K. White, H. Martin, A. Cheng, E. Quirk, Bictegravir, emtricitabine, and tenofovir alafenamide versus dolutegravir, abacavir, and lamivudine for initial treatment of HIV-1 infection (GS-US-380-1489): a double-blind, multicentre, phase 3, randomised controlled non-inferiority trial, Lancet, 390 (2017) 2063-2072, https://doi.org/10.1016/S0140-6736(17)32299-7.
[335] N.D. Diaco, C. Strickler, S. Giezendanner, S.A. Wirz, P.E. Tarr, Systematic De-escalation of Successful Triple Antiretroviral Therapy to Dual Therapy with Dolutegravir plus Emtricitabine or Lamivudine in Swiss HIV-positive Persons, EClinicalMedicine, 6 (2018) 21-25, https://doi.org/10.1016/j.eclinm.2018.11.005.
[336] M. Aboud, C. Orkin, D. Podzamczer, J.R. Bogner, D. Baker, M.A. Khuong-Josses, D. Parks, K. Angelis, L.P. Kahl, E.A. Blair, K. Adkison, M. Underwood, J.E. Matthews, B. Wynne, K. Vandermeulen, M. Gartland, K. Smith, Efficacy and safety of dolutegravir-rilpivirine for maintenance of virological suppression in adults with HIV-1: 100-week data from the randomised, open-label, phase 3 SWORD-1 and SWORD-2 studies, Lancet HIV, 6 (2019) e576-e587, https://doi.org/10.1016/S2352-3018(19)30149-3.
[337] P. Cahn, Madero, J. S., Arribas, J. R., Antinori, A., Ortiz, R., Clarke, A. E., Hung, C. C., Rockstroh, J. K., Girard, P. M., Sievers, J., Man, C. Y., Urbaityte, R., Brandon, D. J., Underwood, M., Tenorio, A. R., Pappa, K. A., Wynne, B., Gartland, M., Aboud, M., van Wyk, J., Smith, K. Y., Durable Efficacy of Dolutegravir Plus Lamivudine in Antiretroviral Treatment–Naive Adults With HIV-1 Infection-- 96-Week Results From the GEMINI-1 and GEMINI-2 Randomized Clinical Trials, J Acquir Immune Defic Syndr, 83 (2020) 310-318, 10.1097/QAI.0000000000002275.
[338] P.E. Sax, Rockstroh, J. K., Luetkemeyer, A. F., Yazdanpanah, Y., Ward, D., Trottier, B., Rieger, A., Liu, H., Acosta, R., Collins, S. E., Brainard, D. M., Martin, H., Gs-Us-Investigators, Switching to Bictegravir, Emtricitabine, and Tenofovir Alafenamide in Virologically Suppressed Adults With Human Immunodeficiency Virus, Clin Infect Dis, 73 (2021) e485-e493, https://doi.org/10.1093/cid/ciaa988.
[339] T.W. Chun, L. Stuyver, S.B. Mizell, L.A. Ehler, J.A. Mican, M. Baseler, A.L. Lloyd, M.A. Nowak, A.S. Fauci, Presence of an inducible HIV-1 latent reservoir during highly active

antiretroviral therapy, Proc Natl Acad Sci U S A, 94 (1997) 13193-13197, https://doi.org/10.1073/pnas.94.24.13193.
[340] J.B. Whitney, A.L. Hill, S. Sanisetty, P. Penaloza-MacMaster, J. Liu, M. Shetty, L. Parenteau, C. Cabral, J. Shields, S. Blackmore, J.Y. Smith, A.L. Brinkman, L.E. Peter, S.I. Mathew, K.M. Smith, E.N. Borducchi, D.I. Rosenbloom, M.G. Lewis, J. Hattersley, B. Li, J. Hesselgesser, R. Geleziunas, M.L. Robb, J.H. Kim, N.L. Michael, D.H. Barouch, Rapid seeding of the viral reservoir prior to SIV viraemia in rhesus monkeys, Nature, 512 (2014) 74-77, https://doi.org/10.1038/nature13594.
[341] A.I. Hernández Cordero, C.X. Yang, J. Yang, Li, X,, S. Horvath, T. Shaipanich, J. MacIsaac, D. Lin, L. McEwen, M.S. Kobor, S. Guillemi, M. Harris, W. Lam, S. Lam, M. Obeidat, R.M. Novak, F. Hudson, H. Klinker, N. Dharan, J. Montaner, S.F.P. Man, K. Kunisaki, D.D. Sin, J.M. Leung, INSIGHT START Pulmonary and Genomic Substudy Groups, HIV-1 and T cell dynamics after interruption of highly active antiretroviral therapy (HAART) in patients with a history of sustained viral suppression, EBioMedicine, 83 (1999) 10246, https://doi.org/10.1016/j.ebiom.2022.104206.
[342] L. Ahdieh Grant, M.J. Silverberg, H. Palacio, H. Minkoff, K. Anastos, M.A. Young, M. Nowicki, A. Kovacs, M. Cohen, A. Muñoz, Discontinuation of potent antiretroviral therapy predictive value of and impact on CD4 cell counts and HIV RNA levels, AIDS, 15 (2001) 2101-2108, https://doi.org/10.1097/00002030-200111090-00005.
[343] W. Stohr, S. Fidler, M. McClure, J. Weber, D. Cooper, G. Ramjee, P. Kaleebu, G. Tambussi, M. Schechter, A. Babiker, R.E. Phillips, K. Porter, J. Frater, Duration of HIV-1 viral suppression on cessation of antiretroviral therapy in primary infection correlates with time on therapy, PLoS One, 8 (2013) e78287, https://doi.org/10.1371/journal.pone.0078287.
[344] D.J. Colby, L. Trautmann, S. Pinyakorn, L. Leyre, A. Pagliuzza, E. Kroon, M. Rolland, H. Takata, S. Buranapraditkun, J. Intasan, N. Chomchey, R. Muir, E.K. Haddad, S. Tovanabutra, S. Ubolyam, D.L. Bolton, B.A. Fullmer, R.J. Gorelick, L. Fox, T.A. Crowell, R. Trichavaroj, R. O'Connell, N. Chomont, J.H. Kim, N.L. Michael, M.L. Robb, N. Phanuphak, J. Ananworanich, R.V.s. group., Rapid HIV RNA rebound after antiretroviral treatment interruption in persons durably suppressed in Fiebig I acute HIV infection, Nat Med, 24 (2018) 923-926, https://doi.org/10.1038/s41591-018-0026-6.
[345] J.S.Y. Lau, M.Z. Smith, S.R. Lewin, J.H. McMahon, Clinical trials of antiretroviral treatment interruption in HIV-infected

individuals, AIDS, 33 (2019) 773-791, https://doi.org/10.1097/QAD.0000000000002113.
[346] J. Blazkova, Gao, F., Marichannegowda, M. H., Justement, J. S., Shi, V., Whitehead, E. J., Schneck, R. F., Huiting, E. D., Gittens, K., Cottrell, M., Benko, E., Kovacs, C., Lack, J., Sneller, M. C., Moir, S., Fauci, A. S., Chun, T. W., Distinct mechanisms of long-term virologic control in two HIV-infected individuals after treatment interruption of anti-retroviral therapy, Nat Med, 27 (2021) 1893-1898, https://doi.org/10.1038/s41591-021-01503-6.
[347] A.P. Burke, W. Benson, J.L. Ribas, D. Anderson, W.S. Chu, J. Smialek, R. Virmani, Postmortem localization of HIV-1 RNA by in situ hybridization in lymphoid tissues of intravenous drug addicts who died unexpectedly, Am J Pathol, 142 (1993) 1701-1713.
[348] T.W. North, J. Higgins, J.D. Deere, T.L. Hayes, A. Villalobos, L. Adamson, B.L. Shacklett, R.F. Schinazi, P.A. Luciw, Viral sanctuaries during highly active antiretroviral therapy in a nonhuman primate model for AIDS, J Virol, 84 (2010) 2913-2922, https://doi.org/10.1128/JVI.02356-09.
[349] S. Siddiqui, S. Perez, Y. Gao, L. Doyle-Meyers, B.T. Foley, Q. Li, B. Ling, Persistent Viral Reservoirs in Lymphoid Tissues in SIV-Infected Rhesus Macaques of Chinese-Origin on Suppressive Antiretroviral Therapy, Viruses, 11 (2019), https://doi.org/10.3390/v11020105.
[350] M. Horiike, S. Iwami, M. Kodama, A. Sato, Y. Watanabe, M. Yasui, Y. Ishida, T. Kobayashi, T. Miura, T. Igarashi, Lymph nodes harbor viral reservoirs that cause rebound of plasma viremia in SIV-infected macaques upon cessation of combined antiretroviral therapy, Virology, 423 (2012) 107-118, https://doi.org/10.1016/j.virol.2011.11.024.
[351] S. Siddiqui, Perez, S., Gao, Y., Doyle-Meyers, L., Foley, B. T., Li, Q., Ling, B. , Persistent Viral Reservoirs in Lymphoid Tissues in SIV-Infected Rhesus Macaques of Chines-Origin on Suppressive Antiretroviral Therapy, Viruses, 11 (2019) 105, https://doi.org/10.3390/v11020105.
[352] J.P. Freeling, R.J. Ho, Anti-HIV drug particles may overcome lymphatic drug insufficiency and associated HIV persistence, Proc Natl Acad Sci U S A, 111 (2014) E2512-2513, https://doi.org/10.1073/pnas.1406554111.
[353] J. Stein, M. Storcksdieck Genannt Bonsmann, H. Streeck, Barriers to HIV Cure, HLA, 88 (2016) 155-163, https://doi.org/10.1111/tan.12867.
[354] C.V. Fletcher, A.T. Podany, Antiretroviral Drug Penetration into Lymphoid Tissue, in: T.J. Hope, Richman,

D. D., Stevenson, M. (Ed.) Encyclopedia of AIDS, Springer, New York, 2018.
[355] A.S. Devanathan, M.L. Cottrell, Pharmacology of HIV Cure: Site of Action, Clin Pharmacol Ther, 109 (2021) 841-855, https://doi.org/10.1002/cpt.2187.
[356] S. Cao, Y. Jiang, H. Zhang, N. Kondza, K.A. Woodrow, Core-shell nanoparticles for targeted and combination antiretroviral activity in gut-homing T cells, Nanomedicine, 14 (2018) 2143-2153, http://doi.org/10.1016/j.nano.2018.06.005.
[357] Y. Du, Y. Xia, Y. Zou, Y. Hu, J. Fu, J. Wu, X.D. Gao, G. Ma, Exploiting the Lymph-Node-Amplifying Effect for Potent Systemic and Gastrointestinal Immune Responses via Polymer/Lipid Nanoparticles, ACS Nano, 13 (2019) 13809-13817, http://doi.org/10.1021/acsnano.9b04071.
[358] J. McCright, A. Ramirez, M. Amosu, A. Sinha, A. Bogseth, K. Maisel, Targeting the Gut Mucosal Immune System Using Nanomaterials, Pharmaceutics, 13 (2021), http://doi.org/10.3390/pharmaceutics13111755.
[359] W.N.A. Charman, V.J. Stella, Estimating the maximal potential for lymphatic transport of lipophilic drug molecules, International Journal of Pharmaceutics, 34 (1986) 175-178, https://doi.org/10.1016/0378-5173(86)90027-X.
[360] Y. Chu, Qin, C., Feng, W., Sheriston, C., Jane Khor, Y., Medrano-Padial, C., Watson, B. E., Chan, T., Ling, B., Stocks, M. J., Fischer, P. M., Gershkovich, P., Oral administration of tipranavir with long-chain triglyceride results in moderate intestinal lymph targeting but no efficient delivery to HIV-1 reservoir in mesenteric lymph nodes, Int J Pharm, 602 (2021) 120621, https://doi.org/10.1016/j.ijpharm.2021.120621.
[361] V. Cento, Perno, C. F., Dolutegravir Plus Lamivudine Two-Drug Regimen: Safety, Efficacy and Diagnostic Considerations for Its Use in Real-Life Clinical Practice-A Refined Approach in the COVID-19 Era, Diagnostics (Basel), 11 (2021), https://doi.org/10.3390/diagnostics11050809.
[362] D. Carroll, Genome engineering with zinc-finger nucleases, Genetics, 188 (2011) 773-782, https://doi.org/10.1534/genetics.111.131433.
[363] J. Stappaerts, S. Geboers, J. Snoeys, J. Brouwers, J. Tack, P. Annaert, P. Augustijns, Rapid conversion of the ester prodrug abiraterone acetate results in intestinal supersaturation and enhanced absorption of abiraterone: in vitro, rat in situ and human in vivo studies, Eur J Pharm Biopharm, 90 (2015) 1-7, https://doi.org/10.1016/j.ejpb.2015.01.001.

[364] C.G. Thompson, Rosen, E. P., Prince, H. M. A., White, N., Sykes, C., de la Cruz, G., Mathews, M., Deleage, C., Estes, J. D., Charlins, P., Mulder, L. R., Kovarova, M., Adamson, L., Arora, S., Dellon, E. S., Peery, A. F., Shaheen, N. J., Gay, C., Muddiman, D. C., Akkina, R., Garcia, J. V., Luciw, P., Kashuba, A. D. M., Heterogeneous antiretroviral drug distribution and HIV/SHIV detection in the gut of three species, Sci Transl Med, 11 (2019), https://doi.org/10.1126/scitranslmed.aap8758.
[365] L. Labarthe, T. Gele, H. Gouget, M.S. Benzemrane, P. Le Calvez, N. Legrand, O. Lambotte, R. Le Grand, C. Bourgeois, A. Barrail-Tran, Pharmacokinetics and tissue distribution of tenofovir, emtricitabine and dolutegravir in mice, J Antimicrob Chemother, 77 (2022) 1094-1101, https://doi.org/10.1093/jac/dkab501.
[366] N.L. Trevaskis, R.M. Shanker, W.N. Charman, C.J. Porter, The mechanism of lymphatic access of two cholesteryl ester transfer protein inhibitors (CP524,515 and CP532,623) and evaluation of their impact on lymph lipoprotein profiles, Pharm Res, 27 (2010) 1949-1964, https://doi.org/10.1007/s11095-010-0199-2.
[367] Sigma-Aldrich, SAFETY DATA SHEET - Esterase, from porcine liver, in, 2019.
[368] D. Wang, L. Zou, Q. Jin, J. Hou, G. Ge, L. Yang, Human carboxylesterases: a comprehensive review, Acta Pharm Sin B, 8 (2018) 699-712, https://doi.org/10.1016/j.apsb.2018.05.005.
[369] L. Moss, D. Wagner, E. Kanaoka, K. Olson, Y.L. Yueh, G.D. Bowers, The comparative disposition and metabolism of dolutegravir, a potent HIV-1 integrase inhibitor, in mice, rats, and monkeys, Xenobiotica, 45 (2015) 60-70, https://doi.org/10.3109/00498254.2014.942409.
[370] E. Nieschlag, J. Mauss, A. Coert, P. Kićović, Plasma androgen levels in men after oral administration of testosterone or testosterone undecanoate, Acta Endocrinol (Copenh), 79 (1975) 366-374, https://doi.org/10.1530/acta.0.0790366.
[371] V. Bala, S. Rao, E. Bateman, D. Keefe, S. Wang, C.A. Prestidge, Enabling Oral SN38-Based Chemotherapy with a Combined Lipophilic Prodrug and Self-Microemulsifying Drug Delivery System, Mol Pharm, 13 (2016) 3518-3525, https://doi.org/10.1021/acs.molpharmaceut.6b00591.
[372] M. Grove, G.P. Pedersen, J.L. Nielsen, A. Mullertz, Bioavailability of seocalcitol I: Relating solubility in biorelevant media with oral bioavailability in rats--effect of medium and long chain triglycerides, J Pharm Sci, 94 (2005) 1830-1838, https://doi.org/10.1002/jps.20403.

[373] T. Quach, Hu, L., Han, S., Lim, S. F., Senyschyn, D., Yadav, P., Trevaksis, N. L., Simpson, J. S., Porter, C. J. H., Triglyceride-Mimetic Prodrugs of Buprenorphine Enhance Oral Bioavailability via Promotion of Lymphatic Transport, Front Pharmacol, 13 (2022) 879660, https://doi.org/10.3389/fphar.2022.879660.
[374] S.M. Caliph, F.W. Faassen, C.J. Porter, The influence of intestinal lymphatic transport on the systemic exposure and brain deposition of a novel highly lipophilic compound with structural similarity to cholesterol, J Pharm Pharmacol, 66 (2014) 1377-1387, https://doi.org/10.1111/jphp.12268.
[375] G. Lee, Han, S., Lu, Z., Hong, J., Phillips, A. R. J., Windsor, J. A., Porter, C. J. H., Trevaskis, N. L., Intestinal delivery in a long-chain fatty acid formulation enables lymphatic transport and systemic exposure of orlistat, Int J Pharm, 596 (2021) 120247, https://doi.org/10.1016/j.ijpharm.2021.120247.
[376] H. Mu, C.E. Hoy, The digestion of dietary triacylglycerols, Prog Lipid Res, 43 (2004) 105-133, https://doi.org/10.1016/s0163-7827(03)00050-x.
[377] Y. Huang, Yu, Q., Chen, Z., Wu, W., Zhu, Q., Lu, Y., In vitro and in vivo correlation for lipid-based formulations: Current status and future perspectives, Acta Pharmaceutica Sinica B, 11 (2021) 2469-2487, https://doi.org/10.1016/j.apsb.2021.03.025.
[378] A.T. Larsen, P. Sassene, A. Mullertz, In vitro lipolysis models as a tool for the characterization of oral lipid and surfactant based drug delivery systems, Int J Pharm, 417 (2011) 245-255, https://doi.org/10.1016/j.ijpharm.2011.03.002.
[379] N. Thomas, R. Holm, A. Mullertz, T. Rades, In vitro and in vivo performance of novel supersaturated self-nanoemulsifying drug delivery systems (super-SNEDDS), J Control Release, 160 (2012) 25-32, https://doi.org/10.1016/j.jconrel.2012.02.027.
[380] A.T. Larsen, A.G. Ohlsson, B. Polentarutti, R.A. Barker, A.R. Phillips, R.D. Abu-Rmaileh, P. A., B. Abrahamsson, J. Ostergaard, A. Mullertz, Oral bioavailability of cinnarizine in dogs: relation to SNEDDS droplet size, drug solubility and in vitro precipitation, Eur J Pharm Sci, 48 (2013) 339-350, https://doi.org/10.1016/j.ejps.2012.11.004.
[381] L.C. Alskar, J. Keemink, J. Johannesson, C.J.H. Porter, C.A.S. Bergstrom, Impact of Drug Physicochemical Properties on Lipolysis-Triggered Drug Supersaturation and Precipitation from Lipid-Based Formulations, Mol Pharm, 15 (2018) 4733-4744, https://doi.org/10.1021/acs.molpharmaceut.8b00699.

[382] A. Dahan, A. Hoffman, The effect of different lipid based formulations on the oral absorption of lipophilic drugs: the ability of in vitro lipolysis and consecutive ex vivo intestinal permeability data to predict in vivo bioavailability in rats, Eur J Pharm Biopharm, 67 (2007) 96-105, https://doi.org/10.1016/j.ejpb.2007.01.017.
[383] A. Dahan, A. Hoffman, Use of a dynamic in vitro lipolysis model to rationalize oral formulation development for poor water soluble drugs: correlation with in vivo data and the relationship to intra-enterocyte processes in rats, Pharm Res, 23 (2006) 2165-2174, https://doi.org/10.1007/s11095-006-9054-x.
[384] C.J. Porter, A.M. Kaukonen, A. Taillardat-Bertschinger, B.J. Boyd, J.M. O'Connor, G.A. Edwards, W.N. Charman, Use of in vitro lipid digestion data to explain the in vivo performance of triglyceride-based oral lipid formulations of poorly water-soluble drugs-- Studies with halofantrine, J Pharm Sci, 93 (2004) 1110-1121, https://doi.org/10.1002/jps.20039.
[385] A. Larsen, R. Holm, M.L. Pedersen, A. Mullertz, Lipid-based formulations for danazol containing a digestible surfactant, Labrafil M2125CS: in vivo bioavailability and dynamic in vitro lipolysis, Pharm Res, 25 (2008) 2769-2777, https://doi.org/10.1007/s11095-008-9641-0.
[386] D.S. Wishart, Y.D. Feunang, A.C. Guo, E.J. Lo, A. Marcu, J.R. Grant, T. Sajed, D. Johnson, C. Li, Z. Sayeeda, N. Assempour, I. Iynkkaran, Y. Liu, A. Maciejewski, N. Gale, A. Wilson, L. Chin, R. Cummings, D. Le, A. Pon, C. Knox, M. Wilson, DrugBank 5.0: a major update to the DrugBank database for 2018, Nucleic Acids Res, (2017), https://doi.org/10.1093/nar/gkx1037.
[387] R.A. Myers, V.J. Stella, Factors affecting the lymphatic transport of penclomedine (NSC-338720), a lipophilic cytotoxic drug Comparison to DDT and hexachlorobenzene, Int J Pharm, 80 (1992) 51-62, https://doi.org/10.1016/0378-5173(92)90261-Y.
[388] D.J. Hauss, S.C. Mehta, G.W. Radebaugh, Targeted lymphatic transport and modified systemic distribution of CI-976, a lipophilic lipid-regulator drug, via a formulation approach, Int J Pharm, 108 (1994) 85-93, https://doi.org/10.1016/0378-5173(94)90318-2.
[389] N.L. Trevaskis, C.L. McEvoy, M.P. McIntosh, G.A. Edwards, R.M. Shanker, W.N. Charman, C.J. Porter, The role of the intestinal lymphatics in the absorption of two highly lipophilic cholesterol ester transfer protein inhibitors (CP524,515 and CP532,623), Pharm Res, 27 (2010) 878-893, https://doi.org/10.1007/s11095-010-0083-0.

[390] F.B. Padley, Major vegetable fats, in: F.D. Gunstone, Harwood, J. L., Padley, F. B. (Ed.) The Lipid Handbook, Chapman & Hall, London, 1986, pp. 53-147.
[391] M.M. Hussain, A proposed model for the assembly of chylomicrons, Atherosclerosis, 148 (2000) 1-15, https://doi.org/10.1016/s0021-9150(99)00397-4.
[392] J. Bjorkegren, C.J. Packard, A. Hamsten, D. Bedford, M. Caslake, L. Foster, J. Shepherd, P. Stewart, F. Karpe, Accumulation of large very low density lipoprotein in plasma during intravenous infusion of a chylomicron-like triglyceride emulsion reflects competition for a common lipolytic pathway, Journal of Lipid Research, 37 (1996) 76-86, https://doi.org/10.1016/s0022-2275(20)37637-9.
[393] D.A. Smith, K. Beaumont, T.S. Maurer, L. Di, Volume of Distribution in Drug Design, J Med Chem, 58 (2015) 5691-5698, https://doi.org/10.1021/acs.jmedchem.5b00201.
[394] M. Ellmerer, L. Schaupp, G.A. Brunner, G. Sendlhofer, A. Wutte, P. Wach, T.R. Pieber, Measurement of interstitial albumin in human skeletal muscle and adipose tissue by open-flow microperfusion, Am J Physiol Endocrinol Metab, 278 (2000) E352-356, https://doi.org/10.1152/ajpendo.2000.278.2.E352.
[395] M.J. Reese, P.M. Savina, G.T.T. Generaux, H. Humphreys, J. E., E. Kanaoka, L.O. Webster, K.A. Harmon, J.D. Clarke, J.W. Polli, In vitro investigations into the roles of drug transporters and metabolizing enzymes in the disposition and drug interactions of dolutegravir, a HIV integrase inhibitor, Drug Metab Dispos, 41 (2013) 353-361, https://doi.org/10.1124/dmd.112.048918.
[396] D. Edelstein, S. Basaria, Testosterone undecanoate in the treatment of male hypogonadism, Expert Opin Pharmacother, 11 (2010) 2095-2106, https://doi.org/10.1517/14656566.2010.505920.
[397] W. Cui, S. Zhang, H. Zhao, C. Luo, B. Sun, Z. Li, M. Sun, Q. Ye, J. Sun, Z. He, Formulating a single thioether-bridged oleate prodrug into a self-nanoemulsifying drug delivery system to facilitate oral absorption of docetaxel, Biomater Sci, 7 (2019) 1117-1131, https://doi.org/10.1039/c8bm00947c.
[398] A. Abdel Razik, M.S.E.-H. Metwally, M. F., M.A. El Wardany, Steric substituent effect on the resin catalyzed hydrolysis of alkyl acetate esters, React Kinet Catal Lett, 48 (1992) 279-290, https://doi.org/10.1007/BF02070097.
[399] C.J. Porter, A.M. Kaukonen, A. Taillardat-Bertschinger, B.J. Boyd, J.M. O'Connor, G.A. Edwards, W.N. Charman, Use of in vitro lipid digestion data to explain the in vivo performance of triglyceride-based oral lipid formulations of

poorly water-soluble drugs: Studies with halofantrine, J Pharm Sci, 93 (2004) 1110-1121, https://doi.org/10.1002/jps.20039.
[400] C.J. Porter, A.M. Kaukonen, B.J. Boyd, G.A. Edwards, W.N. Charman, Susceptibility to lipase-mediated digestion reduces the oral bioavailability of danazol after administration as a medium-chain lipid-based microemulsion formulation, Pharm Res, 21 (2004) 1405-1412, https://doi.org/10.1023/b:pham.0000036914.22132.cc.
[401] A. Dahan, A. Hoffman, Evaluation of a chylomicron flow blocking approach to investigate the intestinal lymphatic transport of lipophilic drugs, Eur J Pharm Sci, 24 (2005) 381-388, https://doi.org/10.1016/j.ejps.2004.12.006.
[402] D.G. Fatouros, D.M. Karpf, F.S. Nielsen, A. Mullertz, Clinical studies with oral lipid based formulations of poorly soluble compounds, Ther Clin Risk Manag, 3 (2007) 591-604.
[403] D.J. Hauss, S.E. Fogal, J.V.P. Ficorilli, C. A., T. Roy, A.A.K. Jayaraj, J. J., Lipid-Based Delivery Systems for Improving the Bioavailability and Lymphatic Transport of a Poorly Water-Soluble LTB4 Inhibitor, J Pharm Sci, 87 (1998) 164-169, https://doi.org/10.1021/js970300n.
[404] A.M. Kaukonen, B.J. Boyd, C.J. Porter, W.N. Charman, Drug Solubilization Behavior During in Vitro Digestion of Simple Triglyceride Lipid Solution Formulations, Pharm Res, 21 (2004) 245-253, https://doi.org/10.1023/b:pham.0000016282.77887.1f.
[405] M. Markovic, S. Ben-Shabat, A. Aponick, E.M. Zimmermann, A. Dahan, Lipids and Lipid-Processing Pathways in Drug Delivery and Therapeutics, Int J Mol Sci, 21 (2020), https://doi.org/10.3390/ijms21093248.
[406] A. Siew, Developing Lipid-Based Formulations, Pharmaceutical Technology, 42 (2018).
[407] F. Beilstein, V. Carriere, A. Leturque, S. Demignot, Characteristics and functions of lipid droplets and associated proteins in enterocytes, Exp Cell Res, 340 (2016) 172-179, https://doi.org/10.1016/j.yexcr.2015.09.018.
[408] US Food and Drug Administration, Guidance for industry: extended release oral dosage forms: development, evaluation, and application of in vitro/in vivo correlations., in: Center for Drug Evaluation and Research (CDER) (Ed.), 1997.
[409] A.R. Cillo, J.W. Mellors, Which therapeutic strategy will achieve a cure for HIV-1?, Curr Opin Virol, 18 (2016) 14-19, https://doi.org/10.1016/j.coviro.2016.02.001.

[410] G. Hütter, D. Nowak, M. Mossner, S. Ganepola, A. Müssig, K. Allers, T.H. Schneider, J., C. Kücherer, O. Blau, I.W. Blau, W.K. Hofmann, E. Thiel, Long-term control of HIV by CCR5 Delta32/Delta32 stem-cell transplantation, The New England Journal of Medicine, 360 (2009) 692-698, https://doi.org/10.1056/NEJMoa0802905.
[411] R.K. Gupta, D. Peppa, A.L. Hill, C. Gálvez, M. Salgado, M. Pace, L.E. McCoy, S.A. Griffith, J. Thornhill, A. Alrubayyi, L.E.P. Huyveneers, E. Nastouli, P. Grant, S.G. Edwards, A.J. Innes, J. Frater, M. Nijhuis, A.M.J. Wensing, J. Martinez-Picado, E. Olavarria, Evidence for HIV-1 cure after CCR5Δ32/Δ32 allogeneic haemopoietic stem-cell transplantation 30 months post analytical treatment interruption: a case report, The Lancet HIV, 7 (2020) e340-e347, https://doi.org/10.1016/s2352-3018(20)30069-2.
[412] D. Persaud, H. Gay, C. Ziemniak, Y.H. Chen, M.J. Piatak, T.W. Chun, M. Strain, D.L. Richman, K., Absence of detectable HIV-1 viremia after treatment cessation in an infant, The New England Journal of Medicine, 369 (2013) 1828-1835, https://doi.org/10.1056/NEJMoa1302976.
[413] D.H. Hamer, Can HIV be Cured? Mechanisms of HIV Persistence and Strategies to Combat It, Current HIV Research, 2 (2004) 99-111, https://doi.org/10.2174/1570162043484915.
[414] K. Thorlund, M.S. Horwitz, B.T. Fife, R. Lester, D.W. Cameron, Landscape review of current HIV 'kick and kill' cure research - some kicking, not enough killing, BMC Infectious Diseases, 17 (2017) 595, https://doi.org/10.1186/s12879-017-2683-3.
[415] Y.C. Ho, L. Shan, N.N. Hosmane, J. Wang, S.B. Laskey, D.I. Rosenbloom, J. Lai, J.N. Blankson, J.D. Siliciano, R.F. Siliciano, Replication-competent noninduced proviruses in the latent reservoir increase barrier to HIV-1 cure, Cell, 155 (2013) 540-551, https://doi.org/10.1016/j.cell.2013.09.020.
[416] M.M. Nuhn, S.B.H. Gumbs, N. Buchholtz, L.M. Jannink, L. Gharu, L.D. de Witte, A.M.J. Wensing, S.R. Lewin, M. Nijhuis, J. Symons, Shock and kill within the CNS: A promising HIV eradication approach?, Journal of Leukocyte Biology, (2022), https://doi.org/10.1002/JLB.5VMR0122-046RRR.
[417] M.K. Rothenberger, B.F. Keele, S.W. Wietgrefe, C.V. Fletcher, G.J. Beilman, J.G. Chipman, A. Khoruts, J.D. Estes, J. Anderson, S.P. Callisto, T.E. Schmidt, A. Thorkelson, C. Reilly, K. Perkey, T.G. Reimann, N.S. Utay, K. Nganou Makamdop, M. Stevenson, D.C. Douek, A.T. Haase, T.W. Schacker, Large number of rebounding/founder HIV variants emerge from multifocal infection in lymphatic

tissues after treatment interruption, Proceedings of the National Academy of Sciences of the United States of America, 112 (2015) E1126-1134, https://doi.org/10.1073/pnas.1414926112.
[418] V. Svicher, F. Ceccherini-Silberstein, A. Antinori, S. Aquaro, C.F. Perno, Understanding HIV compartments and reservoirs, Current HIV Research, 11 (2014) 186-194, https://doi.org/10.1007/s11904-014-0207-y.